DOKUZ EYLUL UNIVERSITY
GRADUATE SCHOOL OF NATURAL AND APPLIED SCIENCES

INVESTIGATION OF THE UTILIZATION OF SOME CHROMOIONOPHORES IN MICELLE AND IONIC LIQUID CONTAINING MEDIA FOR ION SENSING PURPOSES

by

Müge ÇÖLDÜR

September, 2011
İZMİR

INVESTIGATION OF THE UTILIZATION OF SOME CHROMOIONOPHORES IN MICELLE AND IONIC LIQUID CONTAINING MEDIA FOR ION SENSING PURPOSES

A Thesis Submitted to the
Graduate School of Natural and Applied Sciences of
Dokuz Eylul University
In Partial Fulfillment of the Requirements for
the Degree of Master of Science in Chemistry Program

by
Müge ÇÖLDÜR

September, 2011
İZMİR

M. Sc. THESIS EXAMINATION RESULT FORM

We have read the thesis entitled **"INVESTIGATION OF THE UTILIZATION OF SOME CHROMOINOPHORES IN MICELLE AND IONIC LIQUID CONTAINING MEDIA FOR ION SENSING PURPOSES"** completed by **MÜGE ÇÖLDÜR** under supervision of of **ASSOCIATED PROFESSOR DR. ÖZLEM ÖTER** and we certify that in our opinion it is fully adequate, in scope and in quality, as a thesis for the degree of Master of Science.

Associated Prof. Dr. Özlem ÖTER

Supervisor

Prof. Dr. Kadriye ERTEKİN

(Jury Member)

Assistant Prof. Dr. Özlem KARADENİZ

(Jury Member)

Prof. Dr. Mustafa SABUNCU

Director Graduate School of Natural and Applied Sciences

ACKNOWLEDGEMENTS

I would like to express sincere gratitute to my supervisor Associated Professor Dr. Özlem Öter for providing the fascinating subject, for her valuable support during this thesis and for the great working conditions at our laborotory.

I gratefully acknowledge the extensive help of my colleague Gizem Demiryas.

I also thank to Prof. Dr. Kadriye Ertekin for her support during my thesis.

Finally, I want to thank to my parents for their tolerant attitude to my working effort during the elaboration of this dissertation and for their incessant support during all the years of my studies.

Müge ÇÖLDÜR

INVESTIGATION OF THE UTILIZATION OF SOME CHROMOIONOPHORES IN MICELLE AND IONIC LIQUID CONTAINING MEDIA FOR ION SENSING PURPOSES

ABSTRACT

In the first part of this work, we have employed tree ionic liquids (1-butyl-3-methylimidazolium tetrafluoroborate,1-ethyl-3-methylimidazolium tetrafluoroborate 1-butyl-3- methylimidazolium thiocyanate) and two micelles (sodium dodecyl sulfate and Triton X-100) as new additives for the determination of Mn(II) with Eosin Y in aqueous solutions by spectrofluorimetric method. In the second part, photophysical constants of three ionic liquids, 1-Butyl-3- methylimidazolium thiocyanate, 1-butyl-3-methylimidazoliumtetrafluoroborate,1-ethyl-3-methylimidazoliumtetrafluoroborate were investigated in aqueous media by UV-visible absorption, emission and excitation spectra. The effect of metal cations (Ca(II), Cu(I), Hg(I), As(V), Mo(II), Li(I), Pb(II), Al(III), Cr(III), Na(I), Mg(II), Zn(II), Cd(II), Fe(III), Co(II) and Ni(II)) to the absorption and fluorescence characteristics of the ionic liquids were investigated and the acid base response of the ionic liquids were also evaluated. It has been observed that all the applied ionic liquids exhibited intense and broad emission bands from 350-600 nm. In the absorption spectra of 1-Butyl-3-methylimidazolium thiocyanate a new absorption maxima was observed by the addition of Fe(II) and Fe(III) ions, which is due to the complex formation of iron ions with SCN^- group of the ionic liquid.

Keywords: ionic liquids, micelle, Eosin Y, manganese, iron

BAZI KROMOİYONOFORLARIN MİSEL VE İYONİK SIVI İÇEREN ORTAMLARDA İYON TAYİNİNE YÖNELİK KULLANILABİLİRLİĞİNİN ARAŞTIRILMASI

ÖZ

Bu çalışmanın birinci bölümünde, üç tür iyonik sıvı (1-butyl-3-methylimidazoliumtetrafluoroborate, 1-ethyl-3-methylimidazolium tetrafluoroborate, 1-butyl-3- methylimidazolium thiocyanate ve iki tür misel (sodium dodecyl sulfate ve Triton X-100), Mn(II) nin Eosin Y ile sulu ortamlarda spektroflorimetrik tayininde katkı maddesi olarak kullanıldı. İkinci bölümde ise, 1-butyl-3-methylimidazolium thiocyanate, 1-butyl-3-methylimidazolium tetrafluoroborate, 1-ethyl-3-methylimidazolium tetrafluoroborate iyonik sıvılarının sulu ortamlardaki fotofiziksel özellikleri absorpsiyon, emisyon ve eksitasyon spektrumları alınarak incelendi. Bu iyonik sıvıların asidik ve bazik ortamlardaki (Ca(II), Cu(I), Hg(I), As(V), Mo(II), Li(I), Pb(II), Al(III), Cr(III), Na(I), Mg(II), Zn(II), Cd(II), Fe(III), Co(II) ve Ni(II)) gibi metal katyonlarını içeren ortamlardaki floresans özellikleri incelendi. Elde edilen sonuçlara gore tüm iyonik sıvıların 350-600 nm aralığında şiddetli ve geniş bantlı floresans özellik gösterdikleri bulundu. Ayrica 1-butyl-3-methylimidazolium thiocyanate iyonik sıvısının, SCN^- grubu ile demir iyonlarının olası kompleks oluşturmasından kaynaklanabilecek, demir iyonlarına büyük oranda absorpsiyon bazlı yanıtı gözlendi.

Anahtar kelimeler: iyonik sıvılar, miseller, Eosin Y, mangan, demir

CONTENTS **Page**

CHAPTER ONE
INTRODUCTION

1.1. Optical Measurement Techniques

1.1.1 Spectroscopic Methods

Most optical and fiber-optic sensors are based on absorption and fluorescence methods.Spectroscopic methods are the main tool of modern chemistry for the identification of molecular structures. In organic chemistry, spectroscopic methods are used to determine and confirm molecular structures, to monitor reactions and to control the purity of compounds. Most essential methods for the organic chemistry are the nuclear magnetic resonant spectroscopy (1H) and 13C NMR-spectroscopy, the mass spectrometry, the infrared and the UV/Vis-spectroscopy. **(**Hesse, Meier, Zeeh & Verlag, 2002*)*

Ultraviolet and visible spectrometers have been in general use for the last 35 years and over this period have become the most important analytical instrument in the modern day laboratory (Figure 1.1). In many applications, other techniques could be employed but UV-Visible spectrometry has been the most intensively used one due to its simplicity, versatility, speed, accuracy and cost-effectiveness.

The absorption in the visible range directly affects the perceived color of the chemicals involved. In this region of the electromagnetic spectrum, molecules undergo electronic transitions. This technique is complementary to fluorescence spectroscopy, in that fluorescence deals with transitions from the excited state to the ground state, while absorption measures transitions from the ground state to the excited state. (Skoog Holler Nieman, 2003)

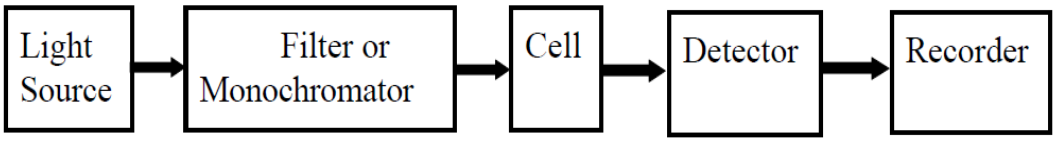

Figure 1.1 Instrument to measure absorption of light-spectrophotometer

1.1.2 Fluorescence

Absorption of UV radiation by a molecule excites it from a vibrational level in the electronic ground state to one of the many vibrational levels in the electronic excited state. This excited state is usually the first excited singlet state. A molecule in a high vibrational level of the excited state will quickly fall to the lowest vibrational level of this state by losing energy to other molecules through collision. The molecule will also partition the excess energy to other possible modes of vibration and rotation. Fluorescence occurs when the molecule returns to the electronic ground state, from the excited singlet state, by emission of a photon. If a molecule which absorbs UV radiation does not fluoresce it means that it must have lost its energy some other way. These processes are called radiationless transfer of energy (Figure 1.2).

Fluorescence spectroscopy, fluorimetry or spectrofluorimetry, is a type of electromagnetic spectroscopy which analyzes fluorescence from a sample. It involves using a beam of light, usually ultraviolet light, that excites the electrons in molecules of certain compounds and causes them to emit light of a lower energy, typically, but not necessarily, visible light. A complementary technique is absorption spectroscopy

In a typical experiment, the different wavelengths of fluorescent light emitted by a sample are measured using a monochromator , holding the excitation light at a constant wavelength. This is called an *emission spectrum*. An *excitation spectrum* is the opposite, whereby the emission light is held at a constant wavelength, and the excitation light is scanned through many different wavelengths.

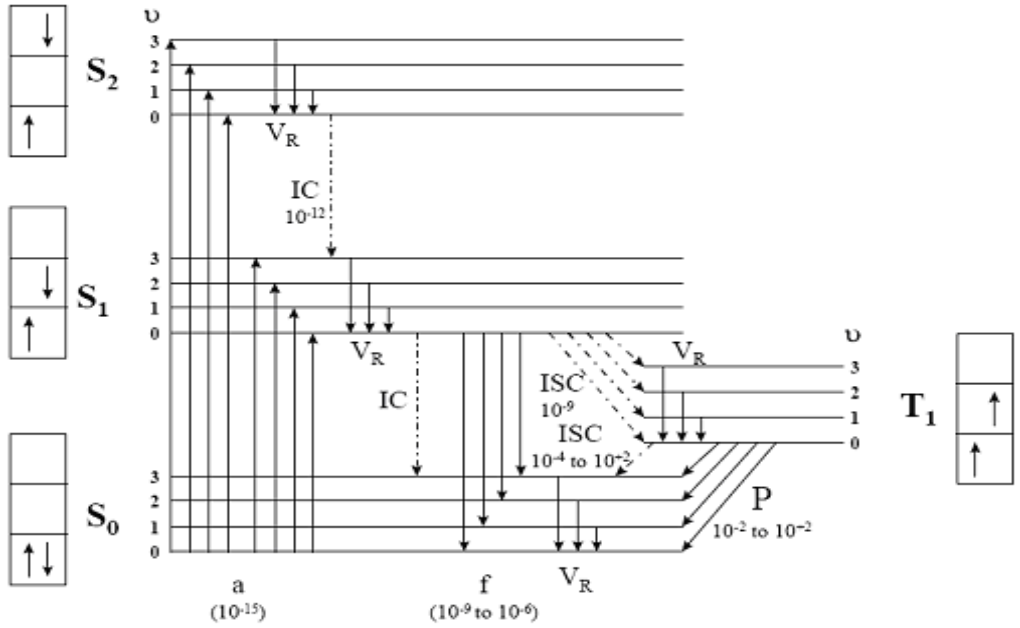

Figure 1.2 Jablonski diagram with the reciprocal rates of transition (taken from Mayr, 1999)

Whether a substance will not do the luminescence, and molecular structure and chemical environment will have an effect, luminescence, while these factors also determines the intensity of emission.

- Dual-bonding, conjugation and aromaticity increases, fluorescence increases.
- -NH_2,-OH groups such as the electron donor fluorescence increases.
- -NO_2-X (F, Cl) -COOH, -CHO, -N = N reduces the fluorescence of groups such as the electron recipient.
- The temperature increases the decrease in fluorescence.
- The molecular mobility increases with decreasing fluorescence. Therefore, the solid phase increases fluorescence, fluorescence of rigid structures is high.
- Solvent molecules in the structure reduce the fluorescence of heavy atoms.
- The fluorescence increases with increasing concentration
- The presence of oxygen dissolved in solution reduces the intensity of fluorescence.

- Internal transition, external transition, the transition between systems increases, fluorescence decreases and the vibrational relaxation (Skoog Holler Nieman p.360-369).

1.1.2.1 Stokes Shift

When a system (be it a molecule or atom) absorbs a photon, it gains energy and enters an excited state. One way for the system to relax is to emit a photon, thus losing its energy (another method would be the loss of heat energy). When the emitted photon has less energy than the absorbed photon, this energy difference is the Stokes shift. (Kitai, 2008)

1.1.2.2 Quantum Yields

The quantum yield of luminescence of a species is the ratio of the number of photons emitted to the number of photons absorbed by the sample. The measured quantum yield of luminescence (fluorescence or phosphorescence) is the measurement made with a fluorescence (phosphorescence) spectrometer when no corrections are made for instrumental response or for sample effects. The corrected quantum yield of luminescence is obtained when the measured quantum yield is corrected for instrumental response, pre- and post-filter effects and refractive index effects. The energy yield of luminescence of a species is defined as the ratio of the energy emitted as luminescence to the energy absorbed by the species.

Quantum yields of fluorescence (phosphorescence) of an analyte are often reduced due to quenching by other species in the analytic solution. (Skoog Holler Nieman, 2003).

1.1 Determination of Heavy Metals

A few decades ago, there was a general feeling that nature could effectively handle hazardous substances. Although, nowadays human beings are more concerned of their sensitive natural environment, pollution is still a problem. Experts estimate

that industrial processes introduce up to a million different pollutants into the atmosphere and the aquatic ecosystem (Förstner & Wittmann, 1981). Heavy metals are one group of these substances, although not all of them are considered harmful to humans **(**Mayr, 2002).

1.2.1 Conventional Methods for the Determination of Heavy Metals

The determination of heavy metals is a challenging subject for analytical chemists regarding concentration ranges set by standards and guidelines for reasons of toxicity. In addition, similar chemistry of these metals is fastidious with respect to selectivity of the determination method.

A variety of analytical methods fulfilling these demands are available. However, only some of them have found application in routine analysis. Recommended procedures for the detection of heavy metals in water samples include photometric methods, flame or graphite furnance atomic absorption spectroscopy (AAS), inductively coupled plasma emission or mass spectrometry (ICP-ES, ICP-MS), total reflection X-Ray fluorimetry (TXRF) and anodic stripping voltammetry (ASV), (Förstner & Wittmann, 1981; Merian, 1991; Fresenius& Quentin, & Schneider, 1988; Klockenkämpfer, 1997). While AAS and photometry are single element methods, ICP-ES, ICP-MS and TXRF are used for multi-element analysis, and voltammetry is an oligo-element approach (Mayr, 2002).

These methods offer good limits of detection and wide linear ranges, but require high cost analytical instruments developed for the use in the laboratories. The necessary collection transportation and pretreatment of a sample is time consuming and a potential source of error (Spichiger & Keller, 1998). However, in the last years smaller and portable and less expensive devices have been brought to the market. On the other hand, the last years have seen a growing development of chemical sensors for a variety of applications. The toxicity of heavy metals makes a continuos supervision of drinking or ground water and lentic or lotic water courses necessary.

Chemical sensors enable on-line and field monitoring and therefore can be an useful alternative tool (Wolfbeis, 1991; Mayr, 2002).

1.2.2 Optical Sensors for the Determination of Heavy Metal Ions

A large number of optical sensors or test strips for heavy metals were developed in the past years and extensively reviewed (Oehme & Wolfbeis, 1997).

The most significant methods are the application of quenchable fluorophores or indicator dyes, which undergo a binding reaction, biosensor assays or the combination of an ionophore with a pH-indicator.

1.3 Ionic Liquids

To date, most chemical reactions have been carried out in molecular solvents. For two millennia, most of our understanding of chemistry has been based upon the behavior of molecules in the solution phase in molecular solvents. Recently, however, a new class of solvent has emerged—ionic liquids. (Earle & Seddon, 2000) Ionic liquids (ILs) are molten salts with the melting point close to or below room temperature.

They are composed of two asymmetrical ions of opposite charges that only loosely fit together (usually bulky organic cations and smaller anions). The good solvating properties, high conductivity, non-volatility, low toxicity, large electrochemical window (i.e. the electrochemical potential range over which the electrolyte is neither reduced nor oxidized on electrodes) and good electrochemical stability, make ILs suitable for many applications. Recently, novel ion selective sensors, gas sensors and biosensors based on ILs have been developed. (Wei & Ivaska, 2002)

Ionic liquids are melts of organic salts existing in the liquid state in a wide temperature range, sometimes below room temperature. As a rule ionic liquids are composed of bulky organic cations and inorganic or organic anions. The unsymmetrical structure and also the spatial separation of the charges impede the

organization of the crystal structure and ensures the ionic (and not molecular) state of the liquid phase. This fact underlies the specific physicochemical properties of ionic liquids: the low melting point and virtually zero pressure of saturated vapor, incombustibility, the ability to dissolve many compounds, high polarity, and also electrochemical stability and conductivity. The possibility to vary the character of the involved ions permits a control of hydrophobicity and other properties of ionic liquids. Therefore ionic liquids are attractive materials for versatile fields of science and technology. (Shvedene, Chernyshov & Pletnev, 2008)

Ionic liquids are termed room-temperature ionic liquids (RTILs) if they are composed of a salt that is liquid at room temperature. ILs almost always contain an organic ion as either the cation or the anion. Typical cations are based on the imidazolium, pyridinium, ammonium, or phosphonium group. Anions are more likely to be inorganic (such as halides, BF_4, PF_6) than are the cations, but organic anions are also common [examples include trifluoromethanesulfonate (triflate) and bis[(trifluoromethyl)sulfonyl]amide (NTF_2)]. The desired anions of a particular IL are often obtained through metathesis reactions. Given the numerous combinations of cations and anions available, ILs have been touted as “designer” compounds. (Hein, Warnke & Armstrong, 2009) The large electrochemical window offers the use of these ionic liquids as unique solvents for electrochemical and spectroscopic investigations. (Suarez, Einloft, Dullius & Dupont, 2006)

The physicochemical properties of RTILs depend on the nature and size of both their cation and anion constituents. (Berthod & Broch, 2006). That properties contributes to increasing importance and can be counted as: they have low vapor pressure, low volatility, they are odorless and inflammable, thermal, chemical and electrochemical stability (Sheldon & ark., 2002; Murugesan & Linhardt, 2005; Ganske & Bornscheuer, 2005).

1.3.1 History

The field of ionic liquids has been reviewed by several authors, including Gabriel, Welton , Holbrey , and Seddon (Earle, 2000)

The first room-temperature ionic liquid Ethanolammonium nitrate (m.p. 52–55 °C) was discovered in 1888 by S. Gabriel and J. Weiner. (Gabriel & Weiner, 1888).

In 1914, Walden (Paul Walden, 1914) reported the synthesis of ethylammonium nitrate, which has a melting point of 13–14◦ C. However, little attention was paid to this report until a synthesis of air- and water-stable ILs based on imidazolium salts was published in 1992 (Wilkes & Zaworotko 1992). These more stable ILs allowed researchers to study and experiment with them in a variety of applications. (Hein, Warnke & Armstrong, 2009)

In the 1970s and 1980s ionic liquids based on alkyl-substituted imidazolium and pyridinium cations, with halide or trihalogenoaluminate anions, were initially developed for use as electrolytes in battery applications (Miller & Osteryoung, 1975).

In 1995, Suarez and coworkers (Jel, Einloft & Dupont, 1995) synthesized 1-n-butyl-3-methylimidazolium (BMIM)BF_4 and (BMIM)PF_6 to serve as a solvent for a two-phase catalysis reaction involving rhodium complexes for the hydrogenation of cyclohexene. Later, (BMIM) BF_4, PF_6, and triflate (trifluoromethanesulfonate) ILs were used in the hydrodimerization of 1,3-butadiene via palladium catalysts in a two-phase system. The Welton group (Boxwell, Dyson & Welton, 2002) that BF_4 was found an even better solvent than dichloromethane for arene hydrogenation using ruthenium catalysts, although other ruthenium catalysts were insoluble in the IL and were rather ineffective (Parker & Welton, 1999). Seddon and coworkers also carried out enzyme-catalyzed reactions in (BMIM)PF_6 in a biphasic system (Cull, Holbrey, & Lye, 2000) and later entirely in an IL (9). By 1999, ILs with organic cations that were not based on imidazolium or pyridinium structures began emerging for specific synthesis tasks (Davis & Forrester, 1999). These studies show how ILs have become

such attractive replacements for traditional organic solvents in these applications. However, because synthesis is not the focus of this review, we do not discuss these applications further. (Hein, Warnke & Armstrong, 2009)

In 1998, the Rogers group (Huddleston, Willauer & Rogers, 1998) began using ILs as solvents for the extraction of simple, substituted benzene derivatives from water. (BMIM)BF_4 and (BMIM)PF_6 displayed partitioning behavior similar to that of the traditional octan-1-ol/water system. Although distribution coefficients were higher in the octan- 1-ol/water system, the IL possessed an adequate extraction power for practical separations. The authors determined that the uncharged forms of ionizable analytes were more efficiently extracted into the IL layer, similar to their behavior with traditional organic solvents. The appeal of using ILs as replacements for organic solvents thus arises from their negligible vapor pressure. (Hein, Warnke & Armstrong, 2009)

Until 2001 the halogen aluminate (III) (in particular [EMIM]$AlCl_4$, which contains the cation 1-ethyl-3-methylimidazolium and the smaller anion tetrachloroaluminate) and the closely related alkylhalogenoaluminate (III) ionic liquids have been by far the most widely studied: nowadays 1,3-dialkyl imidazolium salts are the most popular and investigated classes of room temperature ionic liquids (Dupont, 2004).

1.3.2 Properties

Their unique properties such as nonvolatility, non-flammability, and excellent chemical and thermal stability have made them an environmentally attractive alternative to conventional organic solvents. Ionic liquids have low melting points (<100 °C) and remain as liquids within a broad temperature window (<300 °C). Variations in cations and anions can produce a large number of ionic liquids. Properties of ionic liquids depend on structure of ions. Typical ionic liquid cations (Figure 1.3) include pyridinium, ammonium, sulfonium, phosphine, imidazolium, pyridinium, pyrolidinium, pyrazolium. Comman anions are $[Cl]^-$, $[Br]^-$, $[Al_2Cl_7]^-$, $[Al_3Cl_{10}]^-$, $[Sb_2F_{11}]^-$, $[Fe_2Cl_7]^-$, $[Zn_2Cl_5]^-$, $[Zn_3Cl_7]^-$, $[CaCl_2]^-$, $[SnCl_2]^-$, $[NO_3]^-$,

$[PO_4]^-$, $[HSO_4]^-$, $[SO_4]^{2-}$, $[CF_3SO_3]^-$, $[C_6H_5SO_3]^-$, $[PF_6]^-$, $[SbF_6]^-$, $[BF_4]^-$, $[N(CN)_2]^-$ (Reddy, 2006)

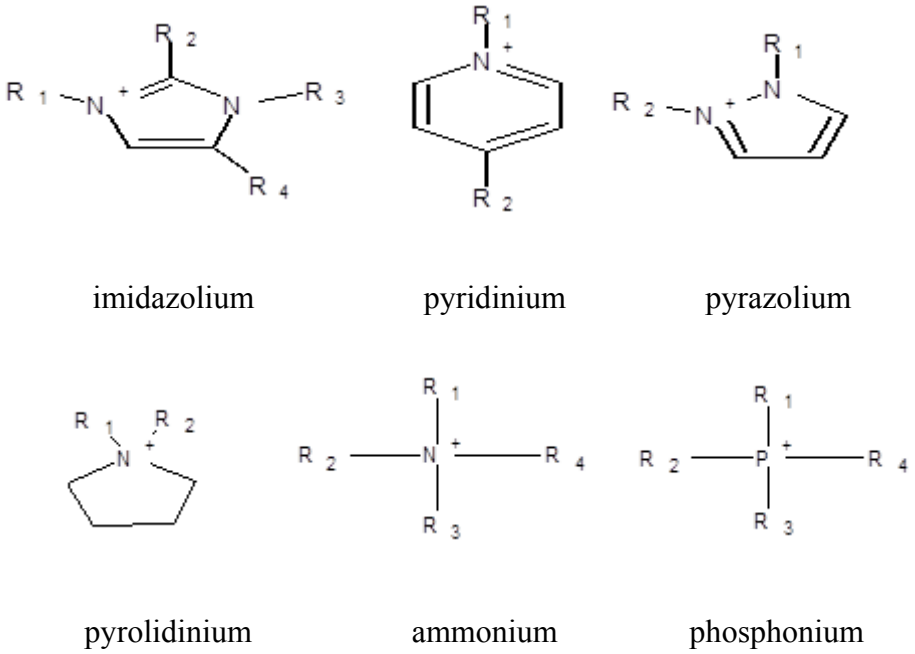

Figure 1.3 Most commonly used cations

Methylimidazolium and pyridine ions proved to be a good starting point for ionic liquids development. Many ionic liquids have been developed for specific synthetic problems. For this reason, ionic liquids have been called as 'designer solvents'. (Wasserscheid, Keim & Angew, 2000)

Ionic liquids have also, low nucleophilicity and capability of providing weekly coordinating or non-coordinating environment, very good solvent properties for a wide variety of organic, inorganic and organometallic compounds: in some cases, the solubility of certain solutes in RTILs can be several orders of magnitude higher than that in traditional solvents. (Yang & Dionysiou,2004)

Despite of their high polarity, most of ionic liquids are hydrophobic and can dissolve up to 1% of water, and the presence of water may affect the physical properties of the ionic liquids (Seddon, Stark & Torres, 2000). However, the solubility of water in ionic liquids varies unpredictably (Rantwijk ,2003). For

example, although 1-butyl-3-methylimidazolium tetrafluoroborate ([BMIM][BF_4]), 1-butyl-3-methylimidazolium hexafluorophosphate ([BMIM][PF_6]), and 1-butyl-3-methyl-imidazolium-bis-(trifluoromethylsulphonyl) imide ([BMIM][TF_2N]) are similar on Reichardt's polarity scale, the former one is completely water-miscible while the latter two are only slightly soluble in water (Park & Kazlauskas, 2003). Ionic liquids have been described as designer solvents (Freemantle,1998), and this means that their properties can be adjusted to suit the requirements of a particular process. Properties such as melting point, viscosity, density, and hydrophobicity can be varied by simple changes to the structure of the ions. For example, the melting points of 1-alkyl-3-methylimidazolium tetrafluoroborates (Holbrey & Seddon,1999) and hexafluorophosphates are a function of the length of the 1-alkyl group, and form liquid crystalline phases for alkyl chain lengths over 12 carbon atoms. Another important property that changes with structure is the miscibility of water in these ionic liquids. For example, 1-alkyl-3-methylimidazolium tetrafluoroborate salts are miscible with water at 25 °C where the alkyl chain length is less than 6, but at or above 6 carbon atoms, they form a separate phase when mixed with water. This behavior can be of substantial benefit when carrying out solvent extractions or product separations, as the relative solubilities of the ionic and extraction phase can be adjusted to make the separation as easy as possible. (Earle & Seddon, 2000)

Ionic liquids are also suitable as the environment for the examination of electrochemical transformation of redox-active compounds. The application of ionic liquids to the electrochemical analysis requires the estimation of their hydrophobicity. Room-temperature ionic liquids are salts with melting points of below *ca.* 100 °C, and sometimes as low as –96 °C, so that they can be used as solvents under conventional organic liquid-phase reaction conditions. They possess a wide liquidus range, in some cases in excess of 400 °C. **(**Seddon, Stark & Torres , 2000)

1.3.3 Application

The recent interest surrounding ILs in regards to Green Chemistry has largely been a result of the fact that they have no measurable vapor pressure, and hence can emit no volatile organic compounds (VOCs). But replacing volatile organic solvents is just part of the story: indeed, ionic liquids are very popular materials and they enjoy a plethora of applications in various domains of physical sciences. (Renner, 2001)

Their application in analytical chemistry, especially in separating analytes, is merited because ILs have some unique properties, such as negligible vapor pressure, good thermal stability, tunable viscosity and miscibility with water and organic solvents, as well as good extractability for various organic compounds and metal ions (Liu , Jhonsson, & Jiang, 2005).

Nowadays ionic liquids find a number of industrial applications which vary greatly in character. A few of their industrial applications are briefly described below; more detailed information can be found in a recent review article (Plechkova & Seddon, 2008).

1.3.4 Advantages of Ionic Liquids

- Stability
    - Temperature
    - Chemical - air, water, one-electron reactivity
    - Volatility
    - Radiation
- Conductivity - connection of electronics to the chemical world
- Control of water content -separation of hydrogen bonding and electrostatics
- Device assembly Wierzbicki & Davis, 2002)

1.3.5 Usage Of Ionic Liquids In The Construction Of Sensors

Ionic liquids are very new matrix materials for sensor design. The high environmental stability, wide potential range and miscibility with organic solvents open new opportunities for use of Room Temperature Ionic Liquids in chemical sensors. It is known, that gases such as ammonia, carbon dioxide, sulfur dioxide, etc have high solubility in RTILs. However, RTILs are not electronic conductors. Therefore, they do not have the ability to transfer chemical information into electrical signal. This drawback can be over-came by mixing them with electronic conductors such as carbon, or conducting polymers. (Josowicz, Jonke & Janata, 2009)

1.2 Micelles

The compounds that make up micelles are also known as *surfactants*. These are compounds that are soluble in both oil and water. They allow compounds that are barely soluble in water to accumulate to higher concentrations within the micellar aggregates. The surfactant properties of these aggregates make them useful as detergents. They can dissolve oily deposits on clothes that will not wash off in water.

There is another type of micelle that is the reverse of the oil-in-water type. It has water-soluble substances dissolved in an organic solution. In this case, however, the polar head groups are in the center of the micelles, while the hydrophobic groups are on the outside, interacting with the organic solvent.

A micelle is an aggregate of surfactant molecules dispersed in a liquid colloid. It is formed when a variety of molecules including soaps and detergents are added to water. The molecule may be a fatty acid, a salt of a fatty acid (soap), phospholipids, or other similar molecules.

The molecule must have a strongly polar "head" and a non-polar hydrocarbon chain "tail". When this type of molecule is added to water, the non-polar tails of the molecules clump into the center of a ball like structure called a micelle, because they

are hydrophobic or "water hating". The polar head of the molecule presents itself for interaction with the water molecules on the outside of the micelle. (Tieleman & Spoel, 2000)

This phase is caused by the insufficient packing issues of single tailed lipids in a bilayer. The difficulty filling all the volume of the interior of a bilayer, while accommodating the area per head group forced on the molecule by the hydration of the lipid head group leads to the formation of the micelle. This type of micelle is known as a normal phase micelle (oil-in-water micelle). Inverse micelles have the head groups at the centre with the tails extending out (water-in-oil micelle). The shape and size of a micelle is a function of the molecular geometry of its surfactant molecules and solution conditions such as surfactant concentration, temperature, pH, and ionic strength.

When surfactants are present above the Critical Micelle Concentration (CMC), they can act as emulsifiers that will allow a compound that is normally insoluble (in the solvent being used) to dissolve. This occurs because the insoluble species can be incorporated into the micelle core, which is itself solubilized in the bulk solvent by virtue of the head groups' favorable interactions with solvent species. (Seddon &Templer, 1995)

Certain molecules may be said to contain two distinct components, differing in their affinity for solutes. The part of the molecule which has an affinity for polar solutes, such as water, is said to be hydrophilic. The part of the molecule which has an affinity for non-polar solutes, such as hydrocarbons, is said to be hydrophobic. Molecules containing both types of components are said to be amphiphilic The proportion of molecules present at the surface or as micelles in the bulk of the liquid depends on the concentration of the amphiphile. At low concentrations surfactants will favor arrangement on the surface. As the surface becomes crowded with surfactant more molecules will arrange into micelles. At some concentration the surface becomes completely loaded with surfactant and any further additions must arrange as micelles. This concentration is called the Critical Micelle Concentration (CMC).

1.4.1 Triton X-100

Triton X-100 ($C_{14}H_{22}O(C_2H_4O)_n$) (Figure 1.4) is a nonionic surfactant which has a hydrophilic polyethylene oxide group (on average it has 9.5 ethylene oxide units) and a hydrocarbon lipophilic or hydrophobic group. The hydrocarbon group is a 4-(1,1,3,3-tetramethylbutyl)-phenyl group. It is related to the pluronic range of detergents marketed. The pluronics are triblock copolymers of ethylene oxide and propylene oxide. The part formed from ethylene oxide is more hydrophilic than the part from propylene oxide. Triton X-100 is very viscous at room temperature and is thus easiest to use after being gently warmed (Kline, 2010).

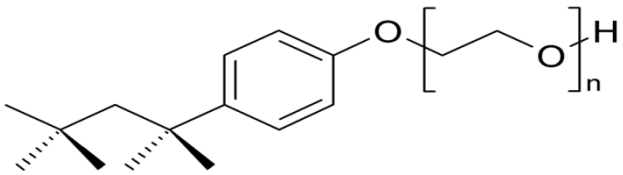

Figure 1.4 Structure of the Triton X-100

Triton X-100 is a commonly used detergent in laboratories. For example: it can be used to permeabilize unfixed (or lightly fixed) eukaryotic cell membranes, it is used in conjunction with zwitterionic detergents such as CHAPS to solubilize membrane proteins in their native state. It can be used in DNA extraction as part of the lysis buffer (usually in a 5% solution in alkaline lysis buffer). It can be used to reduce the surface tension of aqueous solutions during immunostaining (usually in concentration of 0.1-0.5% in TBS or PBS Buffer). Emerging use in dispersion of carbon materials for soft composite materials.

Apart from laboratory use, Triton X-100 can be found in several types of cleaning compound ranging from heavy-duty industrial products to gentle detergents. It is also a popular ingredient in homemade vinyl record cleaning fluids together with distilled water and isopropyl alcohol. Triton X-100 appears as a final ingredient in several yearly influenza vaccines worldwide (Kline, 2010).

1.4.2 Sodium Dodecyl Sulfate

Sodium dodecyl sulfate (SDS) ($C_{12}H_{25}SO_4Na$) (Figure 1.5) is an anionic surfactant used in many cleaning and hygiene products. The salt consists of an anionic organosulfate consisting of a 12-carbon tail attached to a sulfate group, giving the material the amphiphilic properties required of a detergent.

SDS is a highly effective surfactant and is used in any task requiring the removal of oily stains and residues. For example, it is found in higher concentrations with industrial products including engine degreasers, floor cleaners, and car wash soaps. It is used in lower concentrations with toothpastes, shampoos, and shaving foams. It is an important component in bubble bath formulations for its thickening effect and its ability to create a lather.

Research showed that SDS is not carcinogenic when either applied directly to skin or consumed. It has however been shown to irritate the skin of the face with prolonged and constant exposure (more than an hour) in young adults. A clinical study found SDS toothpaste caused a higher frequency of aphthous ulcers than both cocoamidopropyl betaine or a detergent-free paste, on 30 patients with frequent occurrences of such ulcers. A clinical study comparing toothpastes with and without SDS found that it had no significant effect on ulcer patterns (Herlofson & Barkvoll, 1996).

Sodium dodecyl sulfate polyacrylamide gel electrophoresis, is a technique widely used in biochemistry, forensics, genetics and molecular biology to separate proteins according to their electrophoretic mobility (a function of length of polypeptide chain or molecular weight). SDS gel electrophoresis of samples that have identical charge per unit mass due to binding of SDS results in fractionation by size (Marrakchi & Maibach 2006).

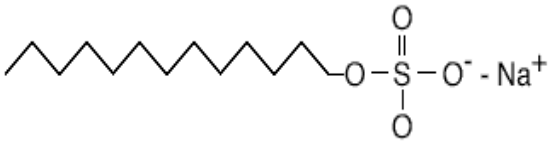

Figure 1.5 Structure of the Sodium Dodecyl Sulfate

1.5 Eosin Y

Eosin Y (Figure 1.6) is a red fluorescent dye in the form of triclinic crystals soluble in spirit, sodium or potassium salts are soluble in water, ethyl ester is alcohol soluble. All Eosins are bromine derivatives of fluorescein, used in dying textiles, in manufacturing, in coloring cosmetics, in coloring gasoline and as a toner. The sodium or potassium salt of Eosin, red to rose-colored crystalline powder, is used in biology to stain cells. Eosin is strongly absorbed by red blood cells, coloring them bright red. Eosin is an acidic dye and shows up in the basic parts of the cell, i.e. the cytoplasm

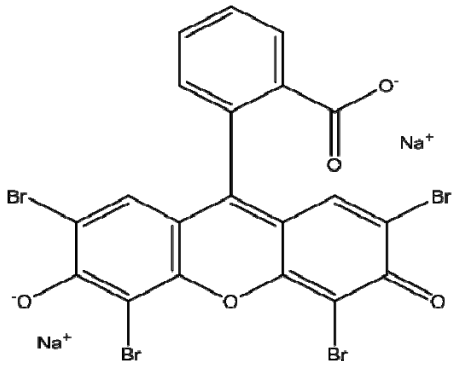

Figure 1.9 Structure of the Eosin Y

The red sodium or potassium salt of this powder, used in biology to stain cells. A red fluorescent dye resulting from the action of bromine on fluorescein. Any of a number of similar red acidic dyes, derivatives of fluorescein, especially Eosin Y (yellowish), 2′,4′,5′,7′-tetrabromofluorescein disodium salt, it is widely used as stains in histology and hematology(Bruce & Gregorios, 1974).

CHAPTER TWO
EXPERIMENTAL METHOD AND INSTRUMENTATION

2.1 Instrumentation

Absorption spectra were recorded using a Shimadzu 1601 UV-Visible spectrophotometer. Steady state fluorescence emission and excitation spectra were measured using Varian Cary Eclipse Spectrofluorometer with a xenon flash lamp as the light source. pH measurements were recorded with a orion pH meter.

All solvents used in this thesis were of analytical grade . Solvents for the spectroscopic studies were used without further purification. The fluorescent dye, 2′,4′,5′,7′-tetrabromofluorescein disodium salt (Eosin Y) was supplied from Aldrich (99.5% purity). The commercial ionic liquid, the 1-Butyl-3- methylimidazolium tetrafluoroborate ([BMIM]BF_4)(IL-I), 1-ethyl-3-methylimidazolium tetrafluoroborate ([EMIM]BF_4)(IL-II), 1-Butyl-3- methylimidazolium thiocyanate ([BMIM][SCN])(IL-III) , ionic liquids and sodium dedecyl sulfate (SDS) and Triton X-100 micelles (TX-100) was supplied from Fluka. All ionic liquids and micelles are soluble in water and in EtOH. The structures of the ionic liquids and the dye were given in Figure 2.1. The buffer solutions in the range of pH 3.0-6.0 were prepared by the same way by adjusting to the desired pH with 0.01 M acetic acid/acetate buffer solutions. The buffer solutions in the range of pH 7.0-9.0 and 10.0-12.0 were prepared by the same way by adjusting to the desired pH with 0.01 M NaH_2PO_4 / Na_2HPO_4 buffer. pH=5.0 was chosen as optimum pH throughout the experiments.

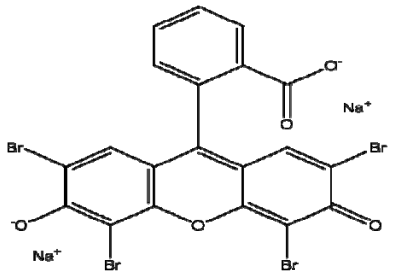

Eosin Y

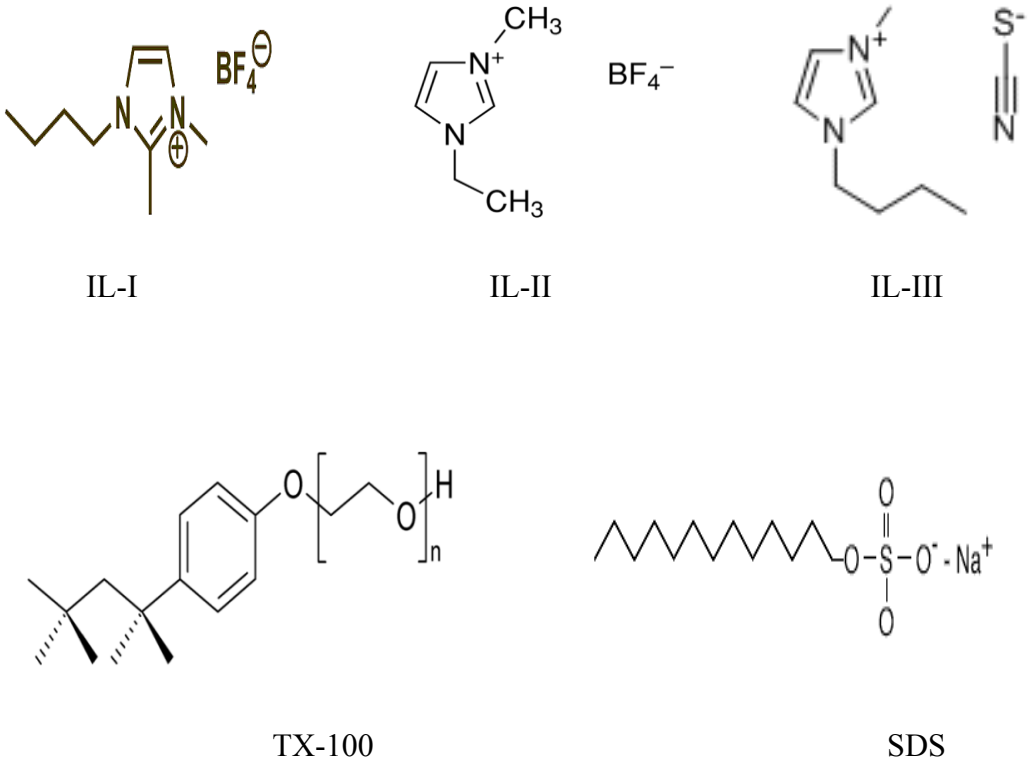

Figure 2.1 Structure of the Eosin Y dye , the ionic liquids and the micelles.

2.1.1 Quantum Yield Calculations

Fluorescence quantum yield values (θ) of the employed dyes were calculated by using the comparative William's method (Williams, Winfield & Miller, 1983). This is a reliable method for recording θ and involves the use of well characterised standard samples with known θ values. Essentially, solutions of the standard and test samples with identical absorbance at the same excitation wavelength can be assumed to be absorbing the same number of photons. Hence, a simple ratio of the integrated fluorescence intensities of the two solutions (recorded under identical conditions) will yield the ratio of the quantum yield values. Since θ for the standard sample is known, it is trivial to calculate the θ for the test sample.

According to this method, the standard samples should be chosen to ensure they absorb at the excitation wavelength of choice for the test sample, and, if possible, emit in a similar region to the test sample. In order to minimise re-absorption effects

(Dhami et al., 1995) absorbances in the 10 mm fluorescence cuvette should never exceed 0.1 at and above the excitation wavelength. Above this level, non-linear effects may be observed due to inner filter effects, and the resulting quantum yield values may be perturbed. This maximum allowable value of the recorded absorbance must be adjusted depending upon the path length of the absorption cuvette being used (for example, 10 mm = 0.1 maximum, 20 mm = 0.2 maximum etc). In this study, standard 10 mm path length fluorescence and absorption cuvettes were used for running the fluorescence and absorbance measurements. The UV-vis absorption (absorbance≤0.10 at the excitation wavelength) and corrected fluorescence emission spectra were recorded for three or more solutions with increasing concentrations of the sample and the standard. The integrated fluorescence intensities (that is, the area of the fluorescence spectrum) were calculated from the fully corrected fluorescence spectrum. Graphs of integrated fluorescence intensity *vs* absorbance were plotted. The gradient of the plots were later used in the quantum yield calculations according to the following equation.

$$\theta_x = \theta_{std}\left(\frac{Grad_x}{Grad_{std}}\right)\left(\frac{n_x^2}{n_{std}^2}\right) \qquad (2.1)$$

Where the subscripts *std* and *x* denote standard and test respectively, θ is the fluorescence quantum yield, *Grad* is the gradient from the plot of integrated fluorescence intensity *vs* absorbance and *n* is the refractive index of the solvent.

2.1.2 Preparation of Buffer Solutions

The pH of the solutions were monitored by use of a digital pH-meter (ORION) calibrated with standard buffers of pH 10.00, 7.00 and 4.00 at 25±1 °C.

In all of the studies ultra pure water of Millipore was used. Deionised water, generated by a Milli-Q deionised water unit, which had a resistance better than 18.2 M cm, was used for the preparation of all the solutions.

Preparation of 0.01 M acetic acid/acetate buffer; 0.572 mL of acetic acid (d=1.05 and 17.48 Molar) were dissolved in 950 mL ultra pure water. The solution was titrated to pH 5 at the lab. temperature of 20 ^{o}C either with 0.1 M HNO_3 or 0.1 M NaOH as needed. The resulting solution was made up to 1000 ml with ultra pure water in a volumetric flask. The buffer solutions in the range of pH 4.0-6.0 were prepared by the same way by adjusting to the desired pH.

Preparation of 0.01 M NaH_2PO_4 / Na_2HPO_4 buffer; 1.56 g of $NaH_2PO_4.2H_2O$ (ma=156.01) and 3.58 g of $Na_2HPO_4.12H_2O$ (ma=358.14) were dissolved in 950 mL ultra pure water. The solution was titrated to pH 7.0 at the lab temperature of 20 ^{o}C either with 0.1 M HNO_3 or 0.1 M NaOH as needed. The resulting solution was made up to 1000 ml with ultra pure water in a volumetric flask. The buffer solutions in the range of pH 7.0-9.0 and 10-12 were prepared by the same way by adjusting to the desired pH.

CHAPTER THREE
DETERMINATION OF MANGANESE WITH EOSIN Y IN IONIC LIQUID OR MICELLE CONTAINING AQUEOUS MEDIA

3.1 Introduction

Manganese plays an significant role in human body as a component of enzymes, such as super oxide dismutase, glutamine syntheses and arginase (Gerber, Leonard & Hantson ,2002). It is also an essential microelement for haemopoietic function and transmission of genetic information (Raya & Perez, 1983). Manganese is important in photosynthetic oxygen evolution in chloroplasts in plants (Seleim, Abu-Bakr& El-Zohry, 2009). Thus, most broad-spectrum plant fertilizers contain manganese (Moreno, Silva & Valcarcel, 1983). Manganese is widely emitted to the atmosphere via metallurgic and chemical industry. It also exists naturally in rivers, lakes, and ground waters. High levels of manganese may cause Parkinsonian disturbances (Zatta, Rensburg & Taylor, 2003) . Because that the prolonged exposure to even low levels of manganese can cause diseases and because of the significant role of manganese in human body, sensitive and selective methods for determination of manganese (II) is of great importance. Mn (II) is the predominant manganese species in neytral acidic waters (Stumm & Morgan ,1996) . Table 3.1 shows the pH dependent distribution of manganese taken from Minteq software.

Table 3.1 pH dependent distribution of manganese

Component	Total dissolved	% dissolved
H^{+1}	4.6822×10^{-6}	100.000
Mn^{+2}	1.0000	100.000

There are several analytical techniques for manganese determination such as flame atomic absorption spectrometry (Santelli, Bezerra, & SantAna, 2005),

electrothermal atomic absorption spectrometry (Almeida, Maria, Morgana,& Silva, 2007), inductively coupled plasma spectrometry (Ren & Salin, 1994), neutron activation analysis (Nguyen, 1994), X-Ray fluorescence(Ruiz, Rodriguez & Olsina, 2002), voltammetry (Ghoneim, 2010) and molecular absorption spectrophotometry(Zolotov & Ryukarev, 1995). Among these spectrophotometric methods are widely used because of their relatively simplicity and low cost. However, existing methods are still complicated and require long oxidation and heating steps, contains hazardous solvents and are lack of sensitivity ranging in higher concentrations than ppb levels. The peroxydisulfate and periodate methods are commonly used spectrophotometric methods ("Handbook of Analytical Chemistry", Meites, 1963), but the reducing chloride ion forms interfering complexes with the samples (Purdy & Hume, 1955). The colorimetric determination of permanganate with 4,4'-tetramethyldiaminotriphenylmethane, is a sensitive method however the forming complex is only stable for five minutes in a darkened laboratory conditions. Some methods such as zincon, dithizone and Arsenazo III methods have the disadvantages of time requiring extraction procedures (Ahrland & Herman, 1975). One of the most applied method for determination of manganese; the "permanganate method" has the necessity to remove chloride and needs oxidation procedure . Several more sensitive methods based on the formation of complexes with organic reagents have been also proposed such as formaldoxime method (Okac &. Barlusek, 1960). Many kinetic methods have been also reported for the determination of manganese (II), based on its catalytic behavior on the oxidation of organic compounds most frequently with hydrogen peroxide and the periodate ion. However, most of these methods lack of sufficient sensitivity for determining manganese (II) at or below ppm levels. Therefore, there is a need to develop new analytical procedures for manganese determination which do not have these disadvantages (Seleim, Hashem & El-Zohry, 2009).

In this study, Eosin Y was tested for the first time for determination of manganese (II) ions in presence of different ILs and micelles in aqueous solutions by spectrofluorimetric method. In some studies, it is reported that the addition of cationic and anionic surfactants into the sensing media increase the sensitivity and

the selectivity of the proposedmethod. In most of the sol-gel based sensor designs, the non-ionic surfactant Triton X-100, in which electrostatic interactions are absent, has been intensively used. When the charged surfactants (e.g. sodium dodecyl sulphate (SDS) and cetyltrimethyl ammonium bromide (CTAB)) were used, increased relative signal changes were reported [Garcia, Fernandez, & Garcia, 2005). There are also some studies indicating that the IL type salts may constitute a new class of surfactants with special properties causing some considerable shifts in the spectra (Aydogdu & Oter, 2010 ; Merrigan & Davis, 2000). The effect of the surfactant type, IL type, IL concentration, pH and the interfering ions were also evaluated and a new method with a detection limit of nanogram per liter concentrations is proposed.

3.2 Experimental

The stock dye (Eosin Y) solution was prepared as 10^{-3} M in EtOH. The dye concentration in the cuvette was optimized and 10^{-5} M. The ionic liquid concentration in the optimized solution was 1.0-40 % by volume. The stock solution of Mn^{2+} and the other metals were 1000 mgL^{-} AAS standard solutions and were diluted to desired concentrations with Milipore ultrapure water. 0.01 M acetic acid/acetate buffer solution of pH=5.0 was used throughout the experiments as the optimum pH.

The determination of Mn (II) with Eosin Y indicator in aqueous solutions were performed in the different additives of [BMIM][BF_4], [EMIM][BF4], [BMIM][SCN], SDS and TX-100 in pH 5.0 buffer:EtOH mixture (60:40).

The solutions were freshly prepared prior to experiments to contain 10^{-5} M Eosin Y and 40 % ethanol, 60 % buffer solution at pH 5.0, by volume. Solution 1; contains 2.5 ml buffer:EtOH mixture (60:40 v:v) and 10^{-5} M Eosin Y in EtOH. Solution 2; contains 2.5ml buffer:EtOH mixture (60:40 v:v), 10^{-5} M Eosin Y in EtOH and 1 % IL-I. Solution 3; contains 2.5 ml buffer:EtOH mixture (60:40 v:v), 10^{-5} M Eosin Y in EtOH and 1 % IL-II. Solution 4; contains 2.5 ml buffer:EtOH mixture (60:40 v:v), 10^{-5} M Eosin Y in EtOH and 1 % IL-III. Solution 5; contains buffer:EtOH mixture

(60:40 v:v), 10^{-5} M Eosin Y in EtOH and 10^{-2} M SDS (Critical micelle concentration of SDS 10^{-3}M). Solution 6; buffer:EtOH mixture (60:40 v:v), 10^{-5} M Eosin Y in EtOH and 0.2×10^{-2} M TX-100 (Critical micelle concentration of TX-100 2.0×10^{-4}M). Table 3.1 shows the composite of solutions.

Table 3.1 Compositions of the solutions

Solution	Dye	Media	Additive
S-1	10^{-5} M Eosin Y	2.5 ml pH 5.0 buffer:EtOH mixture (60:40 v:v)	-
S-2	10^{-5} M Eosin Y	2.5 ml pH 5.0 buffer:EtOH mixture (60:40 v:v)	IL-I (1% by volume)
S-3	10^{-5} M Eosin Y	2.5 ml pH 5.0 buffer:EtOH mixture (60:40 v:v)	IL-II (1% by volume)
S-4	10^{-5} M Eosin Y	2.5 ml pH 5.0 buffer:EtOH mixture (60:40 v:v)	IL-III (1% by volume)
S-5	10^{-5} M Eosin Y	2.5 ml pH 5.0 buffer:EtOH mixture (60:40 v:v)	SDS (10^{-2} M)
S-6	10^{-5} M Eosin Y	2.5 ml pH 5.0 buffer:EtOH mixture (60:40 v:v)	TX-100 (0.2×10^{-2} M)
S-7	10^{-5} M Eosin Y	2.5 ml pH 5.0 buffer:IL-I mixture (60:40 v:v)	IL-I
S-8	10^{-5} M Eosin Y	2.5 ml pH 5.0 buffer :IL-II mixture (60:40 v:v)	IL-II
S-9	10^{-5} M Eosin Y	2.5 ml pH 5.0 buffer:IL-III mixture (60:40 v:v)	IL-III

3.3 Results and discussion

3.3.1 Spectral Characterization of the Eosin Y Dye

Spectral characterization of Eosin Y was performed in the cocktail solutions of S1-S6. Eosin Y concentrations of the solutions were 10^{-5} mol. Figure 3.1 and Table 3.2 show the emission spectra of Eosin Y in the concerned coctails. The spectra of the complex in all media exhibited broad emission bands ranging from 510 to 660 nm. The emission maximum of the dye was between the range of 545-554 nm. The ionic liquid concentrations in S-2, S-3, S-4, S-7, S-8, S-9 were 5.3×10^{-5} M, 6.46×10^{-5} M, 5.42×10^{-5} M, 2.14×10^{-3} M, 2.61×10^{-3} M, 2.16×10^{-3} M, respectively. This concentrations of ionic liquid didn't affect the maximum emission wavelength and the fluorescence intensity. The dye only exhibited a red shift of 3 nm in presence of 10^{-2} M SDS. TX-100 (0.2×10^{-2} M) caused moderately longer red shift of 9 nm and a slight decrease in fluorescence intensity. Safavi et al. investigated the interactions of an imidazolium based IL with two sulfonated anionic dyes, azocarmine G and methyl orange and showed their resemblance to surfactant interactions (Safavi A, 2008) They told that at surfactant concentrations at critical micelle concentration (CMC) values and above, the solubilizing effect of the micelles begins to be important and probably, the ion-association complexes are incorporated into the micelles, and some new changes in spectral responses have been reported b(Garcia & Sanz-Medel, 1986). A probable quenching of the Eosin-Y with the IL was expected because of the competing complex formation of IL both with the dye and can interfere with the quenching response of Eosin Y with metals. In our previous study we have observed the interference of the ionic liquid with the morin dye and with the morin aluminum complex and after this concentration (1.76×10−3 mol/L), due to the formation of the dye–IL complexes, the fluorescence intensity of morin–aluminum complex was decreased (Oter, 2010). In this study, we didnt observe a significant decrease in fluorescence intensity till 40 % ionic liquid concentration (IL-I 2.14×10^{-3} M, IL-II 2.61×10^{-3} M, IL-III 2.16×10^{-3} M). The decrease in fluorescence intensity was maximum for IL-II and was 15 %. Longer spectral shifts or a quenching of

fluorescence intencity is not wanted so higher concentrations of ionic liquid and the surfactants were not applied.

Table 3.2 Emission spectra related data of Eosin Y in the solvents of buffer:EtOH mixture with the different additives. (Eosin Y 10^{-5} M)

solution	λ_{max}^{em} (nm)	F.I.
S-1	548	906
S-2	545	992
S-3	546	812
S-4	545	997
S-5	545	980
S-6	554	992
S-7	548	960
S-8	548	812
S-9	545	863

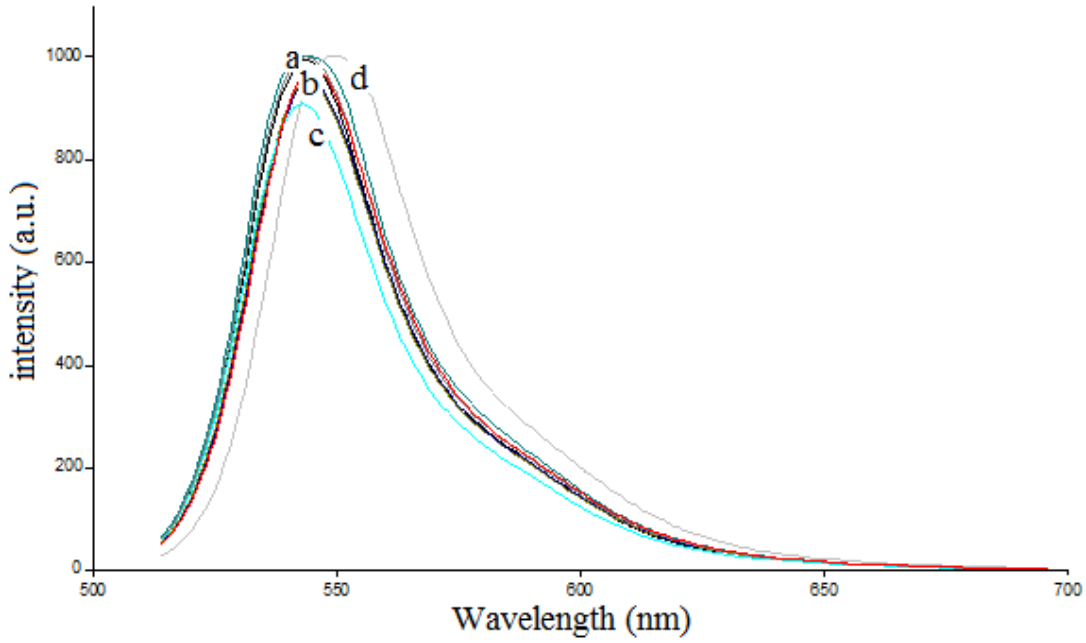

Figure 3.1 Emission spectra of Eosin Y dye in pH 5.0 buffer:EtOH mixture (60:40 v:v) in presence of different additives a) emission of S-2, S-4, S-5, S-9 λ_{max}^{em}=545nm b) emission of S-1, S-7, S-3 λ_{max}^{em}=548 nm c) emission of S-8 λ_{max}^{em}=546nm d) emission of S-6 λ_{max}^{em}=554nm

3.3.2 Response of Eosin Y to Different Cations and Anions in Absence of Additives

Response of Eosin Y to metal ions was investigated by exposure to 1.0 mg L^{-1} solutions of Ca^{2+},Cu^{2+}, Hg^{+}, Hg^{2+}, As^{5+}, Mo^{2+}, Li^{+}, $Pb^{2+,}$ Al^{3+}, Cr^{3+},Na^{+}, $Mg^{2+,}$ Zn^{2+}, Cd^{2+}, Fe^{3+},Co^{2+} and Ni^{2+}. Response of Eosin Y to the anions was also investigated by exposure to the anions of SO_4^{2-}, I^{-}, Cl^{-}, NO_2^{-}, Br^{-}, NO_3^{-}, PO_4^{2-} and anion standard solution of Dionex. Anion standard contains 151 mgL^{-} SO_4^{2-}, 20.2 mgL^{-} Fl^{-}, 30.2 mgL^{-} Cl^{-}, 100 mgL^{-} NO_2^{-}, 100 mgL^{-} Br^{-}, 102 mgL^{-} NO_3^{-}, 151 mgL^{-} PO_4^{2}. Figure 3.2, 3.3 and 3.4 reveal emission-based response of Eosin Y to the concerned metal cations and anions in acetic acid/acetate buffered/EtOH mixture at pH 5.0. Results were plotted as relative signal changes, $((I_0-I)/I_0)$, where I is the fluorescence intensity of the sensor membrane after exposure to ion-containing solutions and I_0 is the fluorescence intensity of the sensor slide in ion-free buffer solution. Table 3.3 and 3.4 show the spectra related data of response of Eosin Y to the metal cations. Figure 3.5, 3.6, 3.7, 3.8, 3.9 show the emission based response of Eosin Y to the metal ions in presence of employed additives (IL-I, IL-II, IL-III, SDS and TX-100).

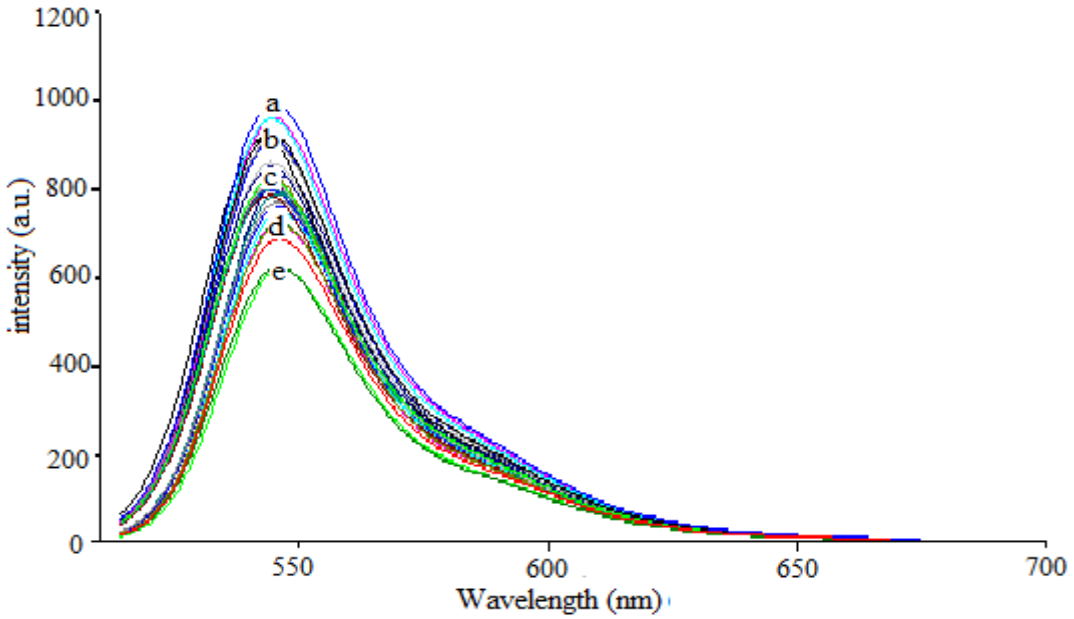

Figure 3.2 Emission based 1.0 mgL^{-1} metal response of Eosin Y in in acetic acid/acetate buffered/EtOH mixture at pH 5.0. a) Mo^{2+}, Na^{+}, Li^{+} b) No metal, Ca^{2+}, Co^{2+}, Cu^{2+}, Hg^{+} c)Hg^{2+}, As^{5+}, Ni^{2+}, Cr^{2+}, Al^{3+} d) Cd^{2+}, Pb^{2+}, Mg^{2+}, Fe^{2+}, Fe^{3+}, Zn^{2+} e) Mn^{2+}

Table 3.3 Emission spectra related data of response of Eosin Y to the metal cations

Metal Cations	$\lambda_{\max}^{em}$	Fluorescence Intensity (a.u.)
-	545	802
Al^{3+}	545	762
Cd^{2+}	544	690
Ca^{2+}	545	813
Pb^{2+}	543	725
Co^{2+}	546	825
Cu^{2+}	545	827
Cr^{2+}	544	788
Na^{+}	543	862
Mn^{2+}	545	598
Mg^{2+}	544	720
Ni^{2+}	544	786
As^{2+}	543	774
Mo^{2+}	546	916
Li^{+}	546	836
Hg^{+}	546	812
Hg^{2+}	545	786
Fe^{2+}	544	672
Fe^{3+}	544	722
Zn^{2+}	545	690

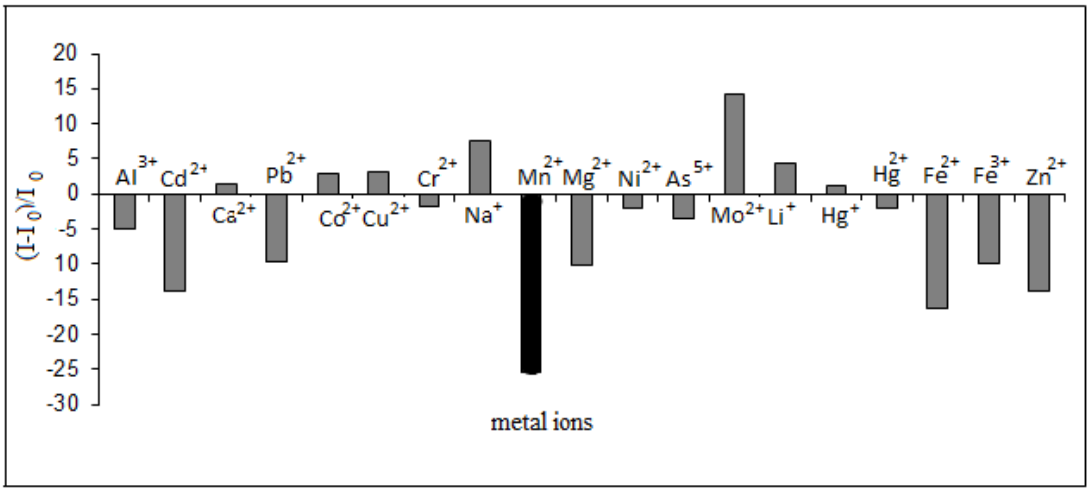

Figure 3.3 Metal-ion response test results for Eosin Y in S-1 buffered solution.

Table 3.4 Emission spectra related data of response of Eosin Y to the anions

Anions	λ_{max}^{em}	Fluorescence Intensity (a.u.)
-	545	802
Cl^-	544	803
NO_2^-	546	817
SO_4^{2-}	545	823
Br^-	544	910
I^-	544	890
PO_4^{3-}	543	875
NO_3^-	545	902

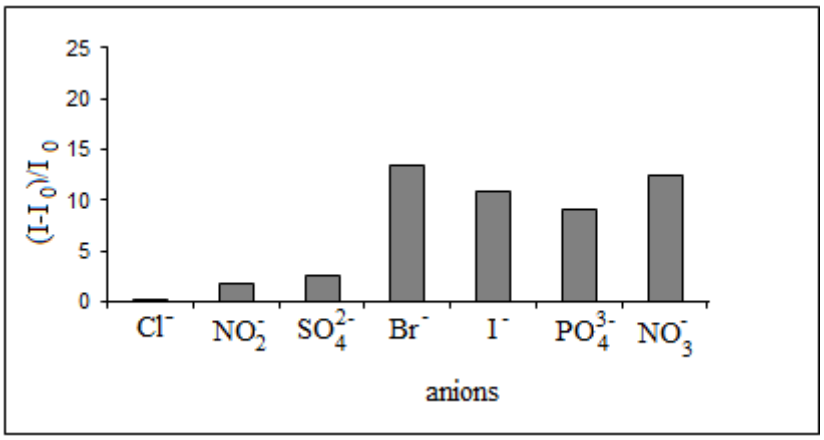

Figure 3.4 Anion response test results for Eosin Y in S-1 solution.

3.3.3 Response of Eosin Y to Metal Cations With Different Additives

Five different solutions (S-2, S-3, S-4, S-5, S-6) were prepared for the 1.0 mgL^- metal solutions response of Eosin Y with different additives (IL-I, IL-II, IL-III, SDS, TX-100, respectively, Table 3.1) Figure 3.5, 3.6, 3.7, 3.8 and 3.9 reveal emission-based response of Eosin Y to the metal cations in acetic acid/acetate buffered/EtOH mixture at pH 5.0 with different additives. In the additive containing solutions we have observed no response for the metal ions of Ca^{2+},Cu^{2+}, Hg^+, Hg^{2+}, As^{5+}, Li^+, Al^{3+}, Cr^{3+}, Co^{2+} and Ni^{2+} ions (See table 3.5). Thus, the presence of both the ionic liquids and the surfactants increased the selectivity of the dye. Besides, they have decreased the % response of the other metal ions except Mn^{2+}.

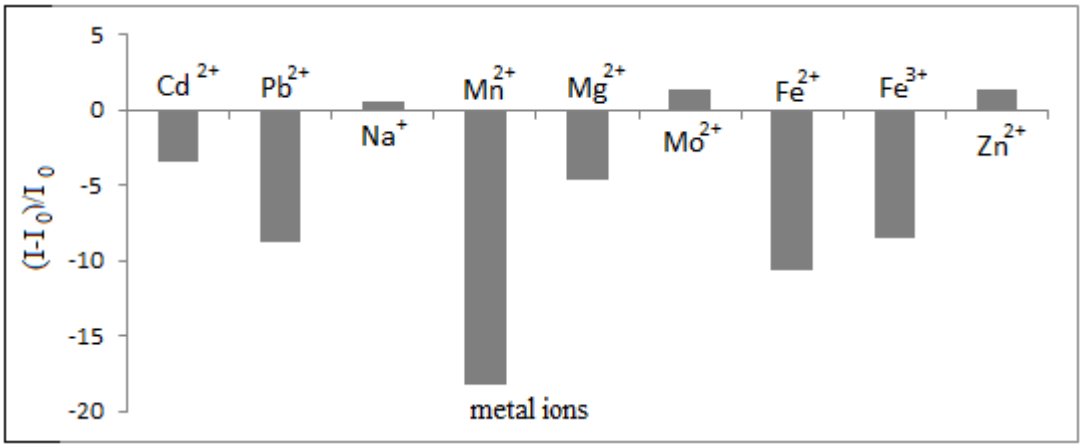

Figure 3.5 Metal-ion response test results for Eosin Y in S-2 (with IL-I) solution.

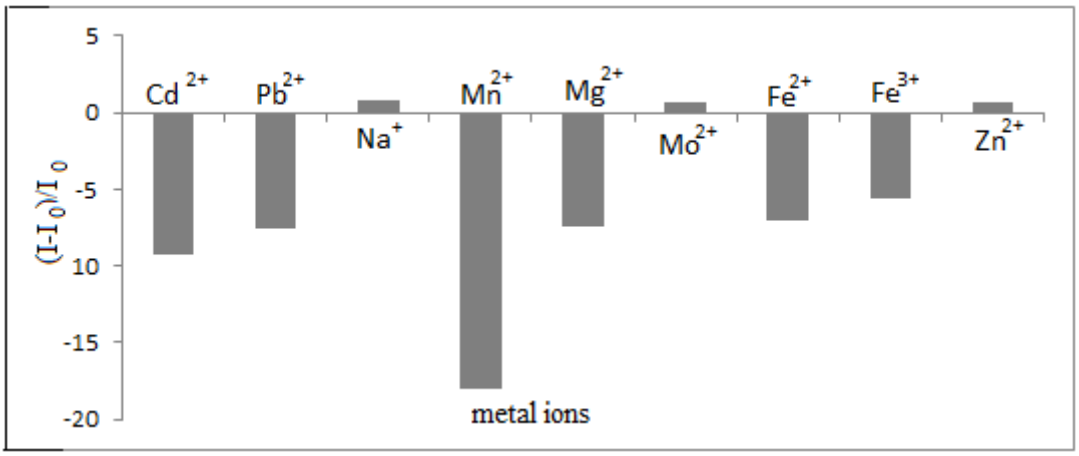

Figure 3.6 Metal-ion response test results for Eosin Y in S-3 (with IL-II) solution.

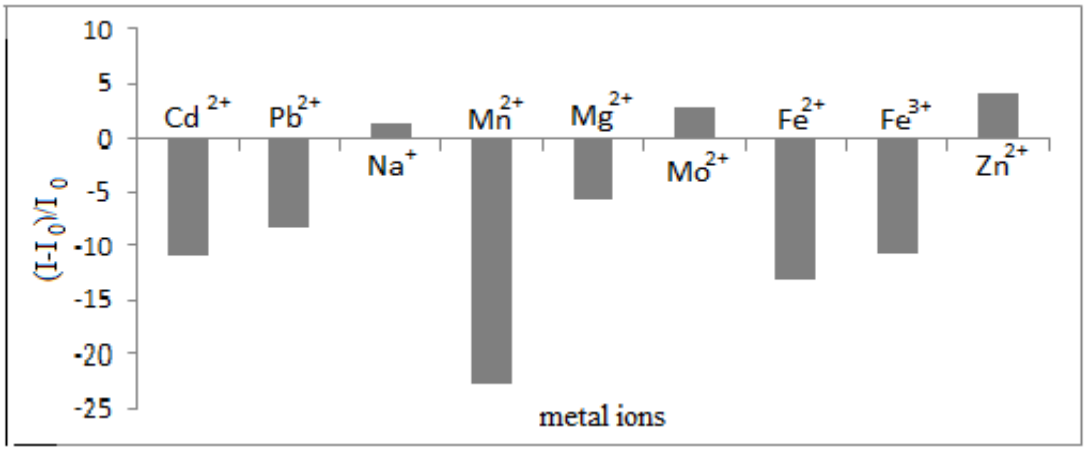

Figure 3.7 Metal-ion and anion response test results for Eosin Y in S-4 (with IL-III) solution.

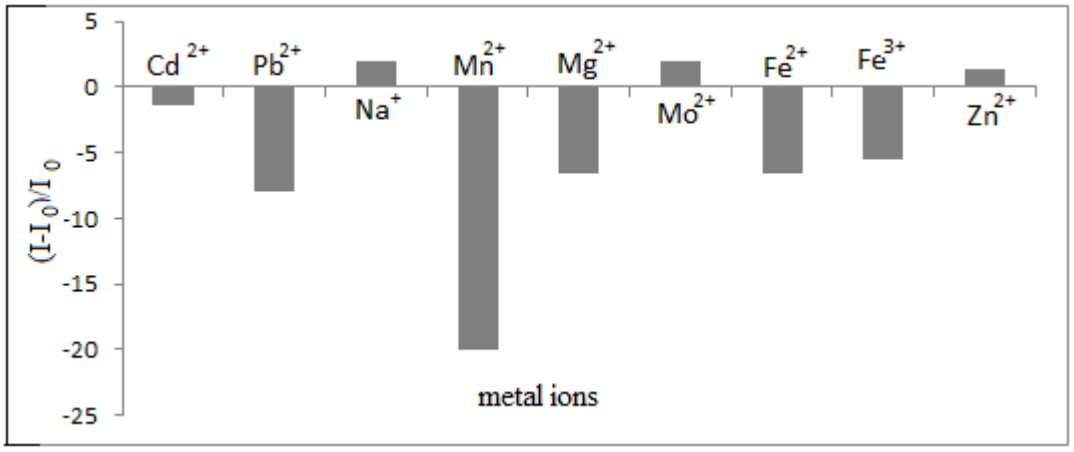

Figure 3.8 Metal-ion and anion response test results for Eosin Y in S-5 (with SDS) solution.

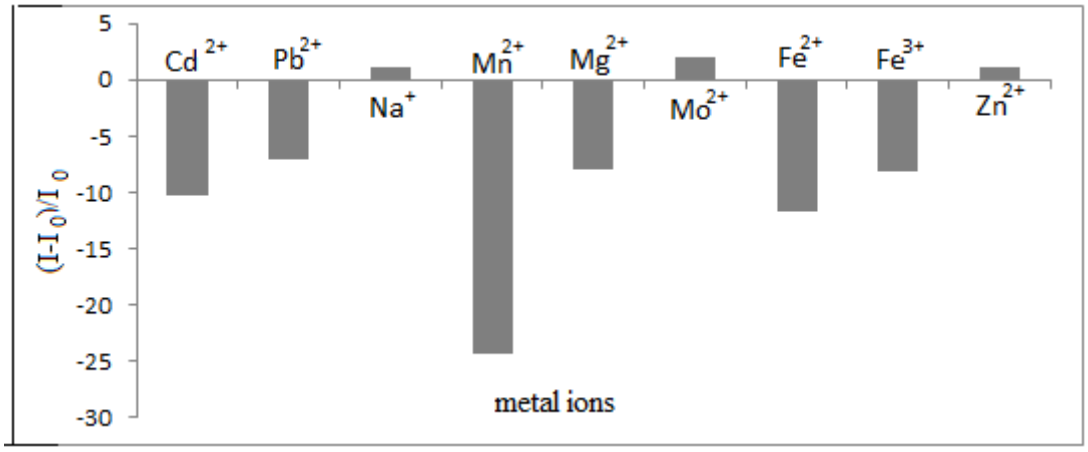

Figure 3.9 Metal-ion and anion response test results for Eosin Y in S-6 (with TX-100) solution.

Table 3.5 % change in fluorescence intensity after exposure to 1.0 mg L^- of metal solutions

	S-1	S-2	S-3	S-4	S-5	S-6
Cd^{2+}	-14	-10	-3	-9	-1	-8
Pb^{2+}	-10	-8	-6	-8	-6	-7
Na^{+}	7	1	1	1	2	1
Mn^{2+}	-25	-23	-18	-18	-20	-24
Mg^{2+}	-10	-6	-5	-7	-7	-8
Mo^{2+}	14	3	1	1	2	2
Fe^{2+}	-16	-13	-11	-7	-7	-10
Fe^{3+}	-10	-11	-9	-5	-6	-8
Zn^{2+}	-14	4	1	1	1	1
anion std	23	1	0	1	3	4

3.3.4 Emission of Eosin Y at Different pH in Absence of Metal Ions

The effect of pH to the excitation and emission spectra of Eosin Y was investigated in the metal free buffered solution of S-1. Solutions were prepared with 0.01 M pH buffer and EtOH mixture (60:40 v:v). The emission based relative signal changes of Eosin Y were shown in figure 3.10 and table 3.6 in the pH range of 3.0-9.0. Eosin Y exhibited a decrease in signal intensity upon exposure to proton in the pH range of 3.0-9.0. The pKa value of the dye in the employed solution matrix was found according to the following equation:

$$pKa = pH+\log [(I_x-I_b)/(I_a-I_x)] \qquad (3.1)$$

Where I_a and I_b are the absorbance intensities of acidic and basic forms and Ix is the intensity at a pH near to the midpoint. The calculated pKa value is 4.79.

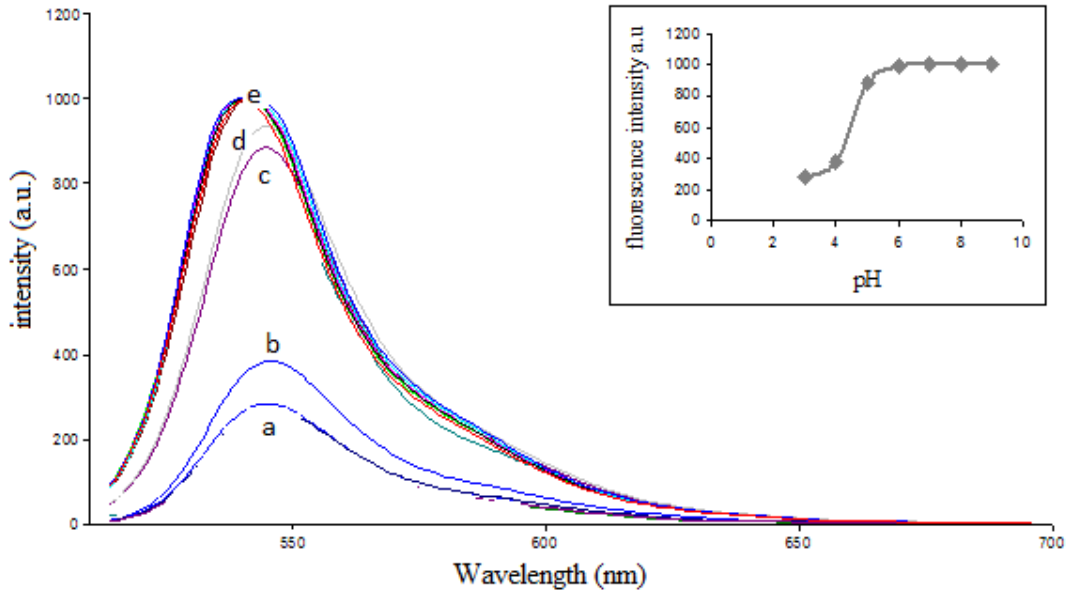

Figure 3.10 pH induced emission spectra of the 10^{-5} M Eosin Y after exposure to buffer solutions of (a) pH=3 (b) pH=4 (c) pH=5 (d) pH= 6 (e) pH= 7.0, 8.0, 9.0.

Table 3.6 pH based response of Eosin Y in S-1 solution in absence of metal ions

pH	λ_{max}^{em} (nm)	Fluorescence Intensity (a.u.)
3.0	546	283
4.0	545	383
5.0	545	886
6.0	540	990
7.0	535	1000
8.0	533	1000
9.0	533	1000

3.3.4.1 Response of Eosin Y at Different pH in the Presence of Mn^{2+}

The pH dependency of interaction of the dye with Mn^{2+} was also investigated at fixed Mn^{2+}concentration ($[Mn^{2+}] = 10^{-3}$ M) in the pH range of 3.0–9.0. The quenching of the dye with the metal ion was most effective at pH 5.0 and this value was chosen as the appropriate working pH for further studies (Figure 3.11, Table 3.7). This result is matching with the literature as the dye responses best to the metal ion near its pKa value (Werner & Wolfbeis, 1993).

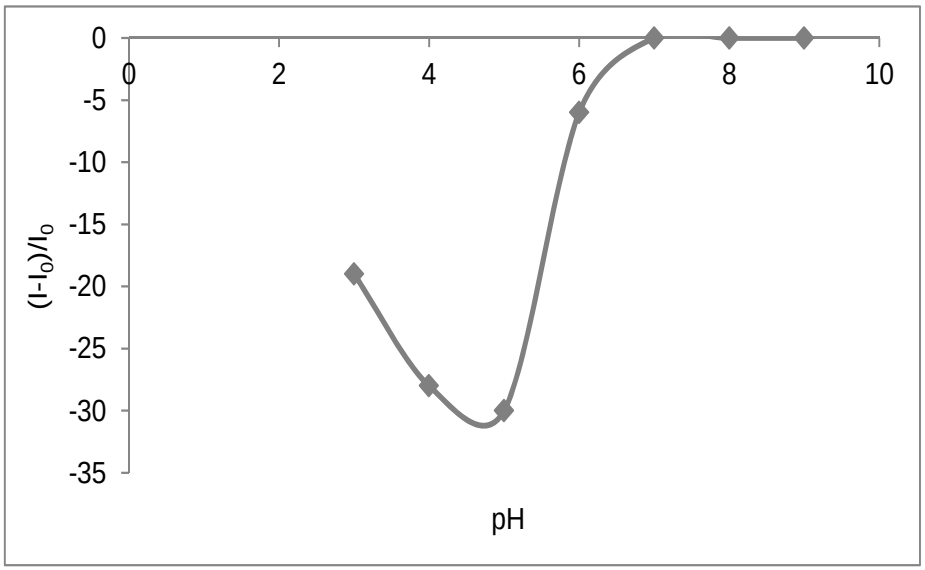

Figure 3.11 Mn^{2+} response of Eosin Y in buffer solutions of different pH

Table 3.7 Max emission wavelenght of Eosin Y in buffer solutions of different pH

pH	λ_{max}^{em} (nm)
3.0	545
4.0	544
5.0	545
6.0	542
7.0	535
8.0	535
9.0	535

3.3.5 Response of Eosin Y to Different Concentrations of Mn^{2+}

Emission based metal response of Eosin Y dye were recorded after exposure to different concentrations of Mn^{2+} solutions (0.001 mg L^- (1.85×10^{-8}M), 0.01 mg L^- (1.85×10^{-7}M), 0.1 mg L^- (1.85×10^{-6}M), 1.0 mg L^- (1.85×10^{-5}M), 2.0 mg L^- (3.7×10^{-5}M), 3.0 mg L^- (5.56×10^{-5}M)) in the concerned solutions of S-1,S-2, S-3, S-4, S-5, S-6, S-7, S-8, S-9. Figure 3.12 shows the emission-based response of the Eosin Y dye to Mn^{2+} (Table 3.8) in S1 solution which do not contain any additive. Figure 3.13, 3.15 and 3.17 show the emission-based response of the Eosin Y dye to Mn^{2+} (Table 3.9, 3.10, 3.11) in S-2, S-3 and S-4 solutions which contain 1 % of IL-I, IL-II and IL-III, respectively. Figure 3.19 and 3.21 show the emission-based response of the Eosin Y dye to Mn^{2+} (Table 3.12, 3.13) in S-5 and S-6 solutions which contain critical miscelle concentrations of SDS (10^{-2} M) and TX-100 (0.2×10^{-2} M). Figure 3.23, 3.25 and 3.27 show the emission-based response of the Eosin Y dye to Mn^{2+} (Table 3.14, 3.15, 3.16) in S-7, S-8 and S-9 solutions which contain 40 % of IL-I, IL-II and IL-III. The insets of figures show the normalized calibration plots of manganese concentration versus relative signal intensity ($(I-I_0)/I_0$). The dye exhibited decreasing response in signal intensity in the concentration range of 0.01–3.0 mg L^- (1.85×10^{-7}M–5.56×10^{-5}M) in S-1, S-2, S-3, S-4, S-5, S-6 solutions with correlation

coefficients of r= 0.98, r=0.9875, r=9741, r=0.9893, r=09803, r=0.9906, respectively. Table 3.17 shows the results and table 3.18 % shows the change in fluorescence intensity after adding 0.001-3ppm Mn^{2+}. The detection limit was the same in the absence and presence of the additives. However, the detection limit decreased to 0.001 mg L^- in 40 % ionic liquid containing solutions. The presence of ionic liquid in this concentration lowered the detection limit of Mn^{2+} by nearly ten times. The dye exhibited decreasing response in signal intensity in the concentration range of 0.001–3.0 mg L^- (1.85×10^{-8}M– 5.56×10^{-5}M) in S-7, S-8 and S-9 solutions yielding correlation coefficients of r=0.9874, r=0.9969, r=0.9893, respectively. In higher concentrations of ionic liquids (> 40%), no response to Mn^{2+} was seen. This result reveals that ionic liquids behaves like surfactants and the response increases at a critical miscelle concentration and decreases again after this concentration. The decrease in fluorescence intensity of Eosin Y after a critical concentration of ionic liquid can be attributed to the competing complex formation of IL the dye. Safavi et al. investigated the interactions of an imidazolium based IL with two sulfonated anionic dyes, azocarmine Gand methyl orange and showed their resemblance to surfactant interactions (Safavi & Zeinali 2008) told that at surfactant concentrations at critical micelle concentration (CMC) values and above, the solubilizing effect of the micelles begins to be important and probably, the ion-association complexes are incorporated into the micelles, and some new changes in spectral responses have been reported (Garcia, M.E. & Sanz-Medel, A., 1986). Since ILs can form aggregates with a similar behavior to micelles, it is thus expected that ILs with a large cationic site behave in a similar manner towards anionic dyes. In addition to electrostatic interaction, another kind of interaction can be considered between IL aggregates and the dye moiety (hydrophobic effect), in which the microenvironment of the dye may be changed from that existing in the bulk aqueous phase, and this change can also be responsible for the changes in fluorescence intensity. In submicellar regions a colloidal solution could be formed which will lessen the interaction of dye with IL which will cause no significant change in fluorescence intensity. By the increasing amounts of IL (more than 2.14×10^{-3} -2.61×10^{-3} mol/L of ILs), the IL concentration was expected to reach the CAC. After this

concentration, due to the formation of the dye–IL complexes, the fluorescence intensity of dye was decreased.

The presence of surfactants of SDS (S-5) and TX-100 (S-6) didn't change the detection limit but significantly enhanced the fluorescence decrease from 63 % (no additive) to 78 % (in presence of Triton X-100) (Figure 3.13). The relative signal changes of Eosin Y to 3.0 mg L^{-} concentration of Mn^{2+} in S-1, S-2, S-3, S-4, S-5, S-6, S-7, S-8 and S-9 solutions were 63 %, 61 %, 62 %, 58 %, 60 %, 78 %, 56 %, 60 % and 60 %, respectively. The best response of Mn^{2+} to Eosin Y was seen in S-6 (with TX-100) solutions.

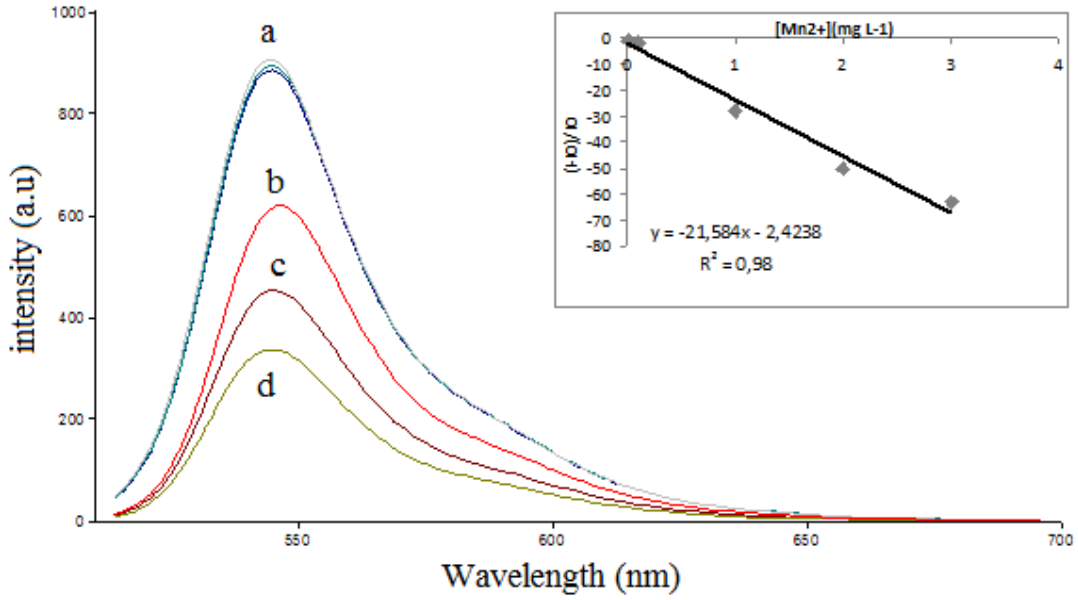

Figure 3.12 Emission based response of Eosin Y dye to Mn^{2+} in solution S-1 in the concentration range of 0.0–3.0 mg L^{-1} Mn^{2+} a) 0.0 ,0.01 , 0.1 mg L^{-1} b) 1.0 mg L^{-1} c) 2.0 mg L^{-1} d) 3.0 mg L^{-1}

Table 3.8 Data of the emission based response of Eosin Y dye to Mn^{2+} in solution S-1 in the concentration range of 0.0–3.0 mg L^{-1} Mn^{2+}

Concentration of Mn^{2+}	λ_{max}^{em} (nm)	Fluorescence Intensity (a.u.)
0.000 mgL^{-1}	545	906
0.010 mgL^{-1}	545	894
0.100 mgL^{-1}	545	885
1.000 mgL^{-1}	545	620
2.000 mgL^{-1}	545	450
3.000 mgL^{-1}	545	334

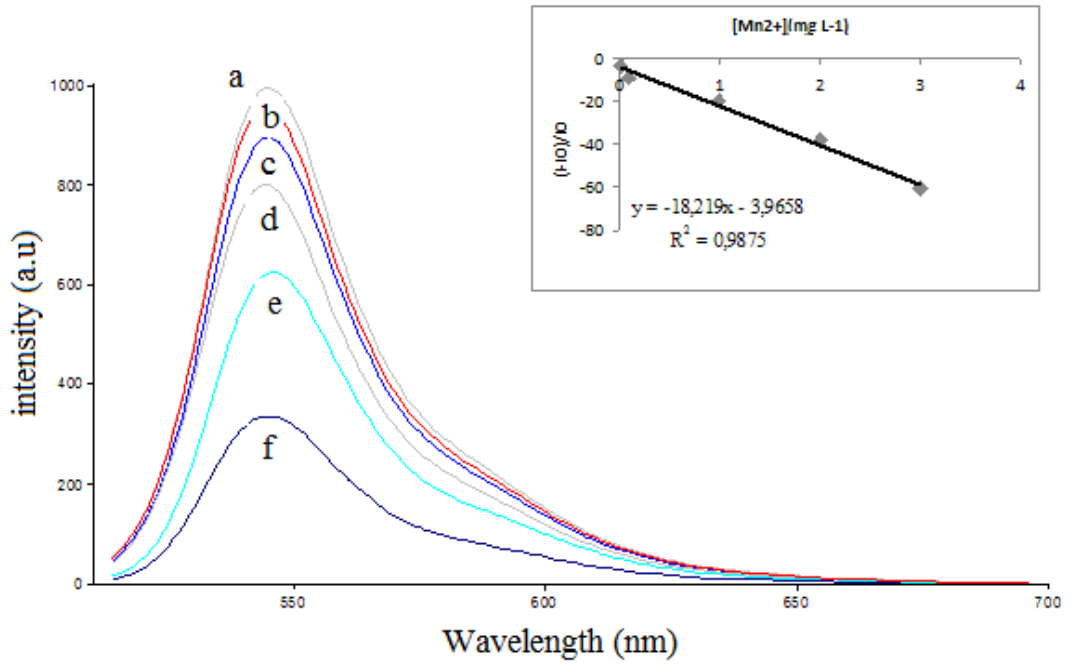

Figure 3.13 Emission based response of Eosin Y dye to Mn^{2+} in solution S-2 in the concentration range of 0.0–3.0 mg L^{-1} Mn^{2+} a) 0.0 mg L^{-1} b) 0.01 mg L^{-1} c) 0.1 mg L^{-1} d) 1.0 mg L^{-1} e) 2.0 mg L^{-1} f) 3.0 mg L^{-1} and Emission based calibration plot of Eosin Y for Mn^{2+}

Table 3.9 Data of the emission based response of Eosin Y dye to Mn^{2+} in solution S-2 in the concentration range of 0.0–3.0 mg L^{-1} Mn^{2+}

Concentration of Mn^{2+}	λ_{max}^{em} (nm)	Fluorescence Intensity (a.u.)
0.000 mgL^{-1}	546	992
0.010 mgL^{-1}	546	962
0.100 mgL^{-1}	546	900
1.000 mgL^{-1}	545	795
2.000 mgL^{-1}	546	612
3.000 mgL^{-1}	545	390

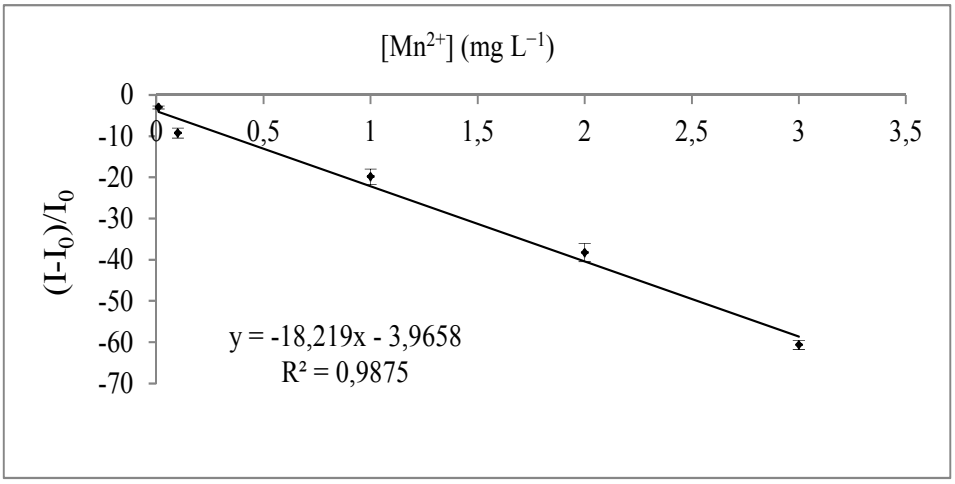

Figure3.14 Emission based calibration plot of three different S-2 solution to Eosin Y for Mn^{2+}

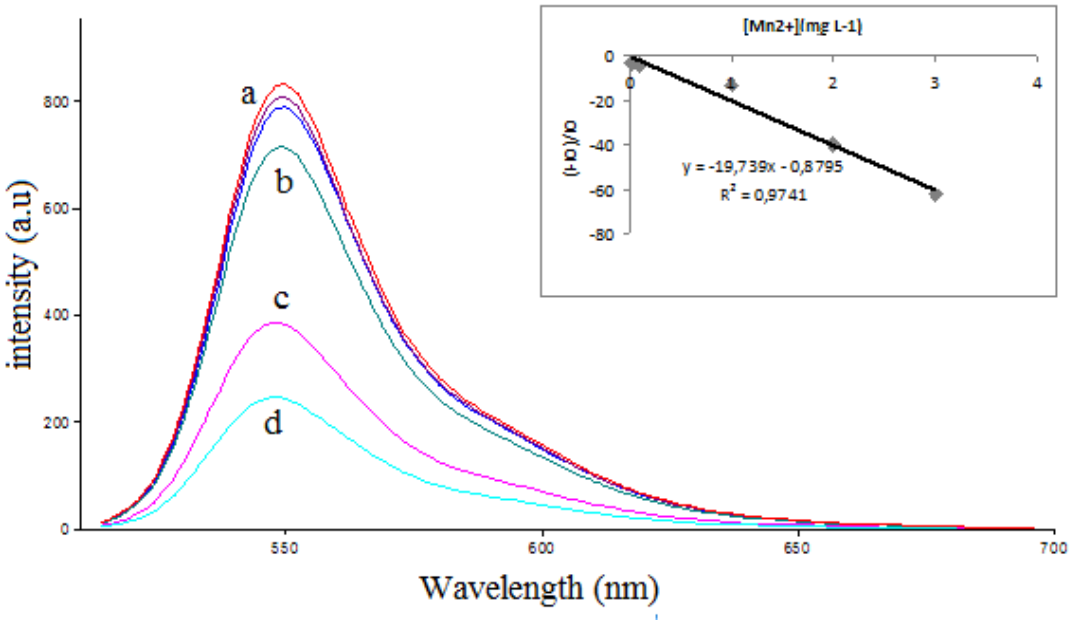

Figure3.15 Emission based response of Eosin Y dye to Mn^{2+} in solution S-3 in the concentration range of 0.0–3.0 mg L^{-1} Mn^{2+} a) 0.0 , 0.01 , 0.1 mg L^{-1} b) 1.0 mg L^{-1} c) 2.0 mg L^{-1} d) 3.0 mg L^{-1} and Emission based calibration plot of Eosin Y for Mn^{2+}

Table 3.10 Data of the emission based response of Eosin Y dye to Mn^{2+} in solution S-3 in the concentration range of 0.0–3.0 mg L^{-1} Mn^{2+}

Concentration of Mn^{2+}	λ_{max}^{em} (nm)	Fluorescence Intensity (a.u.)
0.000 mgL^{-1}	545	812
0.010 mgL^{-1}	545	779
0.100 mgL^{-1}	545	774
1.000mgL^{-1}	545	702
2.000 mgL^{-1}	545	485
3.000 mgL^{-1}	545	305

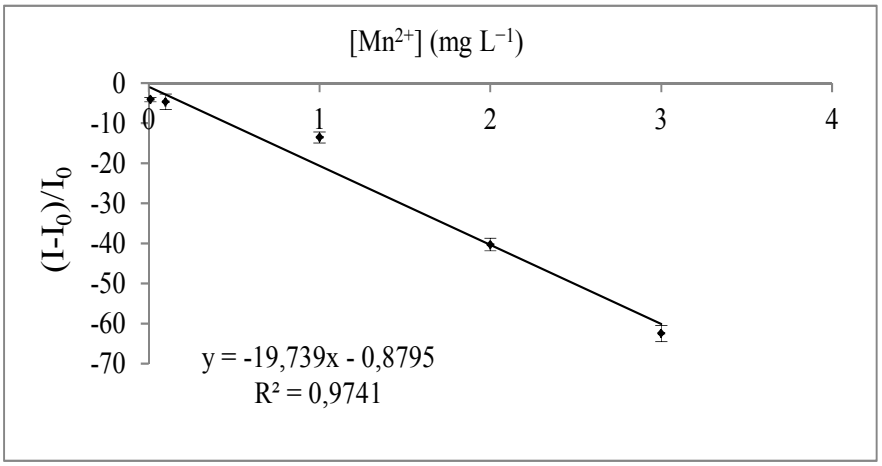

Figure 3.16 Emission based calibration plot of three different S-3 solution to Eosin Y for Mn^{2+}

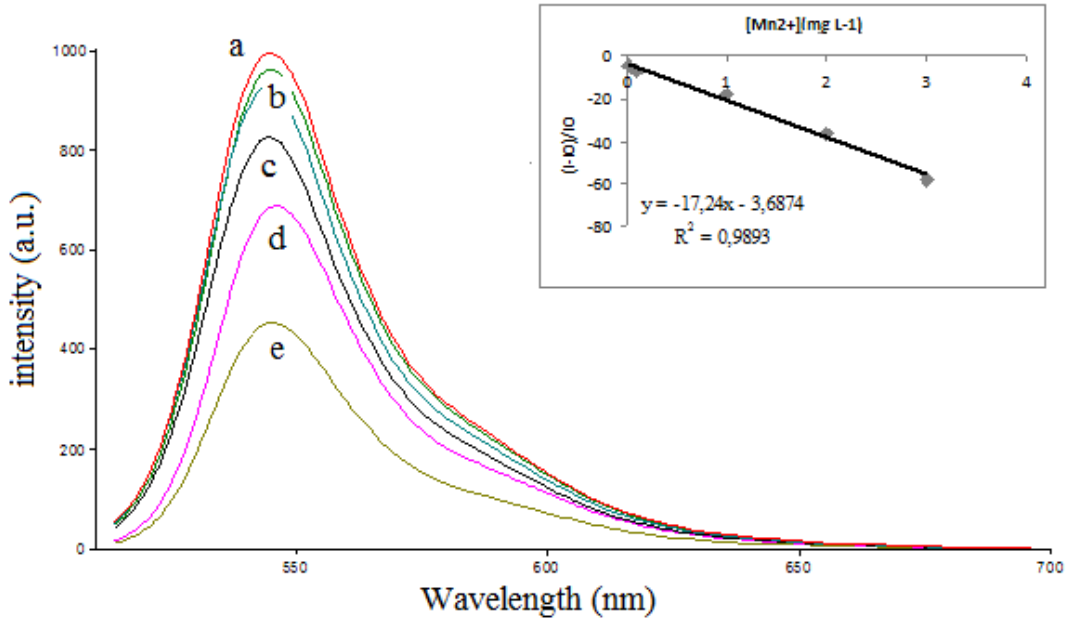

Figure 3.17 Emission based response of Eosin Y dye to Mn^{2+} in solution S-4 in the concentration range of 0.0–3.0 mg L^{-1} Mn^{2+} a) 0.0 mg L^{-1} b) 0.01 , 0.1 mg L^{-1} c) 1.0 mg L^{-1} d) 2.0 mg L^{-1} e) 3.0 mg L^{-1} and Emission based calibration plot of Eosin Y for Mn^{2+}

Table 3.11 Data of the emission based response of Eosin Y dye to Mn^{2+} in solution S-4 in the concentration range of 0.0–3.0 mg L^{-1} Mn^{2+}

Concentration of Mn^{2+}	λ_{max}^{em} (nm)	Fluorescence Intensity (a.u.)
0.000 mgL^{-1}	548	997
0.010 mgL^{-1}	548	950
0.100 mgL^{-1}	548	925
1.000 mgL^{-1}	548	818
2.000 mgL^{-1}	548	635
3.000 mgL^{-1}	548	423

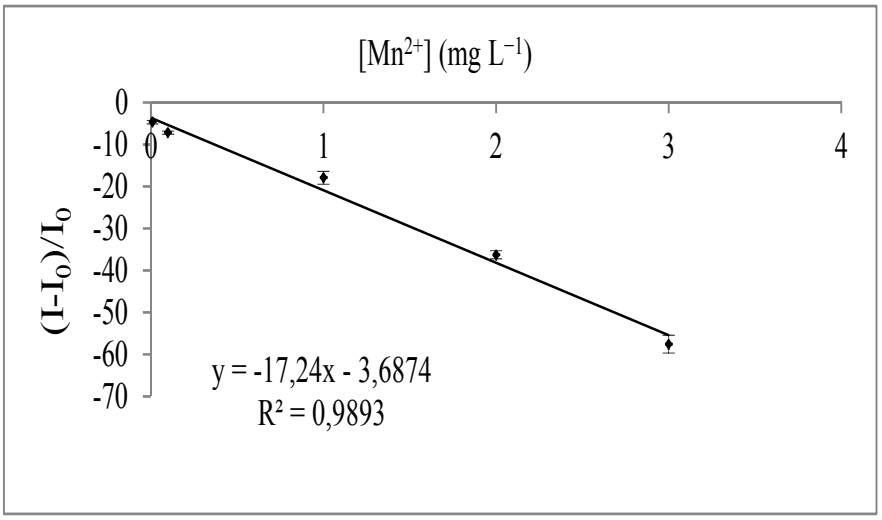

Figure 3.18 Emission based calibration plot of three different S-4 solution to Eosin Y for Mn^{2+}

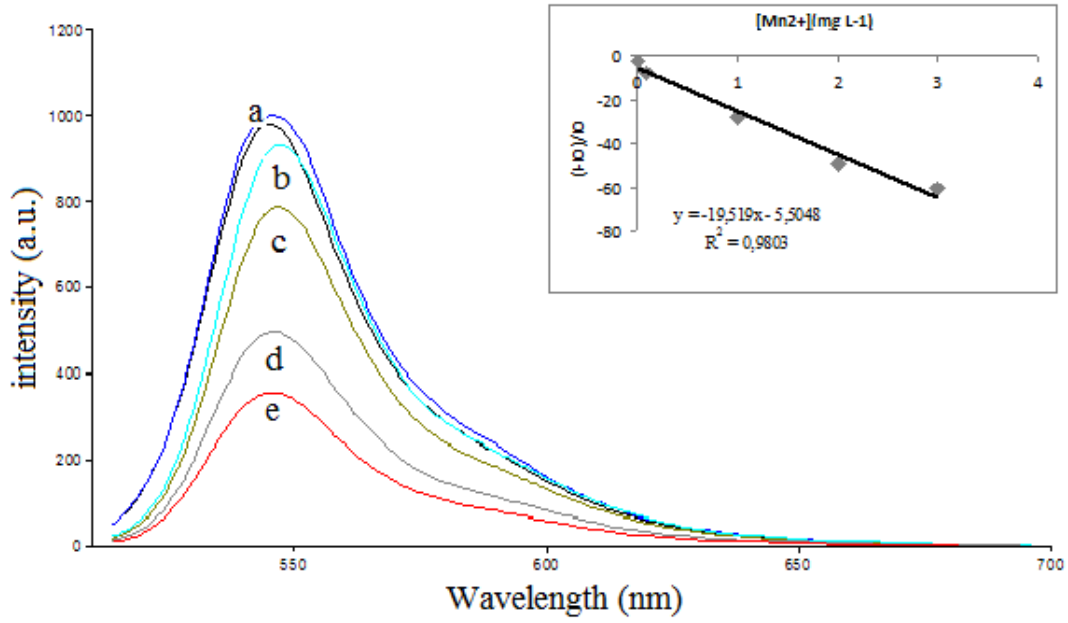

Figure 3.19 Emission based response of Eosin Y dye to Mn^{2+} in solution S-5 in the concentration range of 0.0–3.0 mg L^{-1} Mn^{2+} a) 0.0, 0.01 mg L^{-1} b) 0.1 mg L^{-1} c) 1.0 mg L^{-1} d) 2.0 mg L^{-1} e) 3.0 mg L^{-1} and Emission based calibration plot of Eosin Y for Mn^{2+}

Table 3.12 Data of the emission based response of Eosin Y dye to Mn^{2+} in solution S-5 in the concentration range of 0.0–3.0 mg L^{-1} Mn^{2+}

Concentration of Mn^{2+}	λ_{max}^{em} (nm)	Fluorescence Intensity (a.u.)
0.000 mgL^{-1}	548	996
0.010 mgL^{-1}	548	972
0.100 mgL^{-1}	548	921
1.000 mgL^{-1}	548	720
2.000 mgL^{-1}	548	510
3.000 mgL^{-1}	548	395

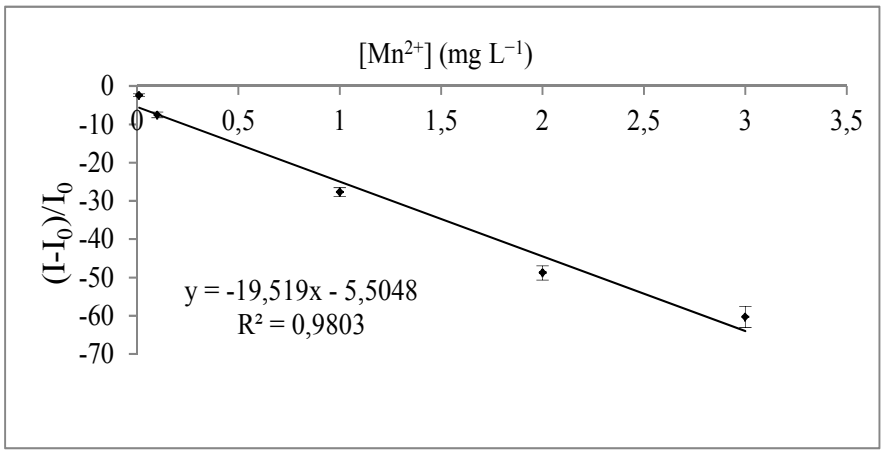

Figure 3.20 Emission based calibration plot of three different S-5 solution to Eosin Y for Mn^{2+}

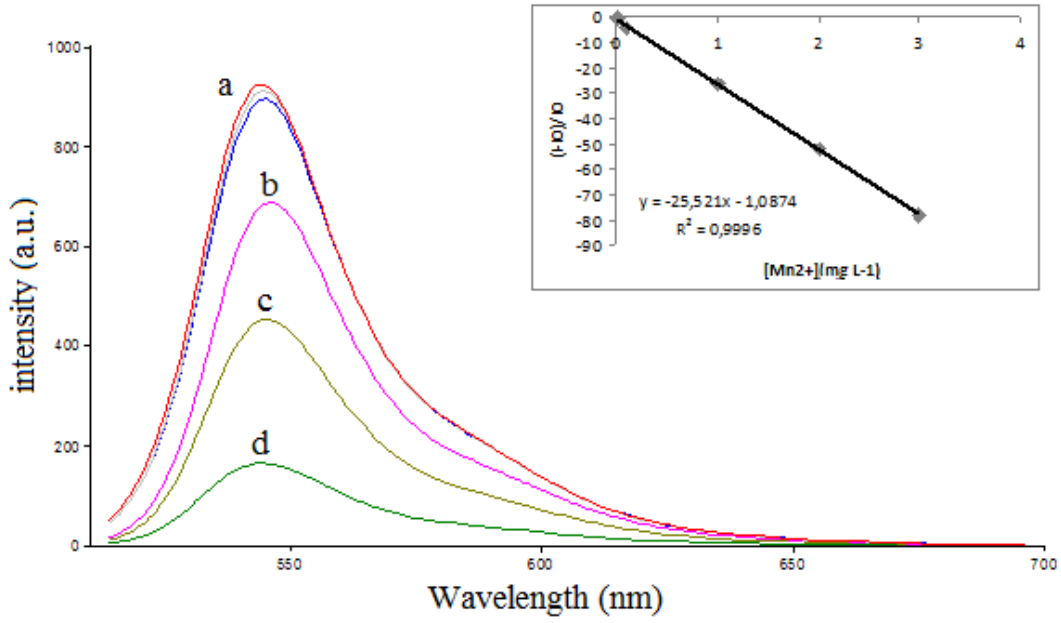

Figure 3.21 Emission based response of Eosin Y dye to Mn^{2+} in solution S-6 in the concentration range of 0.0–3.0 mg L^{-1} Mn^{2+} a) 0.0 , 0.01 , 0.1 mg L^{-1} b) 1.0 mg L^{-1} c) 2.0 mg L^{-1} d) 3.0 mg L^{-1} and Emission based calibration plot of Eosin Y for Mn^{2+}

Table 3.13 Data of the emission based response of Eosin Y dye to Mn^{2+} in solution S-6 in the concentration range of 0.0–3.0 mg L^{-1} Mn^{2+}

Concentration of Mn^{2+}	λ_{max}^{em} (nm)	Fluorescence Intensity (a.u.)
0.000 mgL^{-1}	554	932
0.010 mgL^{-1}	554	925
0.100 mgL^{-1}	554	889
1.000 mgL^{-1}	554	687
2.000 mgL^{-1}	554	450
3.000 mgL^{-1}	554	205

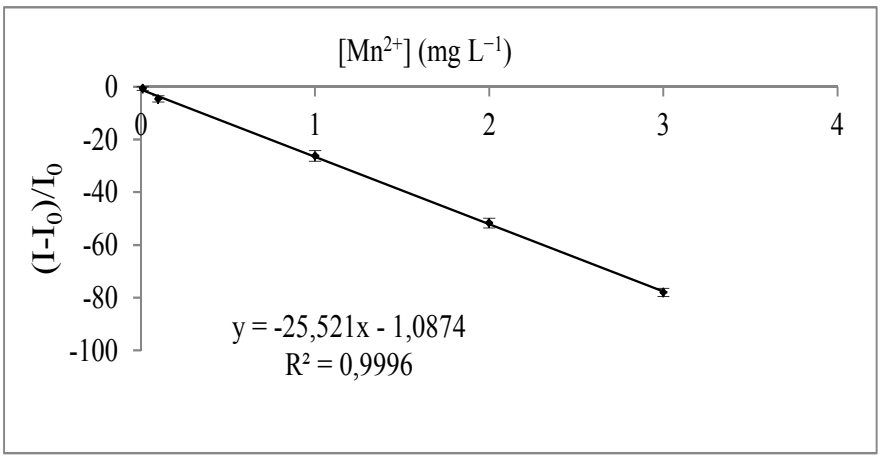

Figure 3.22 Emission based calibration plot of three different S-6 solution to Eosin Y for Mn^{2+}

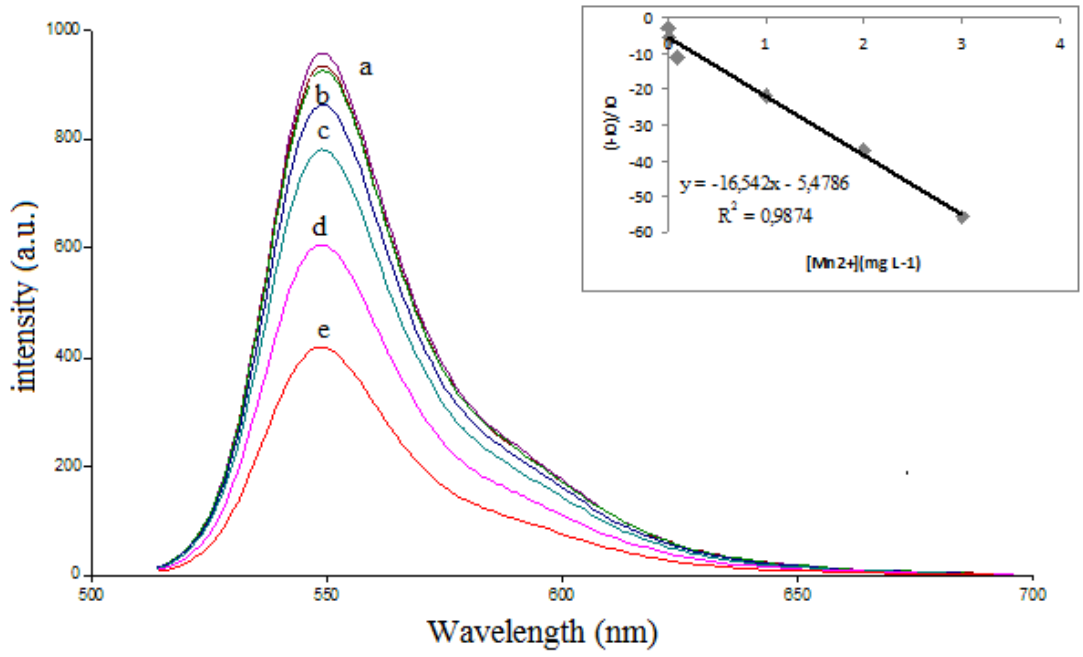

Figure 3.23 Emission based response of Eosin Y dye to Mn^{2+} in solution S-7 in the concentration range of 0.0–3.0 mg L^{-1} Mn^{2+} a) 0.0 , 0.001 , 0.01 mg L^{-1} b) 0.1 mg L^{-1} c) 1.0 mg L^{-1} d) 2.0 mg L^{-1} e) 3.0 mg L^{-1} and Emission based calibration plot of Eosin Y for Mn^{2+}

Table 3.14 Data of the emission based response of Eosin Y dye to Mn^{2+} in solution S-7 in the concentration range of 0.0–3.0 mg L^{-1} Mn^{2+}

Concentration of Mn^{2+}	λ_{max}^{em} (nm)	Fluorescence Intensity (a.u.)
0.000 mgL^{-1}	550	960
0.001 mgL^{-1}	550	935
0.010 mgL^{-1}	550	910
0.100 mgL^{-1}	550	853
1.000 mgL^{-1}	550	750
2.000 mgL^{-1}	551	603
3.000 mgL^{-1}	551	423

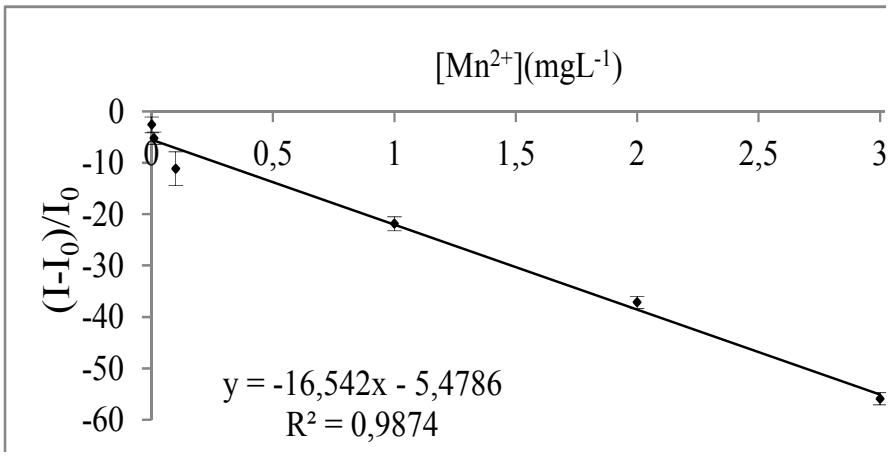

Figure 3.24 Emission based calibration plot of three different S-7 solution to Eosin Y for Mn^{2+}

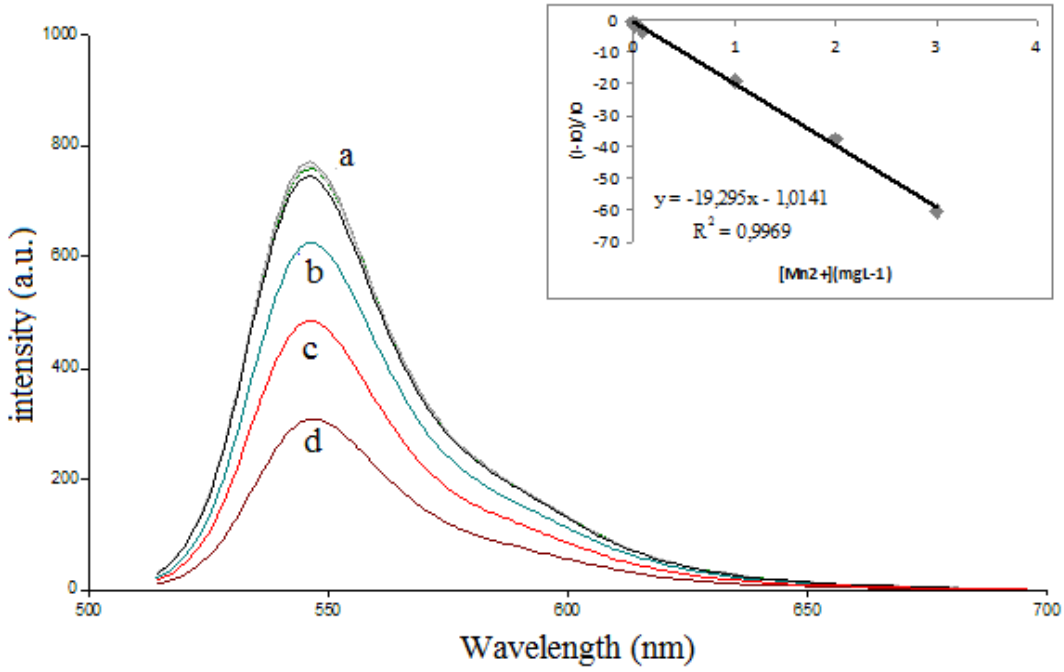

Figure 3.25 Emission based response of Eosin Y dye to Mn^{2+} in solution S-8 in the concentration range of 0.0–3.0 mg L^{-1} Mn^{2+} a) 0.0 , 0.001 , 0.01 mg L^{-1} b) 0.1 mg L^{-1} c) 1.0 mg L^{-1} d) 2.0 mg L^{-1} e) 3.0 mg L^{-1} and Emission based calibration plot of Eosin Y for Mn^{2+}

Table 3.15 Data of the emission based response of Eosin Y dye to Mn^{2+} in solution S-8 in the concentration range of 0.0–3.0 mg L^{-1} Mn^{2+}

Concentration of Mn^{2+}	λ_{max}^{em} (nm)	Fluorescence Intensity (a.u.)
0.000 mgL^{-1}	550	771
0.001 mgL^{-1}	550	763
0.010 mgL^{-1}	550	756
0.100 mgL^{-1}	550	743
1.000 mgL^{-1}	550	623
2.000 mgL^{-1}	551	481
3.000 mgL^{-1}	551	304

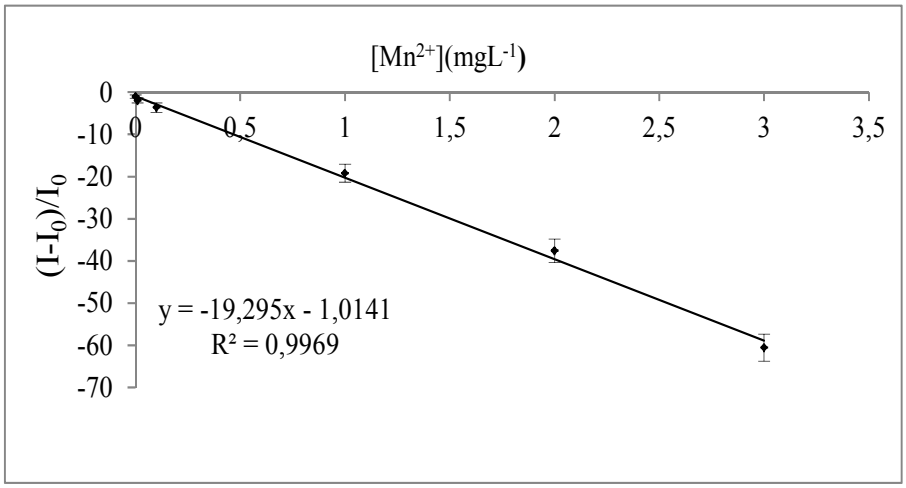

Figure 3.26 Emission based calibration plot of three different S-8 solution to Eosin Y for Mn^{2+}

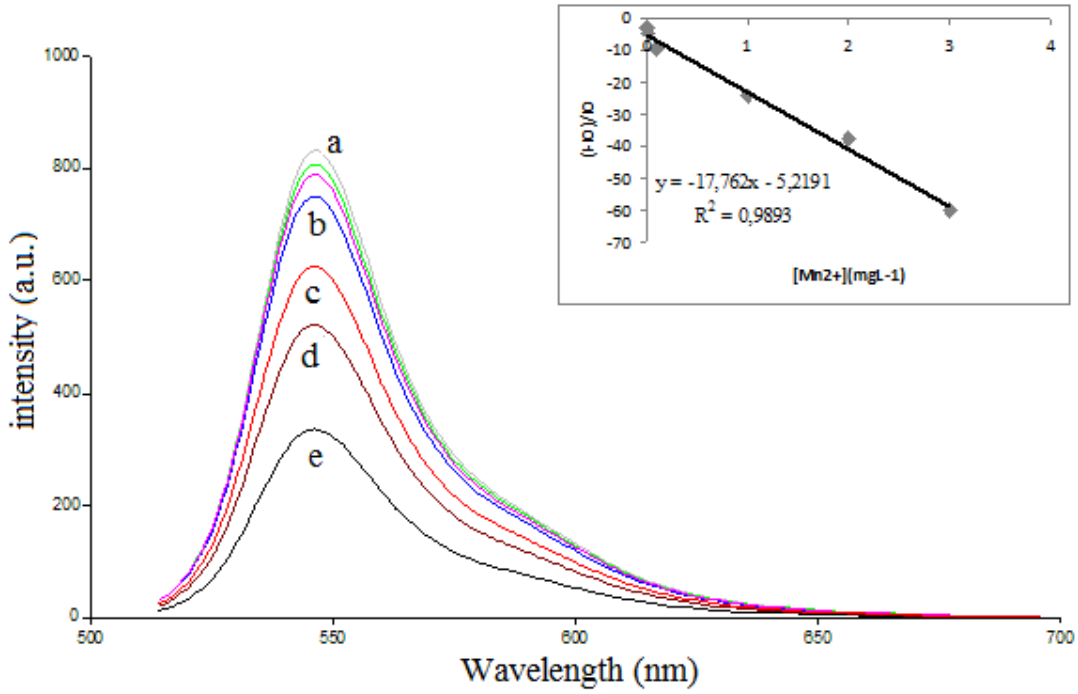

Figure 3.27 Emission based response of Eosin Y dye to Mn^{2+} in buffersolution S-9 in the concentration range of 0.0–3.0 mg L^{-1} Mn^{2+} a) 0.0 , 0.001 , 0.01 mg L^{-1} b) 0.1 mg L^{-1} c) 1.0 mg L^{-1} d) 2.0 mg L^{-1} e) 3.0 mg L^{-1} and Emission based calibration plot of Eosin Y for Mn^{2+}

Table 3.16 Data of the emission based response of Eosin Y dye to Mn^{2+} in solution S-9 in the concentration range of 0.0–3.0 mg L^{-1} Mn^{2+}

Concentration of Mn^{2+}	λ_{max}^{em} (nm)	Fluorescence Intensity (a.u.)
0.000 mgL^{-1}	550	833
0.001 mgL^{-1}	550	808
0.010 mgL^{-1}	550	792
0.100 mgL^{-1}	550	752
1.000 mgL^{-1}	550	628
2.000 mgL^{-1}	551	519
3.000 mgL^{-1}	551	334

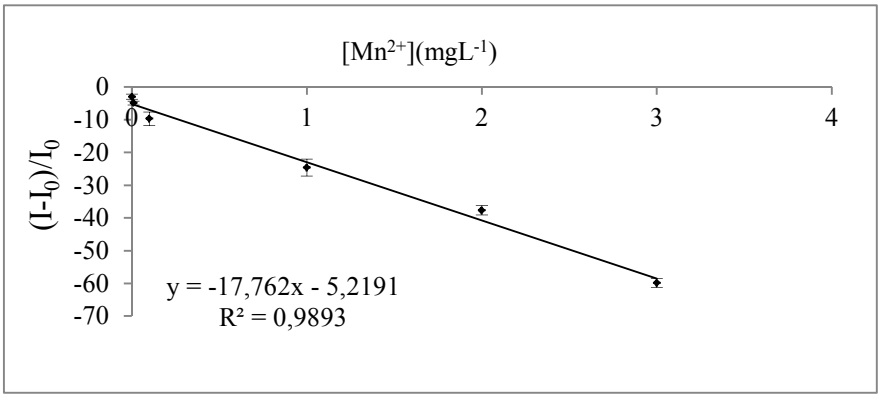

Figure 3.28 Emission based calibration plot of three different S-9 solution to Eosin Y for Mn^{2+}

Table 3.17 Analytical characteristics of solutions

Solution	Linear working range (mg L^{-1})	Regression equation	Limit detection (mgL^{-1})	*r* (*n=3)*
S-1	0.01-3.0	y=-21.584x-2.4238	0.010	0.9800
S-2	0.01-3.0	y=-18.219x-3.9658	0.010	0.9875
S-3	0.01-3.0	y=-19.739x-0.8795	0.010	0.9741
S-4	0.01-3.0	y=-17.24x-3.6874	0.010	0.9893
S-5	0.01-3.0	y=-19.519x-5.5048	0.010	0.9803
S-6	0.01-3.0	y=-25.521x-1.0874	0.010	0.9996
S-7	0.001-3.0	y=-16.542x-5.4786	0.001	0.9874
S-8	0.001-3.0	y=-19.295x-1.0141	0.001	0.9969
S-9	0.001-3.0	y=-17.764x-5.2191	0.001	0.9893

Table 3.18 % change in fluorescence intensity after adding 0.001-3ppm Mn^{2+}

	$(I-I_0)/I_0$ for Mn^{2+}					
solution	0.001ppm (mgL^{-1})	0.010ppm (mgL^{-1})	0.100ppm (mgL^{-1})	1.000ppm (mgL^{-1})	2.000ppm (mgL^{-1})	3.000ppm (mgL^{-1})
S-1	-	-1	-2	-28	-50	-63
S-2	-	-3	-9	-20	-38	-63
S-3	-	-4	-5	-14	-40	-62
S-4	-	-5	-7	-18	-36	-58
S-5	-	-2	-8	-28	-49	-60
S-6	-	-1	-5	-26	-52	-78
S-7	-3	-5	-11	-22	-37	-56
S-8	-2	-3	-5	-20	-38	-60
S-9	-3	-5	-10	-25	-38	-60

3.3.6 Determination of Mn (II) Ions in Ultrapure Water and Drinking Water Samples Using Eosin Y in Different Media

To validate this method, two samples (ultrapure water and drinking water) were used for the Mn^{2+} determination. Each water sample has no Mn^{2+} cation so different concentrations of Mn^{2+} were respectively added in the water samples and then analyzed with the proposed method. The recorded fluorescence intensities of the water samples were employed to the calibration equations. Solution of the calibration equations was yielded the Mn^{2+} concentration of the water samples. Table 3.19 lists the data of Mn^{2+} determination, from which satisfactory results for Mn^{2+} recovery were obtained. This indicates that the Eosin Y can be used for the detection of Mn^{2+} ion in the environmental field.

Table 3.19 Determination of Mn^{2+} in the ultrapure and drinking water

Sample	Solution	Mn^{2+} added (mg L^{-1})	Mn^{2+} found (mg L^{-1}) (mean±S.D.)	Recovery (%)
Ultrapure Water	S-6	1.000	0.945±0.016	94.17
	S-7	1.000	0.953±0.026	95.06
	S-8	1.000	1.080±0.036	92.59
	S-9	1.000	0.925±0.032	91.89
Drinking Water	S-6	0.010	$0.011\pm3.6\times10^{-3}$	90.90
		0.100	0.101±0.072	99.99
		1.000	1.080±0.036	92.59
		2.000	2.020±0.104	99.00
	S-7	0.001	-	-
		0.010	0.011±0.005	90.90
		0.100	0.112±0.083	89.28
		1.000	1.082±0.054	92.42
		2.000	1.959±0.069	97.90

3.3.7 Selectivity studies

The effect of the most strong interferents (Cd^{2+}, Pb^{2+}, Na^{+}, Mg^{2+}, Mo^{2+}, Fe^{2+}, Fe^{3+}, Zn^{2+}, standard anion solution) on the determination of 3mgL^{-} (5.56×10^{-5}M) Mn^{2+} was investigated in all media. We measured the fluorescence of Mn^{2+} Eosin Y without and with interferents added. The tolerance limit was expressed as the maximum interferent concentration to be determined within an error of 5%. The results were shown in Table 3.20. Some species such as Na^{+}, Zn^{2+} and standard anion exhibited less interfering effect in ionic liquids and micelle media. (solutions S-1, S-2, S-3, S-4, S-5, S-6). The tolerance limit of Na^{+}, Zn^{2+} enhance 7 times in presence of ILs and micelle media.

Table 3.20 The tolerance limit of some selected ions in solutions S-1, S-2, S-3, S-4, S-5 and S-6

interferent	S-1	S-2	S-3	S-4	S-5	S-6
Cd^{2+}	0.22	0.32	0.40	0.54	0.32	0.48
Pb^{2+}	0.40	0.40	0.22	0.28	0.40	0.22
Na^{+}	2.80	14.20	10.00	14.00	17.20	8.40
Mg^{2+}	0.22	0.42	0.40	0.42	0.40	0.48
Mo^{2+}	0.40	0.60	0.80	1.00	0.60	0.48
Fe^{2+}	0.40	0.28	0.28	0.32	0.48	0.54
Fe^{3+}	0.40	0.28	0.40	0.40	0.54	0.62
Zn^{2+}	3.20	16.20	5.40	17.40	13.80	4.60

3.3.8 Complex Stoichiometry

The stoichiometry of metal complexes depends on the media. In this study, the complex stoichiometry in TX-100 containing media was determined by using the molar ratio method. In order to determine complex stoichiometry, the emission and absorption spectra of different volumes of 1.5×10^{-5} M Mn^{2+} and 1.5×10^{-5} M Eosin Y of solutions were mixed. Figure 3.29 and 3.30 show the emission and absorption spectra related data of mixtures of 1.5×10^{-5}M Eosin Y and 1.5×10^{-5} M Mn^{2+} solutions. According to the spectra by the addition of Mn^{2+}, no new peaks were observed. The results showed that Eosin Y did not make a complex with Mn^{2+} and the decrease in fluorescence intensity is via fluorescence quenching.

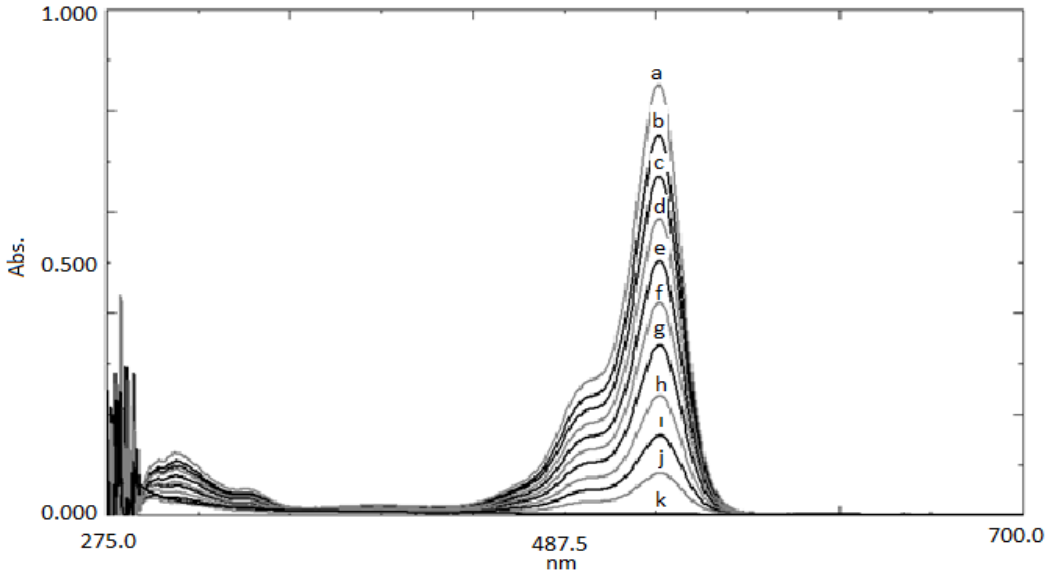

Figure 3.29 Absorption based complex stoichiometry a) 5.0 ml Eosin Y, 0.0 ml Mn^{2+} , b) 4.5 ml Eosin Y, 0.5ml Mn^{2+} c) 4.0 ml Eosin Y, 1.0 ml Mn^{2+}, d) 3.5 ml Eosin Y, 1.5 ml Mn^{2+}, e) 3.0 ml Eosin Y, 2.0 ml Mn^{2+}, f) 2.5 ml Eosin Y, 2.5 ml Mn^{2+}, g) 2 ml Eosin Y, 3.0 ml Mn^{2+}, h) 1.5 ml Eosin Y, 3.5 ml Mn^{2+}, i) 1.0 ml Eosin Y, 4.0 ml Mn^{2+}, j) 0.5 ml Eosin Y, 4.5 ml Mn^{2+}, k) 0.00 ml Eosin Y, 5.0ml Mn^{2+}

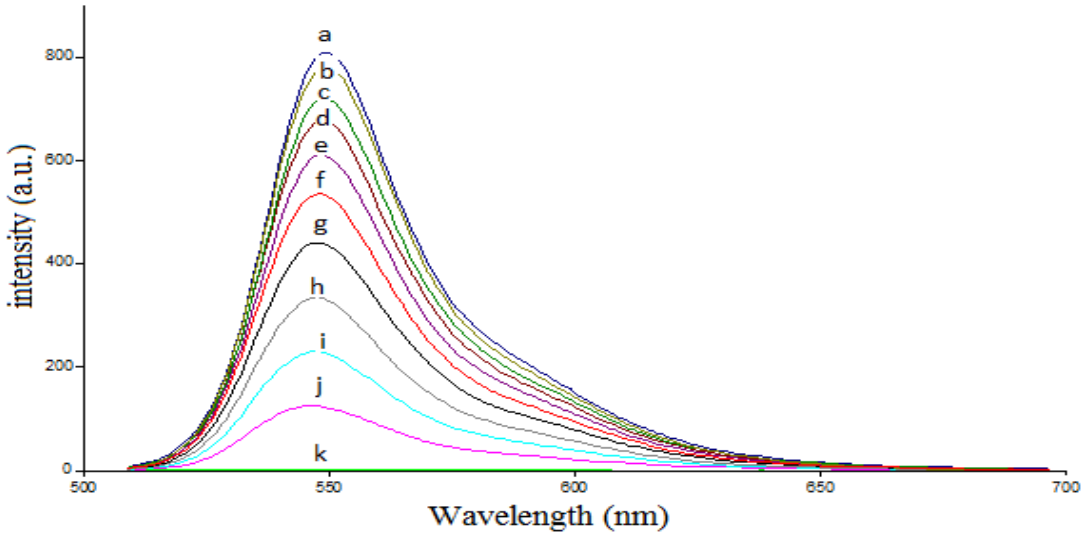

Figure 3.30 Emission based complex stoichiometry a) 5.0 ml Eosin Y, 0.0 ml Mn^{2+} , b) 4.5 ml Eosin Y, 0.5ml Mn^{2+} c) 4.0 ml Eosin Y, 1.0 ml Mn^{2+}, d) 3.5 ml Eosin Y, 1.5 ml Mn^{2+}, e) 3.0 ml Eosin Y, 2.0 ml Mn^{2+}, f) 2.5 ml Eosin Y, 2.5 ml Mn^{2+}, g) 2 ml Eosin Y, 3.0 ml Mn^{2+}, h) 1.5 ml Eosin Y, 3.5 ml Mn^{2+}, i) 1.0 ml Eosin Y, 4.0 ml Mn^{2+}, j) 0.5 ml Eosin Y, 4.5 ml Mn^{2+}, k) 0.00 ml Eosin Y, 5.0ml Mn^{2+}

3.4 Conclusion

In this study we have employed tree ionic liquids (1-butyl-3- methylimidazolium thiocyanate ([BMIM][SCN]), 1-butyl-3- methylimidazolium tetrafluoroborate ([BMIM][BF_4]), 1-ethyl-3-methylimidazolium tetrafluoroborate ([EMIM][BF_4]) and two micelles (sodium dodecyl sulfate (SDS) and Triton X-100) as new additives for the determination of Mn^{2+} with Eosin Y in aqueous solutions by spectrofluorimetric method. The results revealed that the spectra of Eosin Y in all media exhibited broad emission bands ranging from 510 to 650 nm. The emission maximum of the dye was between the range of 545-554 nm. Ionic liquid concentrations in S-2, S-3, S-4, S-7, S-8, S-9 didn't affect the maximum emission wavelength and the fluorescence intensity. TX-100 (0.2×10^{-2} M) caused moderately longer red shift of 9 nm and a slight decrease in fluorescence intensity.

In absence of additives we have observed response for the the metal ions of Ca^{2+},Cu^{2+}, Hg^{+}, Hg^{2+}, As^{5+}, Li^{+}, Al^{3+}, Cr^{3+}, Co^{2+} and Ni^{2+} while we have observed no response in the additive containing solutions ions. Thus, the presence of both the ionic liquids and the surfactants increased the selectivity of the dye. Besides, they have decreased the % response of the other metal ions except Mn^{2+}.

The dye exhibited decreasing response in signal intensity in the concentration range of 0.01–3.0 mg L^{-}(1.85×10^{-7}M–5.56×10^{-5}M) Mn^{2+} in S-1, S-2, S-3, S-4, S-5, S-6 solutions. The detection limit was the same in the absence and presence of the additives. However, the detection limit decreased to 0.001 mg L- in 40 % ionic liquid containing solutions. In higher concentrations of ionic liquids (> 40%), no response to Mn^{2+} was seen. This result reveals that ionic liquids behaves like surfactants and the response increases at a critical miscelle concentration and decreases again after this concentration. The decrease in fluorescence intensity of Eosin Y after a critical concentration of ionic liquid can be attributed to the competing complex formation of IL the dye.

The presence of surfactants of SDS (S-5) and TX-100 (S-6) didn't change the detection limit but significantly enhanced the fluorescence decrease from 63 % (no additive) to 78 % (in presence of Triton X-100). The relative signal changes of Eosin Y to 3.0 mg L- concentration of Mn2+ in S-1, S-2, S-3, S-4, S-5, S-6, S-7, S-8 and S-9 solutions were 63 %, 61 %, 62 %, 58 %, 60 %, 78 %, 56 %, 60 % and 60 %, respectively. The best response of Mn2+ to Eosin Y was seen in S-6 (with TX-100) solutions. The presence of ionic liquid lowered the detection limit of Mn^{2+} by nearly ten times. The interference effect of the other metal ions (Ca^{2+},Cu^{2+}, Hg^{+}, As^{5+}, Mo^{2+}, Li^{+}, $Pb^{2+,}$ Al^{3+}, Cr^{3+},Na^{+}, $Mg^{2+,}$ Zn^{2+}, Cd^{2+}, Fe^{3+},Co^{2+} and Ni^{2+}) to the fluorescence intensity was also investigated. The results showed that Na^{+} and Zn^{2+} ions exhibited less interfering effect in the presence of employed ionic liquids and micelles. The tolerance limit of Na^{+} increased 6 times in presence of [EMIM][BF_4] and the tolerance limit of Zn^{2+} increased 5 times in presence of SDS.

The optimum response was observed at pH 5.0. Because of this the experimens were performed in buffered solutions. One advantage of the IL is that the IL containing solution strongly resisted pH changes due to its buffering effect. Similar behavior of ILs was reported earlier (Zhu, & Yuan, 2006)Formation of such a buffer system enhances the stability of analysis system more than the classical buffer systems and the presence of IL in the analysis solution acts as a sink for acidic or basic species.

CHAPTER FOUR
PHOTOCHARACTERIZATION OF SOME IONIC LIQUIDS AND INVESTIGATION OF THE EFFECT OF SOME CATIONS TO THEIR FLUORESCENCE CHARACTERISTICS

4.1 Introduction

The monitoring of trace levels of iron has raised interest since iron plays an important role in metabolic processes, biological materials and environmental samples. Different dyes have been used for spectral iron detection either in immobilized or free form. On the other hand, the discovery, design and synthesis of new organic fluorescent molecules and their interaction with cations, anions or biomaterials lead exciting advances in sensing, imaging and diagnostic. (Oter, Ertekin & Kirilmis, 2006)

The equilibrium reaction between Fe^{3+} and SCN^- studied , which is represented in aqueous solution by the following product-favored reaction. The $[Fe(H_2O)_5(SCN)]^{2+}$ ion produces a red-orange solution.

$$[Fe(H_2O)_6]^{3+} + SCN^- \text{ <==> } [Fe(H_2O)_5(SCN)]^{2+} + H_2O$$

The utility of ionic liquids as reaction media has taken the place of volatile conventional solvents and has resulted in a large number of studies in recent years (Welton, 1999) A large majority of the studies on ILs are about the characterization of them usually with NMR, IR and Raman spectroscopic techniques (Rodgers, Seddon,2003). The number of UV-visible and fluorimetry based studies on ILs is relatively fewer (Lancaster, Salter & Welton, 2002). These studies have showed the importance of the purity of the IL in spectroscopic studies because of the absorption bands seen in the spectra of ionic liquids. However, it is still not clear that these absorption and emission bands are due to a probable impurity or ionic liquid itself.

In this study, photophysical constants of three ionic liquids (99 % purity), 1-Butyl-3-methylimidazolium tetrafluoroborate ([BMIM]BF_4) (IL-I), 1-ethyl-3-methylimidazolium tetrafluoroborate ([EMIM]BF4) (IL-II) and 1-Butyl-3-methylimidazolium thiocyanate ([BMIM][SCN]) (IL-III) has been declared and their photoluminescent properties were investigated in aqueous media by absorption, emission and excitation spectra. The effect of metal cations (Ca^{2+},Cu^{2+}, Hg^{+}, As^{5+}, Mo^{2+}, Li^{+}, Pb^{2+}, Al^{3+}, Cr^{3+},Na^{+}, Mg^{2+}, Zn^{2+}, Cd^{2+}, Fe^{3+},Co^{2+} and Ni^{2+}) to the absorption and fluorescence characteristics of the ionic liquids were investigated and the acid base response of the ionic liquids were also evaluated.

4.2 Solutions Preparation

All the ionic liquids employed were water soluble, hydrophilic room temperature ionic liquids. The ionic liquid solutions were freshly prepared prior to experiments to contain 0.2%-1.0% IL concentrations (by volume) by diluting with pH 5.0 acetic acid acetate buffer solutions.

4.3 Results and discussion

4.3.1 Spectral Characterization of the Ionic Liquids

In order to evaluate the photoluminescent properties of ionic liquids in aqueous solutions, the absorption, emission and excitation spectra were recorded in the pH 5.0 buffer (Figure 4.1, 4.2, 4.3). The maximum absorption, emission and excitation wavelengths of the IL-I, IL-II, IL-III were given in Table 4.1 and 4.2. All experiments were done at slit 10-10.

In the absorption spectra of ILs, a broad absorption band between 350-700 nm. In the absorption spectra of [BMIM][SCN], new absorption maxima at 460 nm was observed by the addition of Fe^{2+} and Fe^{3+} ions, which is probably due to the

complex formation of iron ions with SCN group of the ionic liquid. All of the ILs exhibited emission bands between 350-600 nm (See Table 4.2).

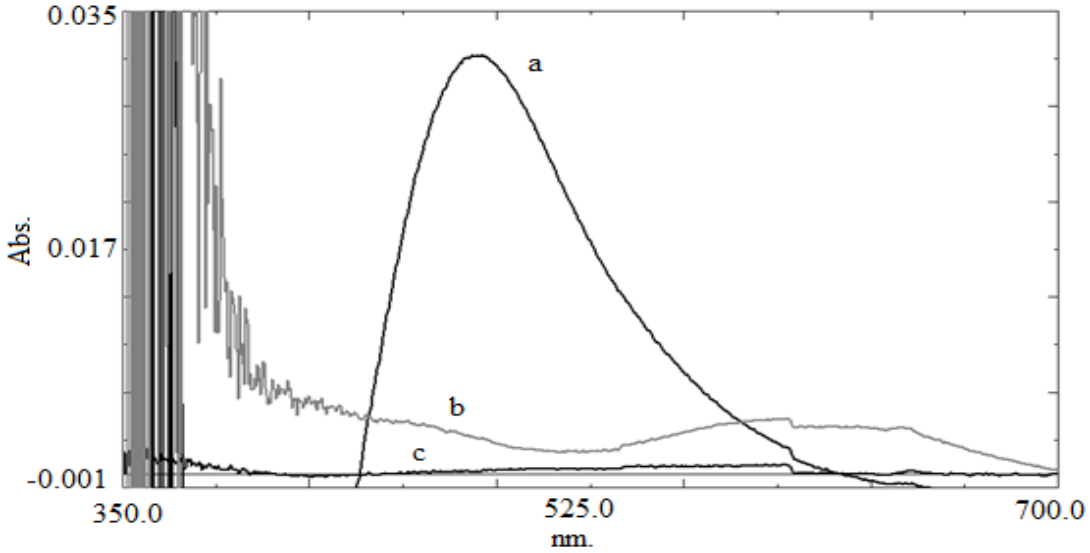

Figure 4.1. Absorption spectra of pure ionic liquids a) IL-III λ^{Abs}_{max} =483.1 A=0.032 b) IL-II λ^{Abs}_{max} =598 A=0.004 c) IL-I λ^{Abs}_{max} =598 A=0.001

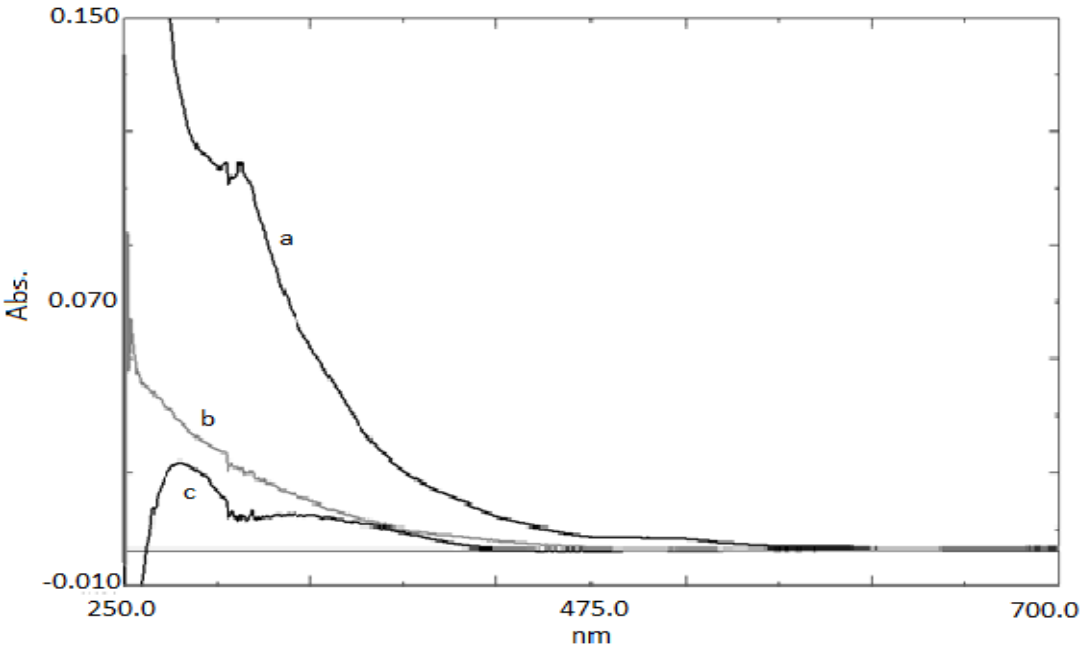

Figure 4.2 Absorption spectra of 1% (by volume) IL-buffer binary mixtures at pH 5. 0 a) IL-I b) IL-II c) IL-III

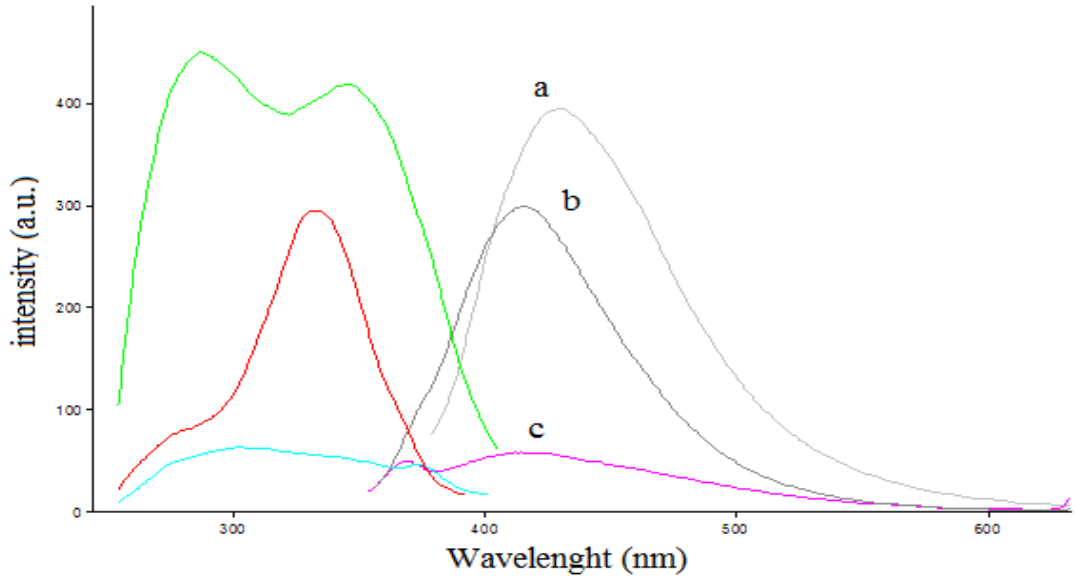

Figure 4.3 Emission and excitation s spectra of 1% (by volume) IL-buffer binary mixtures at pH 5. 0 a) IL-II λ^{ex}_{max}=345nm, λ^{em}_{max}=429nm b) IL-I λ^{ex}_{max}=332nm, λ^{em}_{max}=415nm c) IL-III λ^{ex}_{max}=303nm, λ^{em}_{max}=413nm

Table 4.1. UV/Vis spectra related data of ionic liquids.

Ionic Liquids	Concentration (M)	λ^{Abs}_{max} (nm)	Absorbance	ε
IL-I	0.0532	276	0.025	0.469
IL-II	0.0654	298	0.027	0.413
IL-III	0.0542	309	0.107	1.974

Table 4.2 Emission-excitation spectra related data of ionic liquids.

Ionic Liquids	Concentration (M)	λ^{ex}_{max} (nm)	λ^{em}_{max} (nm)	Stoke's shift	Slit range	Θ_F
IL-I	0.0532	332	415	83	10-10	0.38
IL-II	0.0654	345	429	84	10-10	0.23
IL-III	0.0542	303	413	110	10-10	0.028

In all of the employed matrices the Stoke's shift values, $\Delta\lambda_{ST}$ (the difference between excitation and emission maximum), calculated from the spectral data are quietly high. Stoke's shift is important for fluorescence and optical sensor studies because the high Stoke's shift value allows the emitted fluorescence photons to be easily distinguished from the excitation photons, leading to the possibility of very low background signals and permits the usage of ionic liquids in the construction of fiber optic sensor.

Quantum yield calculations

The fluorescence quantum yield of ionic liquids (IL-I, IL-II, IL-III) in pH 5.0 acetic acid acetate buffer was calculated by William's Method. The Williams method and the calculation of quantum yield values was explained in detail in Chapter 2. For this purpose, the emission spectra of five different concentrations of reference standard (quinine sulfate) were recorded by exciting at 303, 332, 345 nm (Figure 4.4 and 4.5). By similar way, the emission spectra of the five different concentrations of the ionic liquids were recorded (Figure 4.6, 4.7 and 4.8). The integrated fluorescence intensities were plotted vs absorbance for the reference standard, and the ionic liquids. The ratio of gradients of the plots is important and proportional to the quantum yield. The linearized plots of the ionic IL-I, IL-II, IL-III in buffer at pH5 can be described by equations and the relevant correlation coefficients of [y=271130x, R^2= 0.995] , [y=174580x, R^2=0.987] and [y=17415x, R^2=0.9833], respectively. For quantum yield standard; quinine sulfate, the equations are [y=245729x, R_2=0.9912] . The data are also shown in Table 4.2.

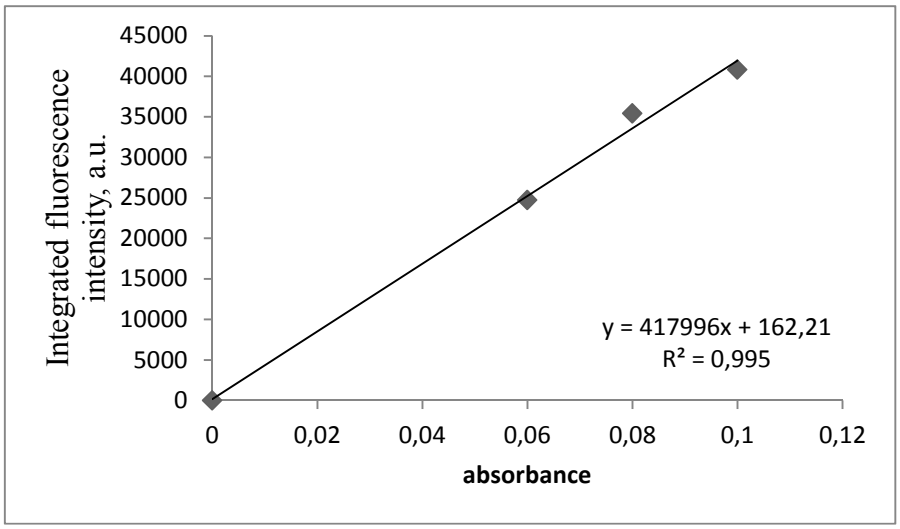

Figure 4.4 The integrated fluorescence intensities vs absorbance values of quinine sulfate in 0.1M H_2SO_4 (excitation at 303 nm).

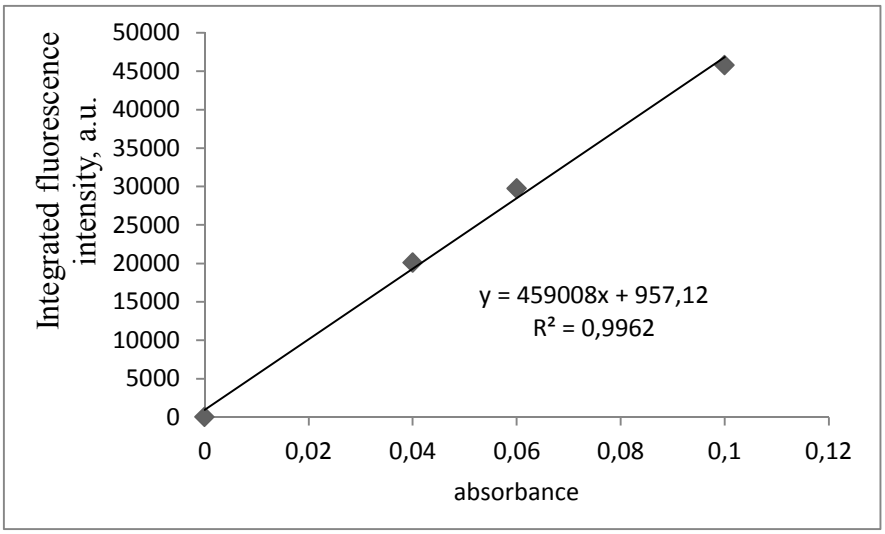

Figure 4.5 The integrated fluorescence intensities vs absorbance values of quinine sulfate in 0.1M H_2SO_4 (excitation at 332 nm).

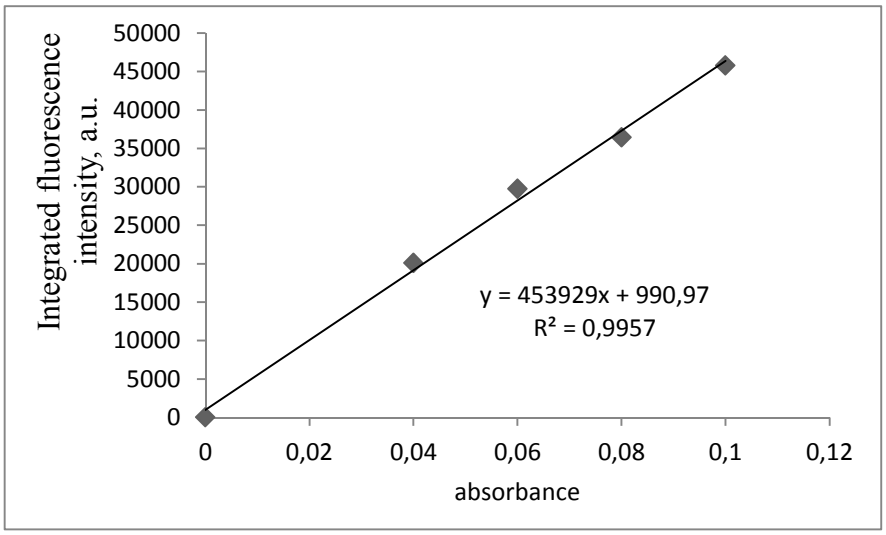

Figure 4.6 The integrated fluorescence intensities vs absorbance values of quinine sulfate in 0.1M H_2SO_4 (excitation at 345 nm).

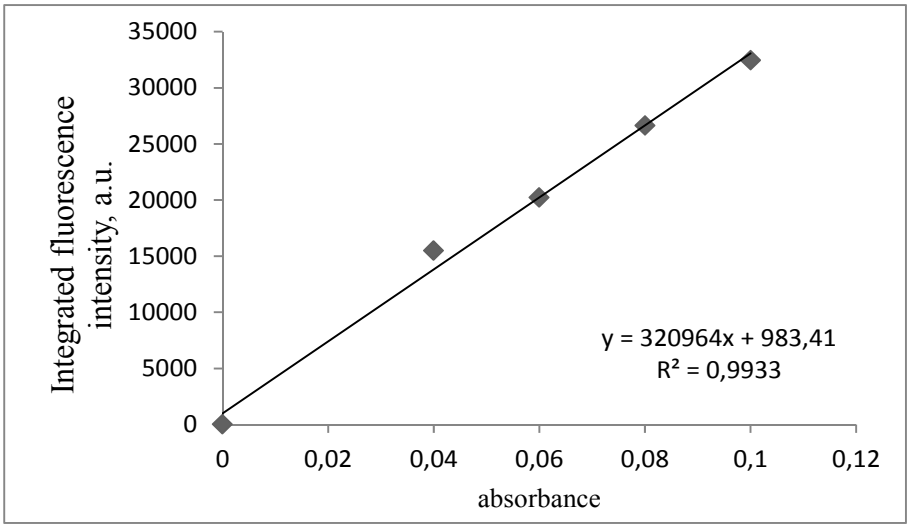

Figure 4.7 The integrated fluorescence intensities vs absorbance values of IL-I in buffer at pH5.

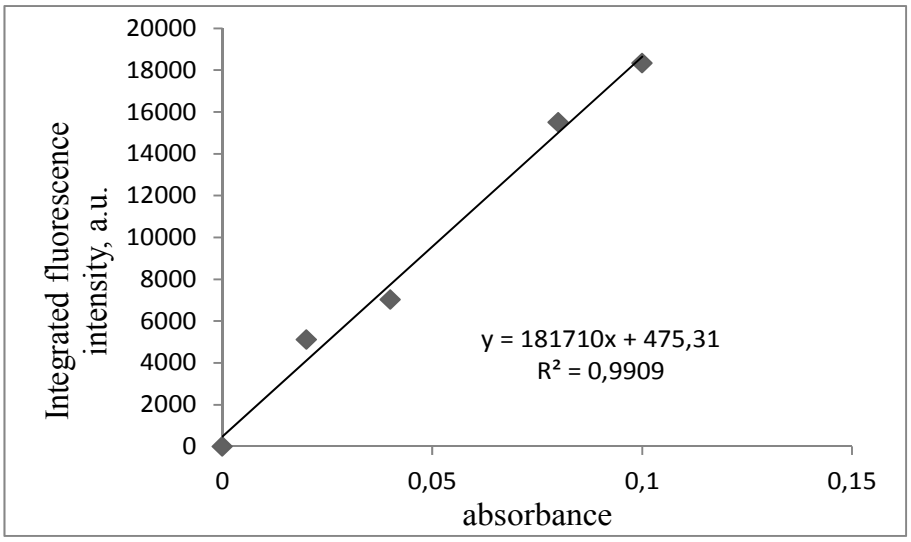

Figure 4.8 The integrated fluorescence intensities vs absorbance values of IL-II in buffer at pH5.

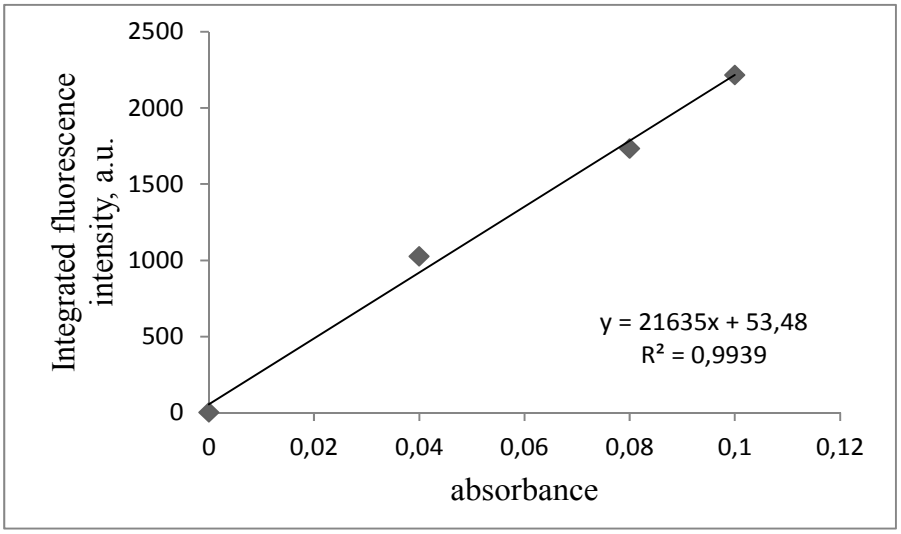

Figure 4.9 The integrated fluorescence intensities vs absorbance values of IL-I in buffer at pH5.

4.3.2 Effect of the pH

The effect of pH on the fluorescence characteristics of ionic liquids were investigated for three pH values (pH 2.0, 5.0 and 10.0) including acidic, slightly acidic and basic region. The emission and excitation based data were shown in Figure 4.9, 4.10, 4. 11. According to the data, the fluorescence intensities of all the

ionic liquids are affected from the pH changes. The relative signal changes due to the pH is maximum for IL-I. Besides, the fluorescence intensities of all of the ionic liquids decrease in strongly acidic and basic media. The maximum fluorescence is observed from slightly acidic to neutral pHs. Because of this the metal response studies of ionic liquids were performed at pH 5.0.

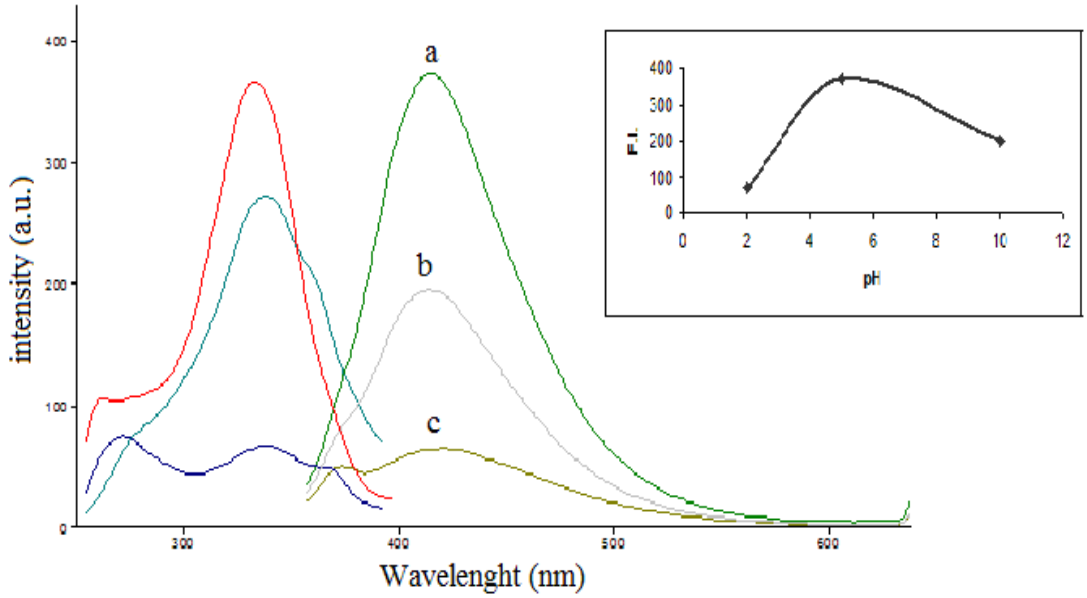

Figure 4.9 pH induced emission spectra of the IL-I after exposure to 1M HNO_3 and 1M NaOH (a) pH5.0 (b) pH10 (c) pH2.0

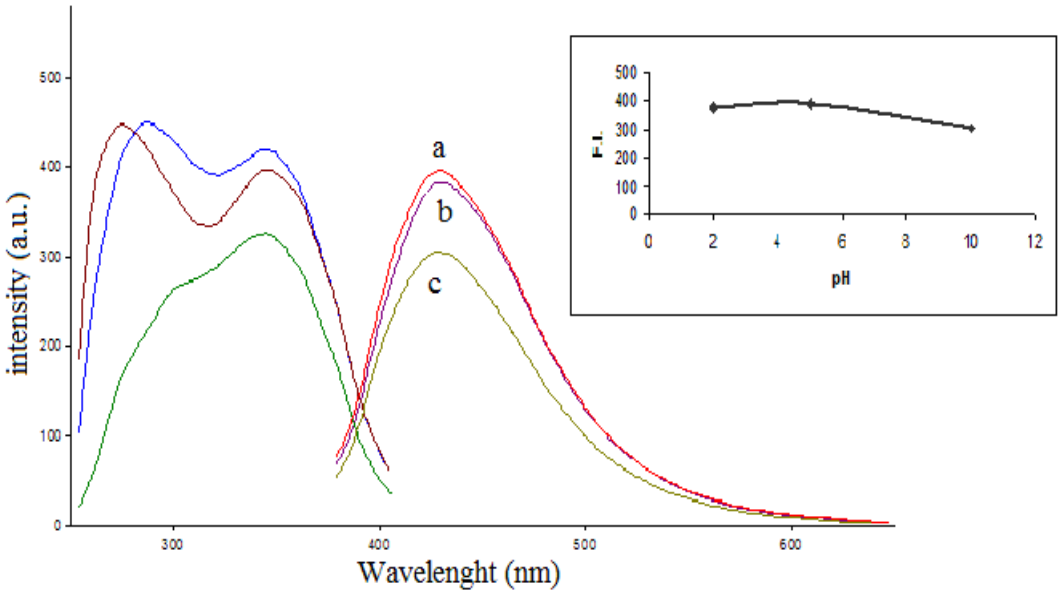

Figure 4.10 pH induced emission spectra of the IL-II after exposure to 1M HNO_3 and 1M NaOH (a) pH5.0 (b) pH2.0 (c) pH10

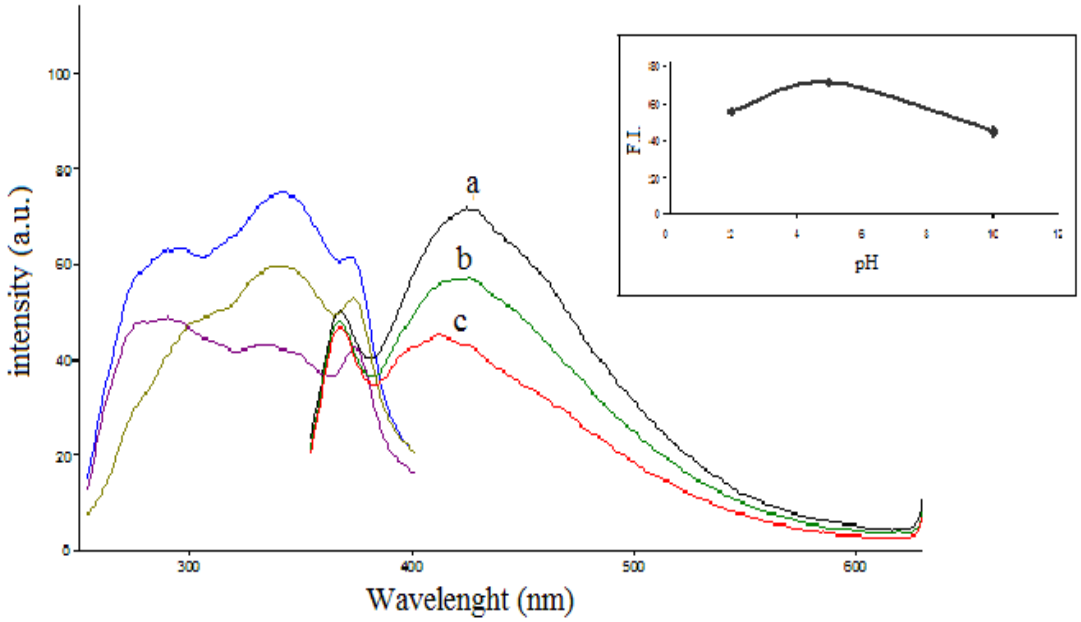

Figure 4.11 pH induced emission spectra of the IL-III after exposure to 1M HNO_3 and 1M NaOH (a) pH5.0 (b) pH2.0 (c) pH10

4.3.3 Response of Ionic Liquids to Different Metal Ion

Response of ionic liquids to metal ions was investigated by exposure to 1.0 mgL^{-} solutions of Ca^{2+},Cu^{2+}, Hg^{+}, Hg^{2+}, As^{5+}, Mo^{2+}, Li^{+}, $Pb^{2+,}$ Al^{3+}, Cr^{3+},Na^{+}, Mg^{2+}, Zn^{2+}, Cd^{2+}, Fe^{2+}, Fe^{3+}, Co^{2+} and Ni^{2+}. The solutions contain 1% IL-pH 5.0 buffer mixture (by volume) and $1mgL^{-1}$ metal ions.

4.3.3.1 Response of IL-I to Different Metal Ions

Figure 4.12, 4.13, 4.14 and Table 4.3 reveal excitation-emission-based response of IL-I to the metal cations in acetic acid/acetate buffered solutions at pH 5.0. Results were plotted as relative signal changes, $((I_0-I)/I_0)$, where I is the fluorescence intensity of the sensor membrane after exposure to ion-containing solutions and I_0 is the fluorescence intensity of the sensor slide in ion-free buffer solution. The fluorescence intensity of IL-I decreased by the addition of the metal ions was between 8 %-25 %. The maximum response was seen for iron ions.

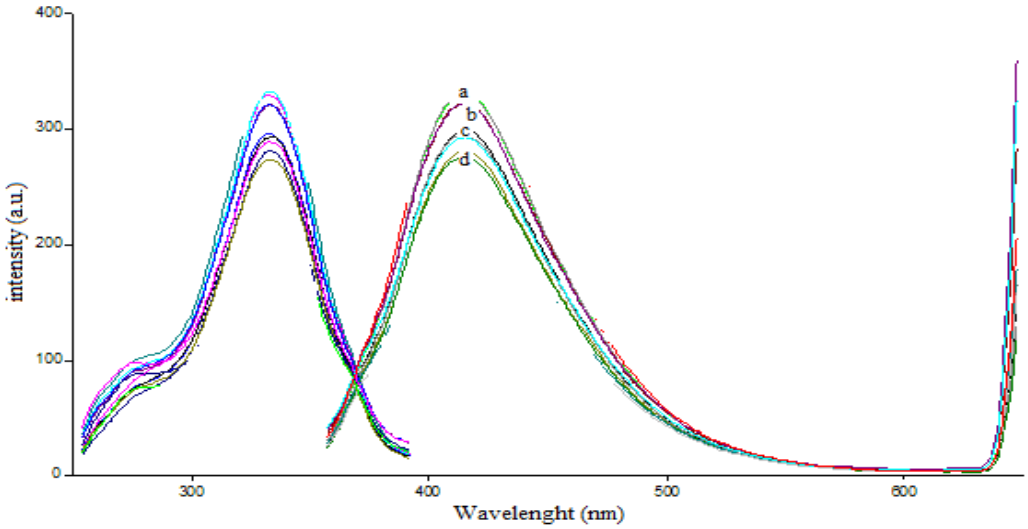

Figure 4.12 Emission and excitation based response of IL-I to metal ions, a) IL –buffer mixture, b) Ca^{2+} , Li^{+} c) Cr^{2+}, Al^{3+} d) Mg^{2+}, Ni^{2+}

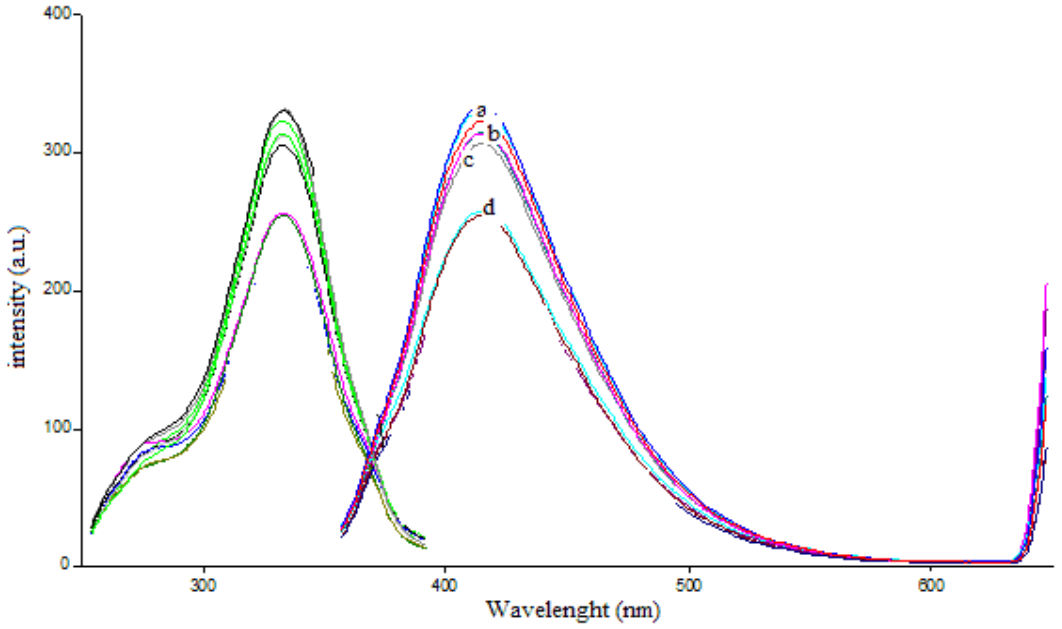

Figure 4.13 Emission and excitation based response of IL-I to metal ions, a) IL –buffer mixture, Co^{2+}, Zn^{2+} b) Mn^{2+}, As^{2+} c) Cu^{2+}, d) Fe^{2+}, Fe^{3+}

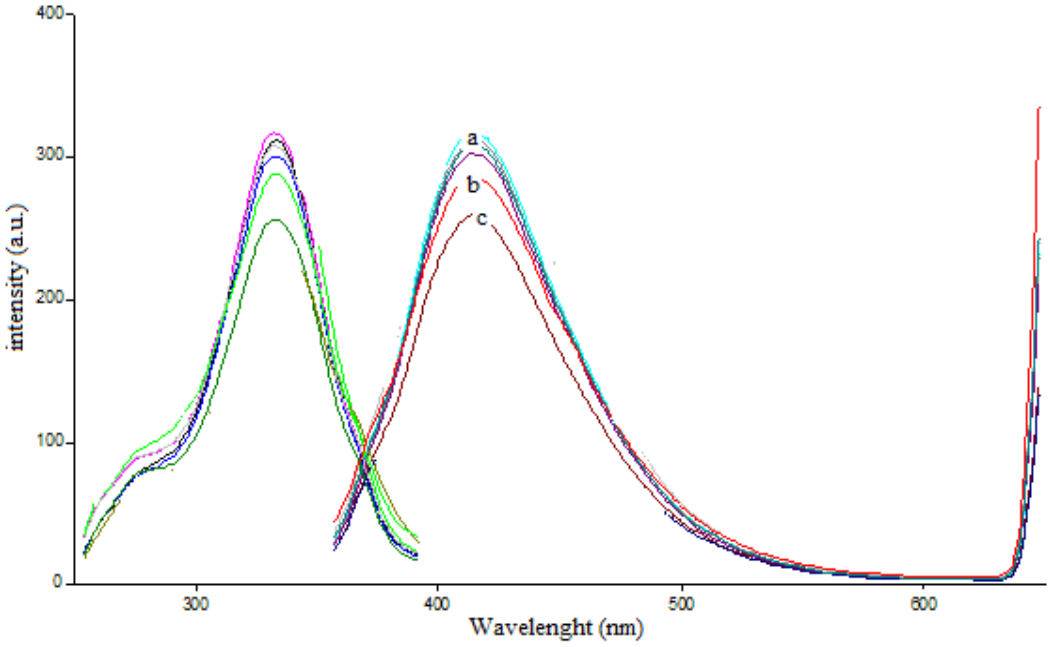

Figure 4.14 Emission and excitation based response of IL-I to metal ions, a) IL –buffer mixture, Hg^{2+}, Hg^{+}, Na^{+}, Mo^{2+} b) Pb^{2+} c) Cd^{2+}

Table 4.3 Emission spectra related data of response of IL-I to the metal cations in the solvents of 1%IL-I-buffer mixture (by volume)

Metal Cations	λ_{max}^{ex} (nm)	λ_{max}^{em} (nm)	Fluorescence Intensity (a.u.) for Excitation	Fluorescence Intensity (a.u.) for Emission
-	332	415	351	350
Al^{3+}	332	415	261	255
Cd^{2+}	331	413	325	328
Ca^{2+}	330	413	348	347
Pb^{2+}	332	415	285	285
Co^{2+}	332	415	348	345
Cu^{2+}	331	414	301	299
Cr^{2+}	331	415	292	289
Na^{+}	330	412	351	349
Mn^{2+}	330	411	257	253
Mg^{2+}	332	415	258	256
Ni^{2+}	330	411	252	248
As^{5+}	329	412	232	229
Mo^{2+}	329	415	314	312
Li^{+}	332	415	338	340
Hg^{+}	332	415	333	335
Hg^{2+}	332	415	340	342
Fe^{2+}	330	412	233	231
Fe^{3+}	330	412	249	247
Zn^{2+}	332	415	348	347

4.3.3.2 Response of IL-II to Different Metal Ions

Figure 4.15, 4.16, 4.17 and Table 4.4 reveal excitation-emission-based response of IL-II to the metal cations in acetic acid/acetate buffered solutions at pH 5.0. The fluorescence intensity of IL-II was effected as a decrease in fluorescence intensity for all of the ions except mercury ions in the range of 5%-8%. The maximum response was observed for iron ions. Mercury ions caused an 8 % increase in fluorescence intensity.

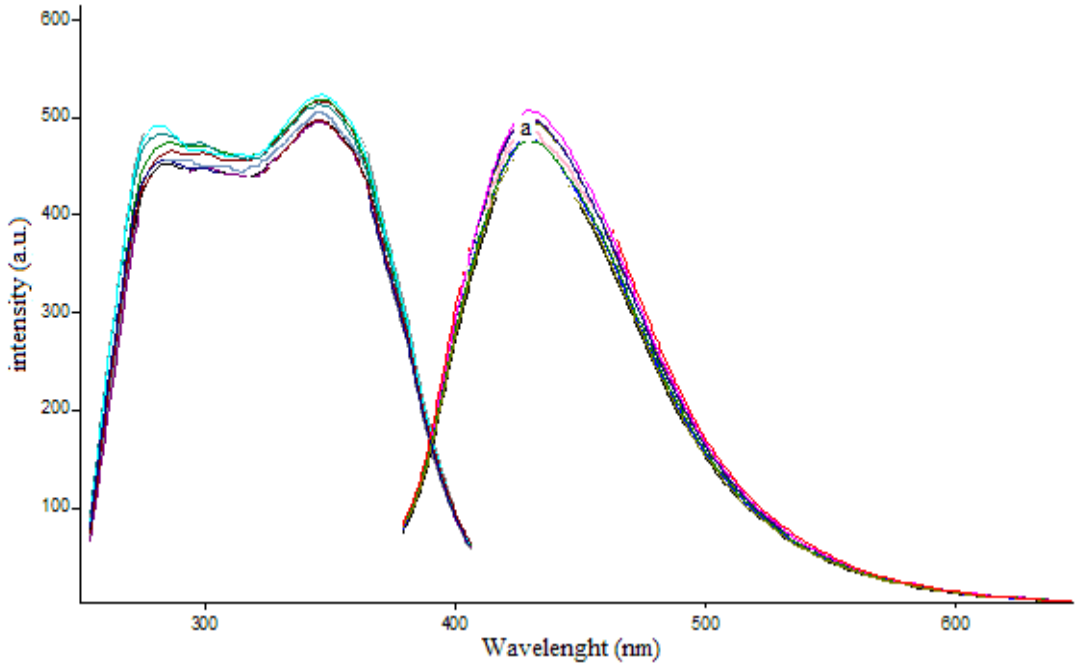

Figure 4.15 Emission and excitation based response of IL-II to metal ions, a) IL –buffer mixture, Hg^{2+}, Hg^{+}, Fe^{2+}, Fe^{3+} ,Ca^{2+}, Co^{2+}

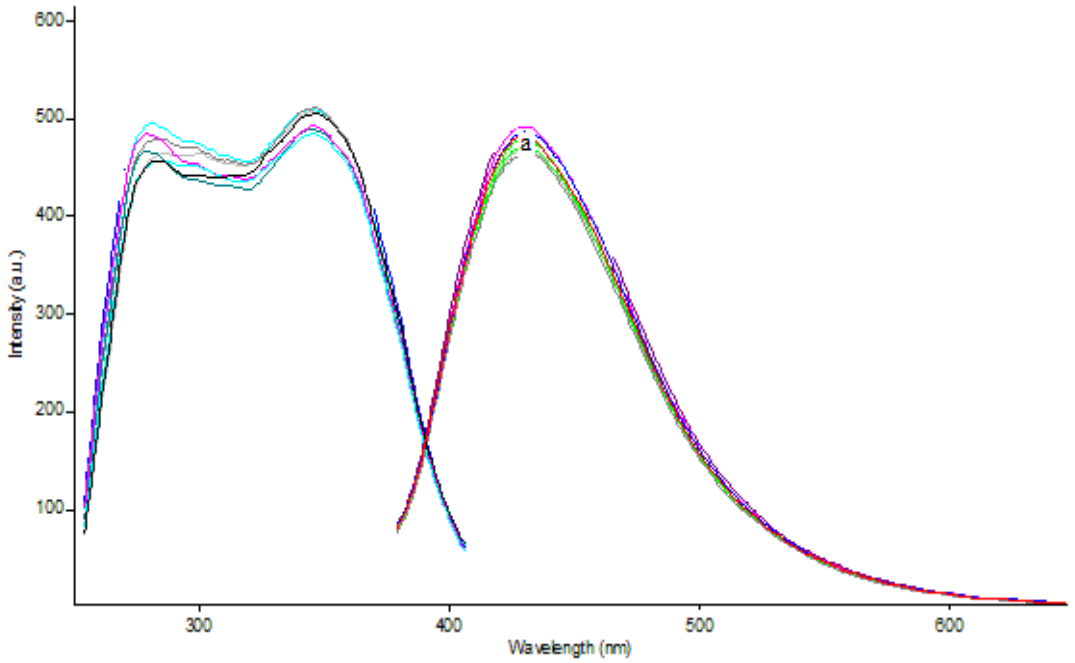

Figure 4.16 Emission and excitation based response of IL-II to metal ions, a) IL –buffer mixture, Na^{+} , Li^{+}, Zn^{2+}, Mn^{2+}, Cr^{2+}, Mg^{2+}, As^{5+}, Ni^{2+}

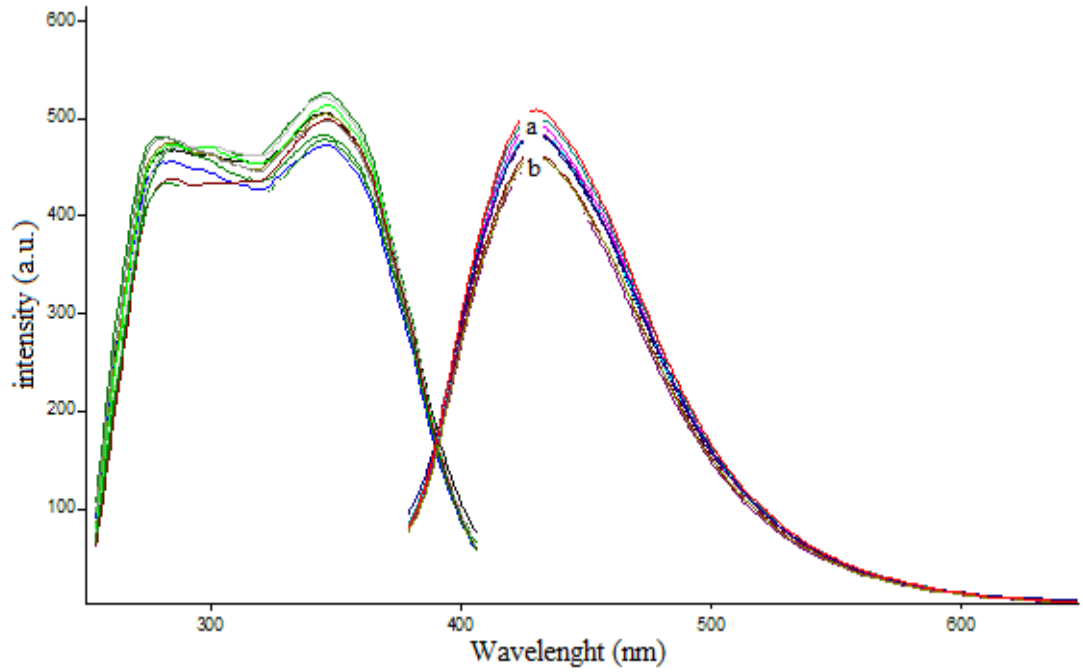

Figure 4.17 Emission and excitation based response of IL-II to metal ions, a) IL –buffer mixture, Al^{3+}, Cu^{2+}, Na^{+}, Pb^{2+}, Cd^{2+}

Table 4.4 Emission spectra related data of response of IL-II to the metal cations in the solvents of 1%IL-II-buffer mixture (by volume)

Metal Cations	λ_{max}^{ex} (nm)	λ_{max}^{em} (nm)	Fluorescence Intensity (a.u.) for Excitation	Fluorescence Intensity (a.u.) for Emission
-	345	429	497	496
Al^{3+}	345	428	508	505
Cd^{2+}	343	429	490	490
Ca^{2+}	343	428	475	476
Pb^{2+}	345	428	477	475
Co^{2+}	345	427	492	490
Cu^{2+}	344	428	478	475
Cr^{2+}	345	427	482	480
Na^{+}	344	427	486	486
Mn^{2+}	346	429	495	493
Mg^{2+}	345	429	493	495
Ni^{2+}	344	429	489	487
As^{5+}	344	430	487	485
Mo^{2+}	345	429	452	450
Li^{+}	345	428	490	490
Hg^{+}	345	430	485	487
Hg^{2+}	344	429	537	537
Fe^{2+}	346	429	487	487
Fe^{3+}	346	429	487	488
Zn^{2+}	345	428	495	496

4.3.3.3 Response of IL-III to Different Metal Ions

Figure 4.18, 4.19 and Table 4.5 reveal excitation-emission-based response of IL-III to the metal cations in acetic acid/acetate buffered solutions at pH 5.0. The fluorescence intensity of IL-III was affected as a decrease in fluorescence intensity in the range of 7 %-26%. The maximum response was observed for iron ions and for IL-III. Because of this further experiments were performed with IL-III for iron sensing purposes. The absorption spectra for IL-III-iron mixtures were also investigated because of the SCN^- group of the IL (Figure 4.21). As expected, the relative signal change was higher in absorption spectra of IL-III-iron mixtures. The IL exhibited a new absorption peak at 460 nm. IL-III was also evaluated in case of the affect of the other metals and the spectra can be seen in Figures

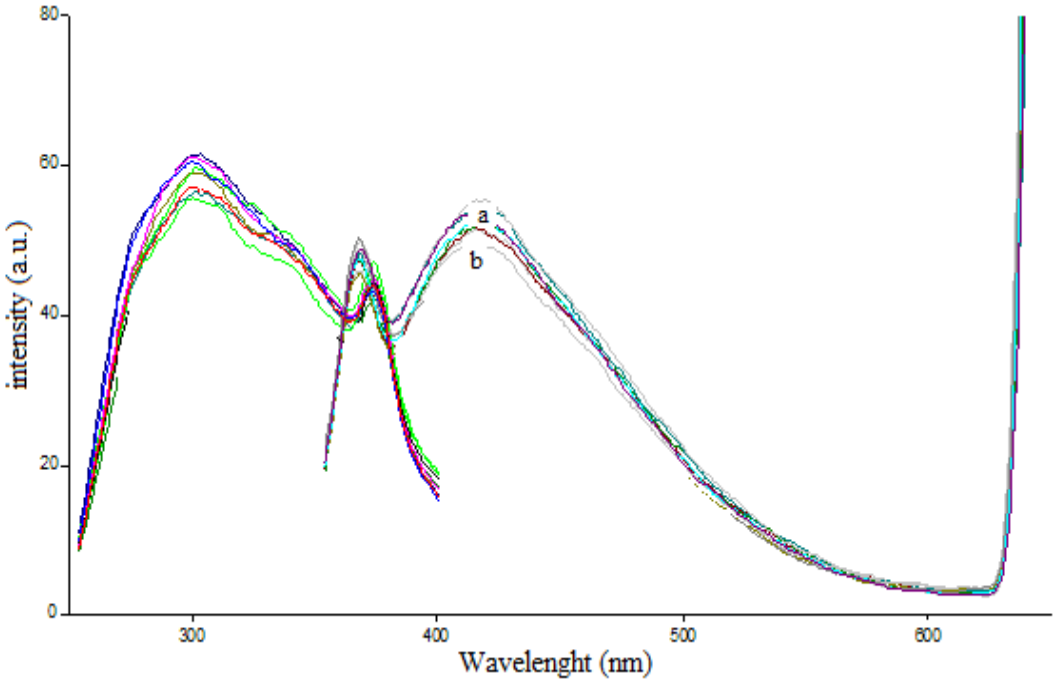

Figure 4.18 Emission and excitation based response of IL-III to metal ions, a) IL –buffer mixture, Hg^{2+}, Ca^{2+}, Co^{2+} , Cu^{2+}, Na^{+}, b) Mo^{2+}

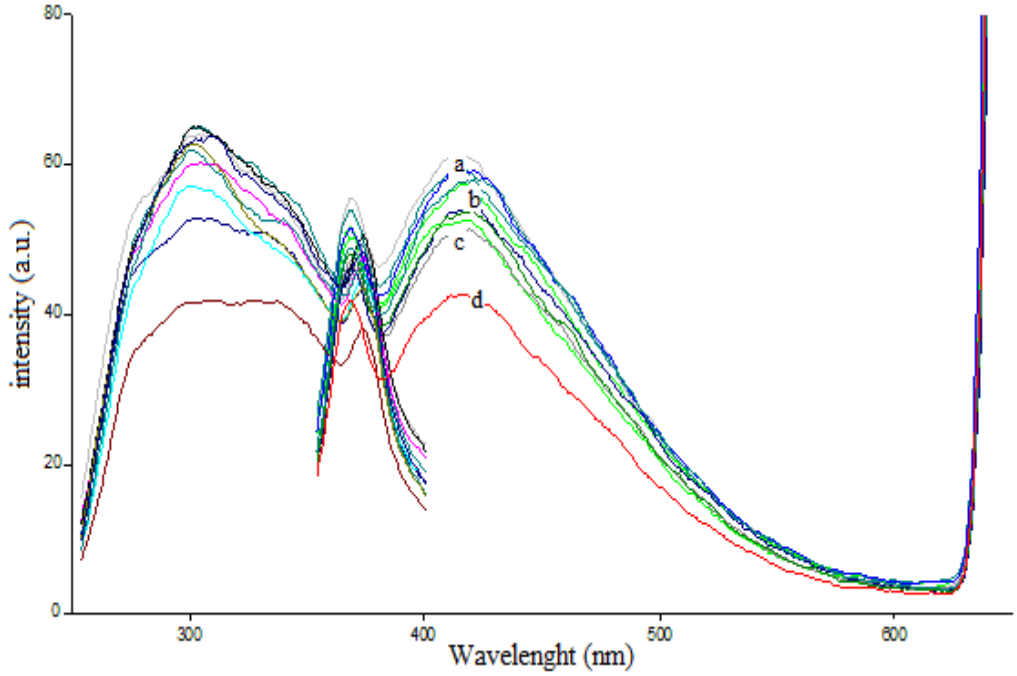

Figure 4.19 Emission and excitation based response of IL-III to metal ions, a) IL –buffer mixture, Hg^{+}, Li^{2+}, b) Ni^{2+}, Mg^{2+}, Mn^{2+}, As^{5+}, Cu^{2+}, Cu^{2+} , Cr^{2+}, Al^{3+} c) Fe^{3+} d) Fe^{3+}

Table 4.5 Emission spectra related data of response of IL-III to the metal cations in the solvents of 1%IL-III-buffer mixture (by volume)

Metal Cations	λ_{max}^{ex} (nm)	λ_{max}^{em} (nm)	Fluorescence Intensity (a.u.) for Excitation	Fluorescence Intensity (a.u.) for Emission
-	303	413	58	63
Al^{3+}	302	41	58	61
Cd^{2+}	303	412	55	49
Ca^{2+}	303	413	58	51
Pb^{2+}	302	411	59	54
Co^{2+}	303	413	59	53
Cu^{2+}	302	412	48	46
Cr^{2+}	302	411	52	47
Na^{+}	303	412	58	52
Mn^{2+}	303	412	57	52
Mg^{2+}	301	413	59	51
Ni^{2+}	301	413	56	50
As^{5+}	300	415	60	58
Mo^{2+}	303	411	53	51
Li^{+}	302	413	54	52
Hg^{+}	303	412	53	50
Hg^{2+}	304	412	56	52
Fe^{2+}	303	416	45	42
Fe^{3+}	303	416	50	49
Zn^{2+}	301	414	54	52

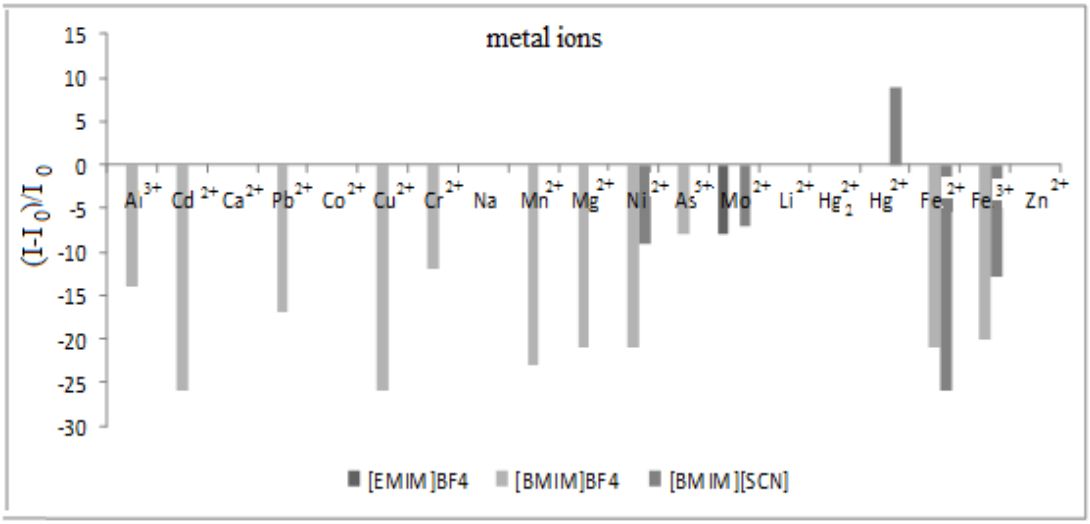

Figure 4.20 Metal-ion response test results for ionic liquids in pH5 buffer. Results are plotted in terms of signal changes, $((I_0-I)/I_0)$, where I is the fluorescence intensity of the sensor membrane after exposure to ion-containing solutions and I_0 is the fluorescence intensity of the sensor slide in ion-free buffer solution.

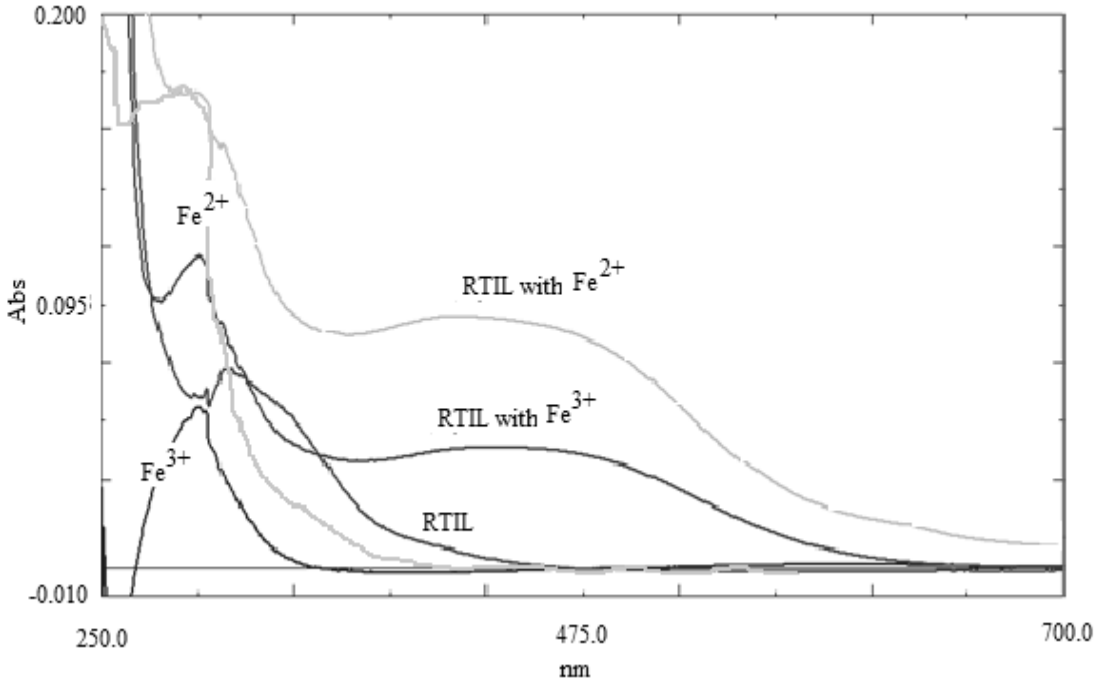

Figure 4.21 Absorption based response of IL-III to Fe^{2+} and Fe^{3+} ions

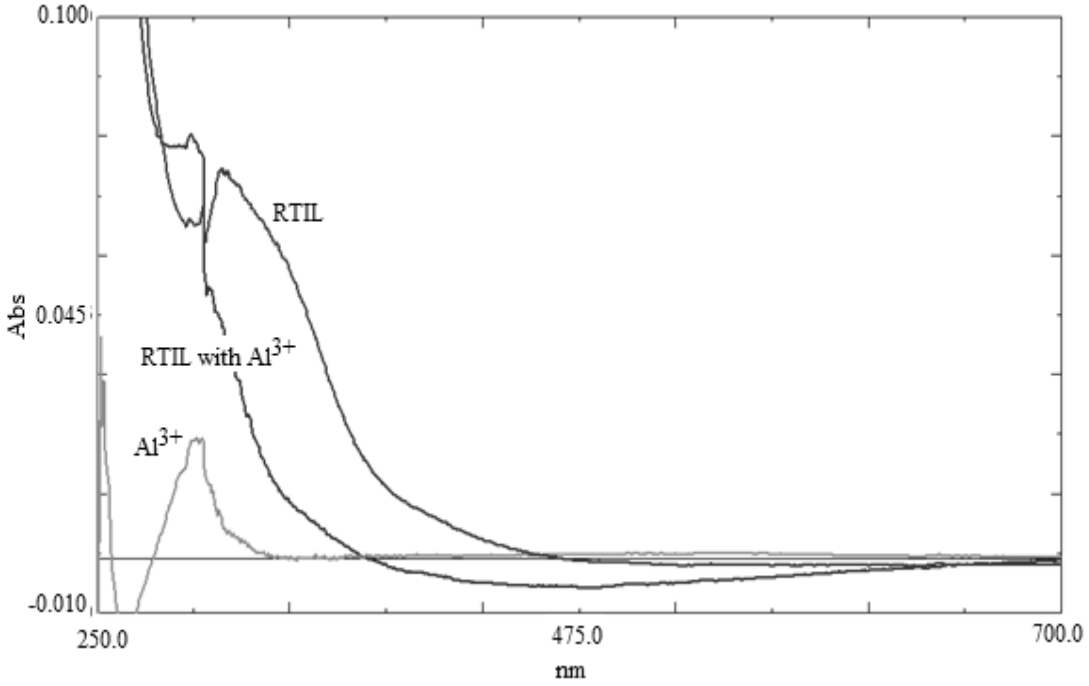

Figure 4.22 Absorption based response of IL-III to Al^{3+} ion

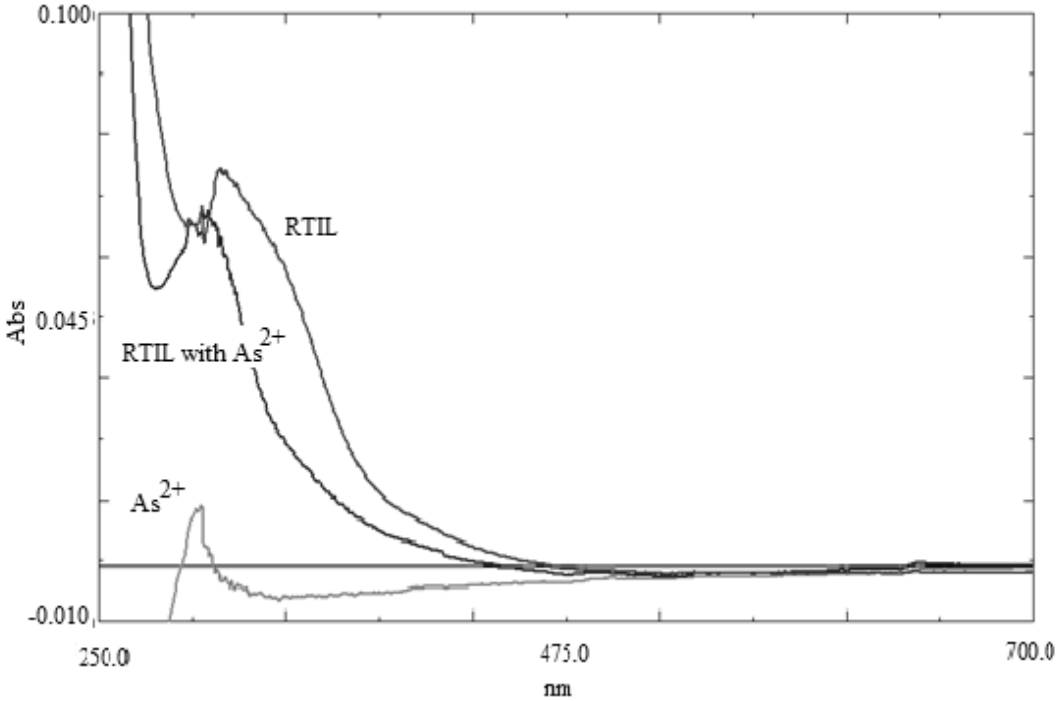

Figure 4.23 Absorption based response of IL-III to As^{5+} ion

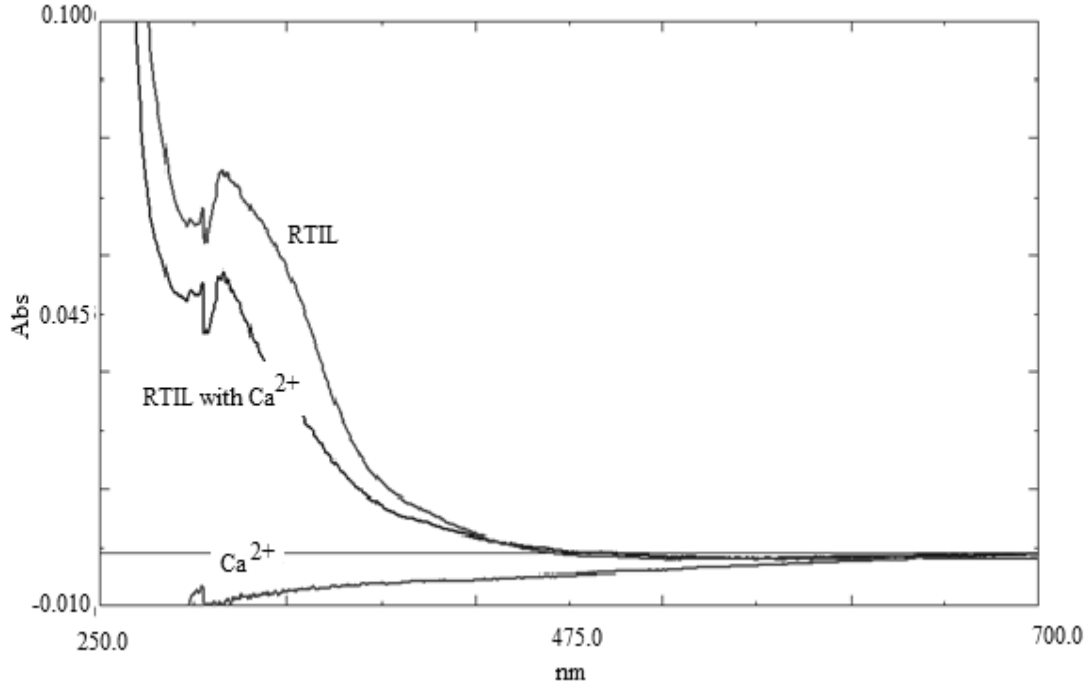

Figure 4.24 Absorption based response of IL-III to Ca^{2+} ion

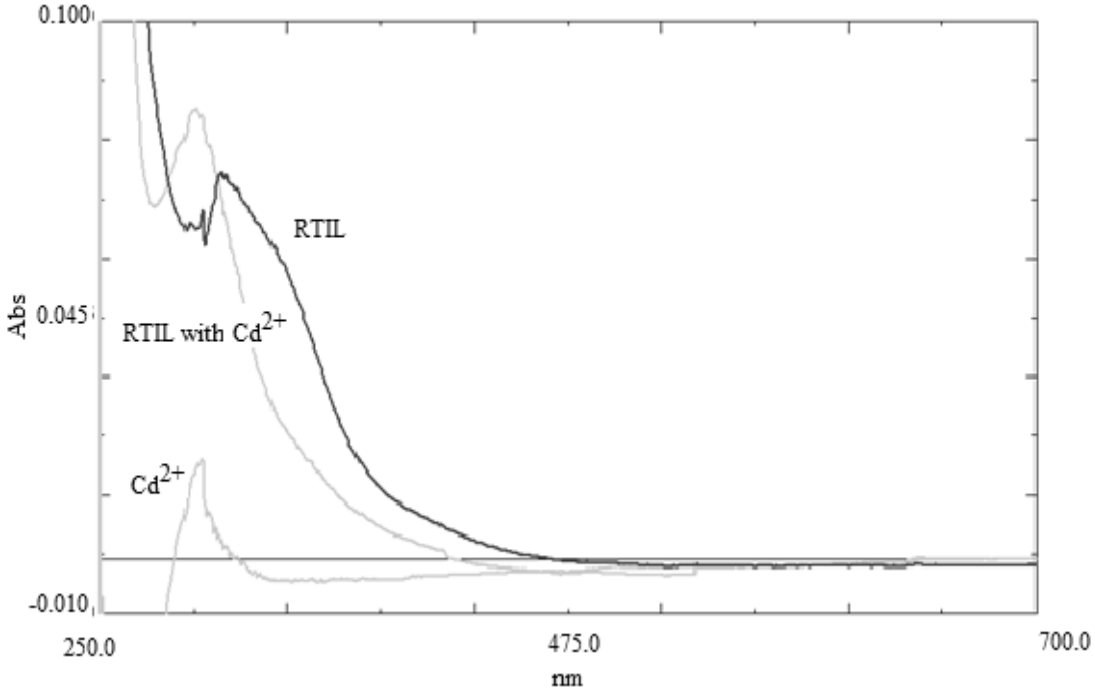

Figure 4.25. Absorption based response of IL-III to Cd^{2+} ion

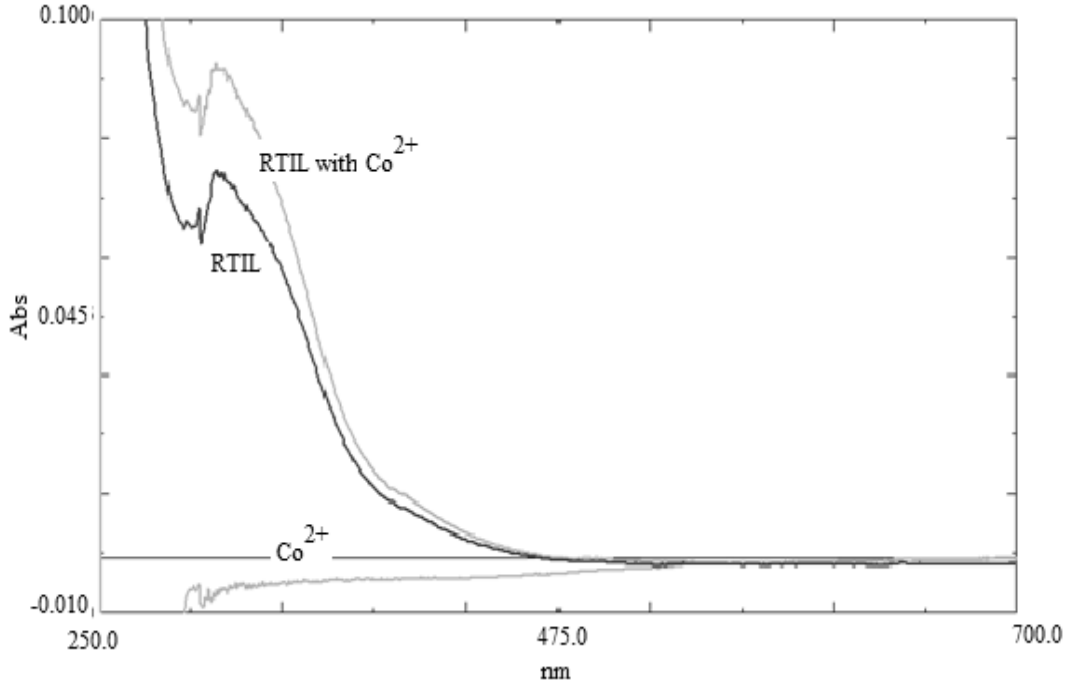

Figure 4.26. Absorption based response of IL-III to Co^{2+} ion

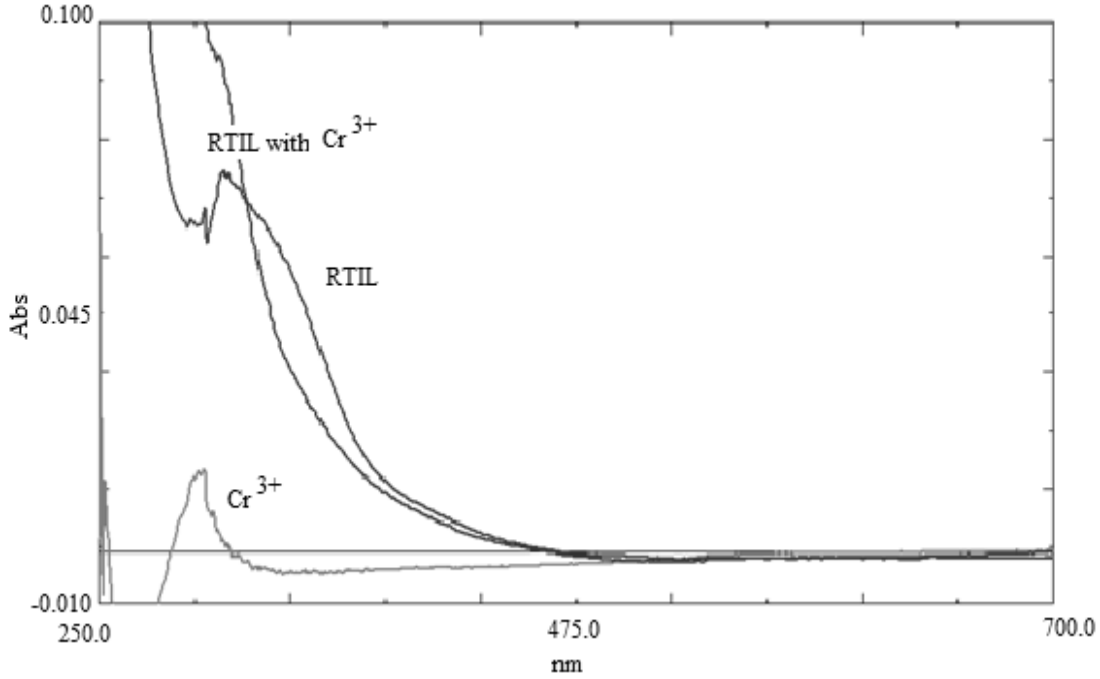

Figure 4.27 Absorption based response of IL-III to Cr^{3+} ion

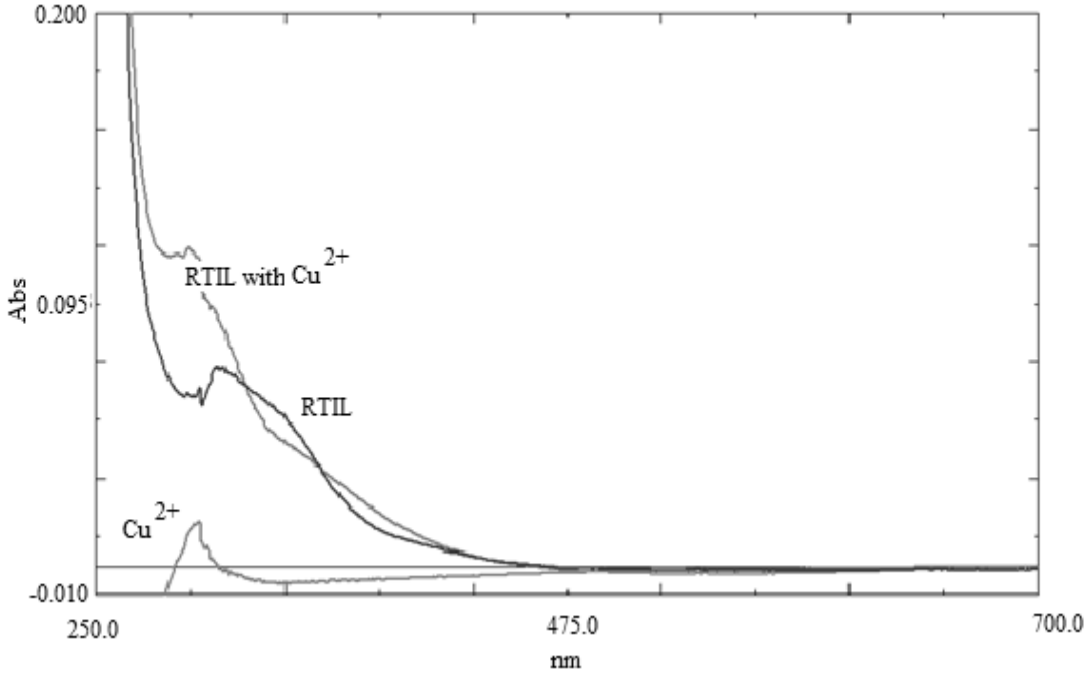

Figure 4.28 Absorption based response of IL-III to Cu^{2+} ion

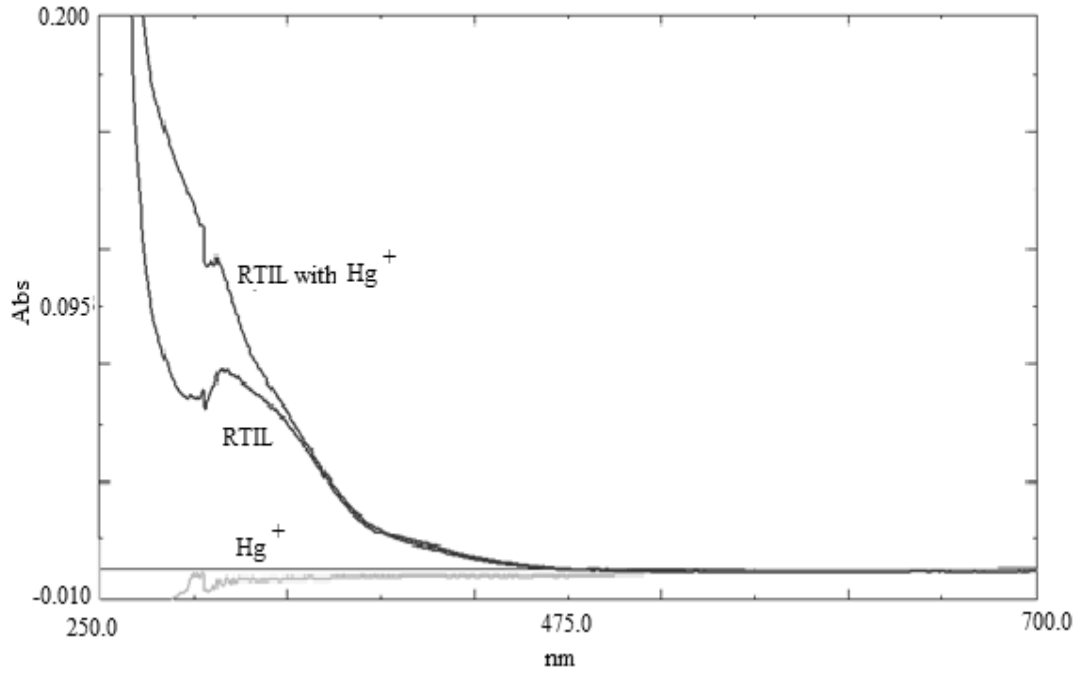

Figure 4.29 Absorption based response of IL-III to Hg_2^{2+} ion

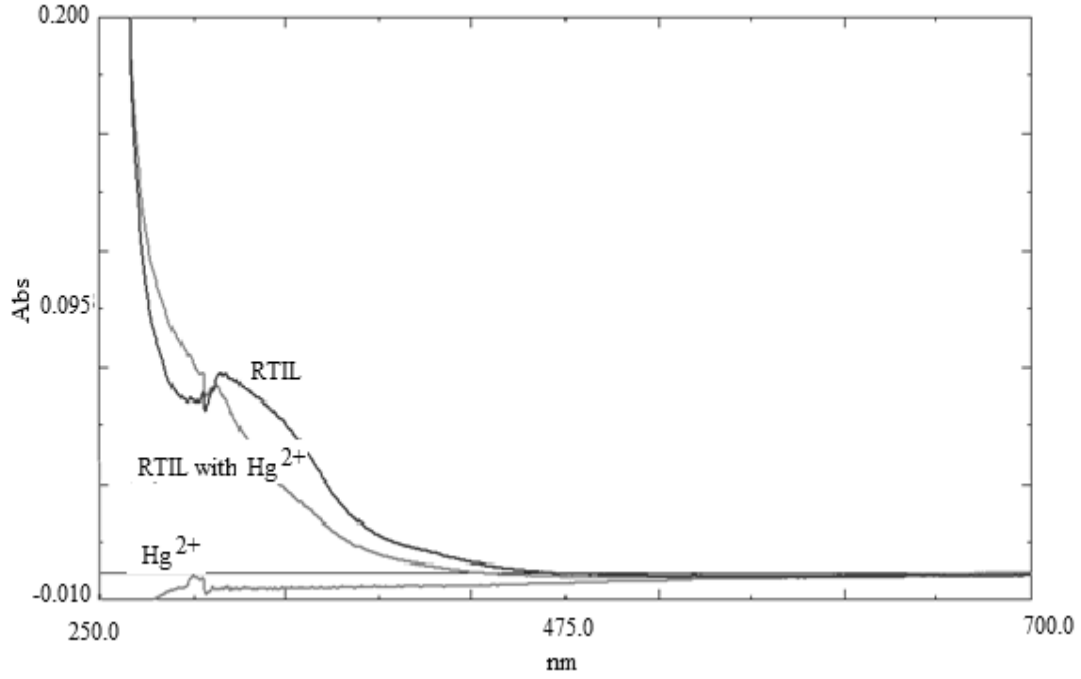

Figure 4.30 Absorption based response of IL-III to Hg^{2+} ion

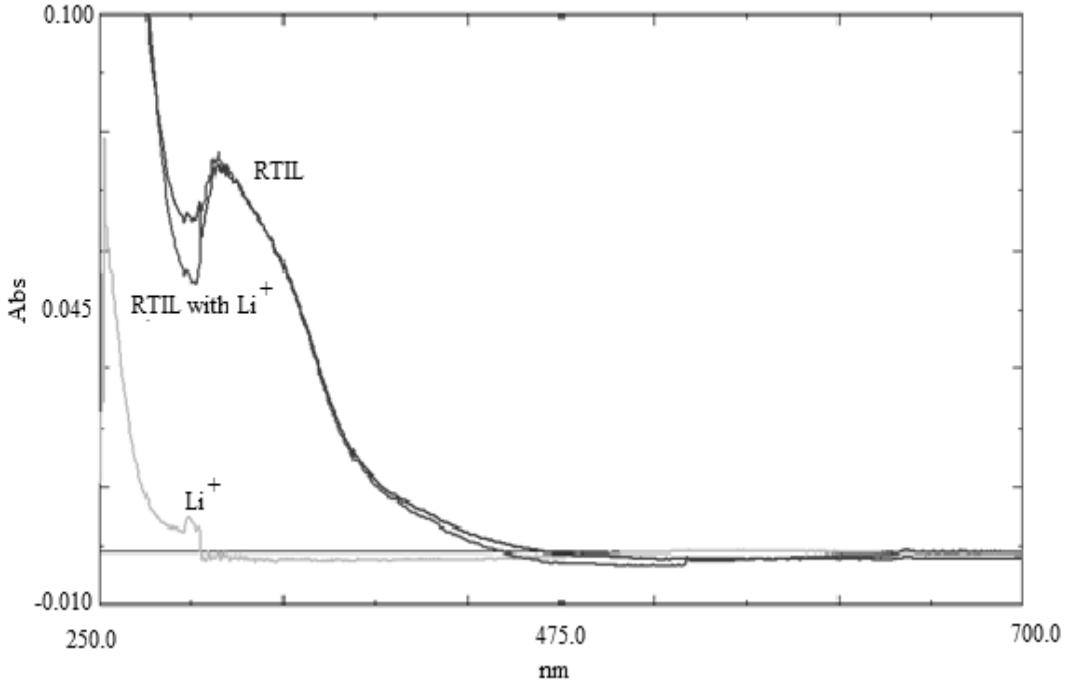

Figure 4.31 Absorption based response of IL-III to Li^{+} ion

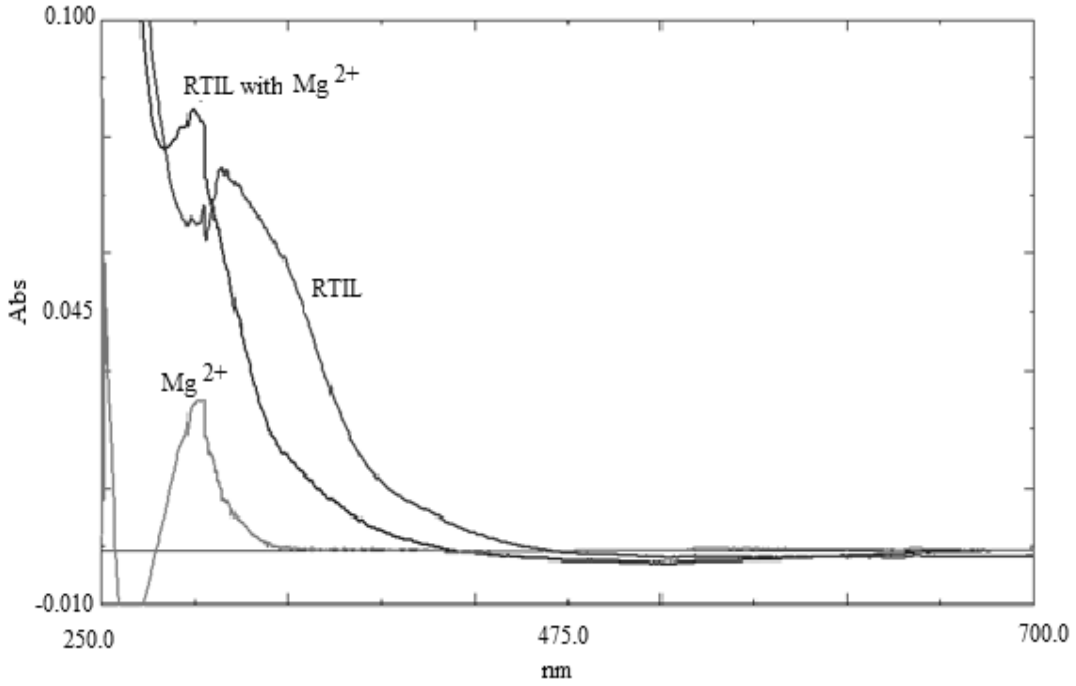

Figure 4.32 Absorption based response of IL-III to Mg^{2+} ion

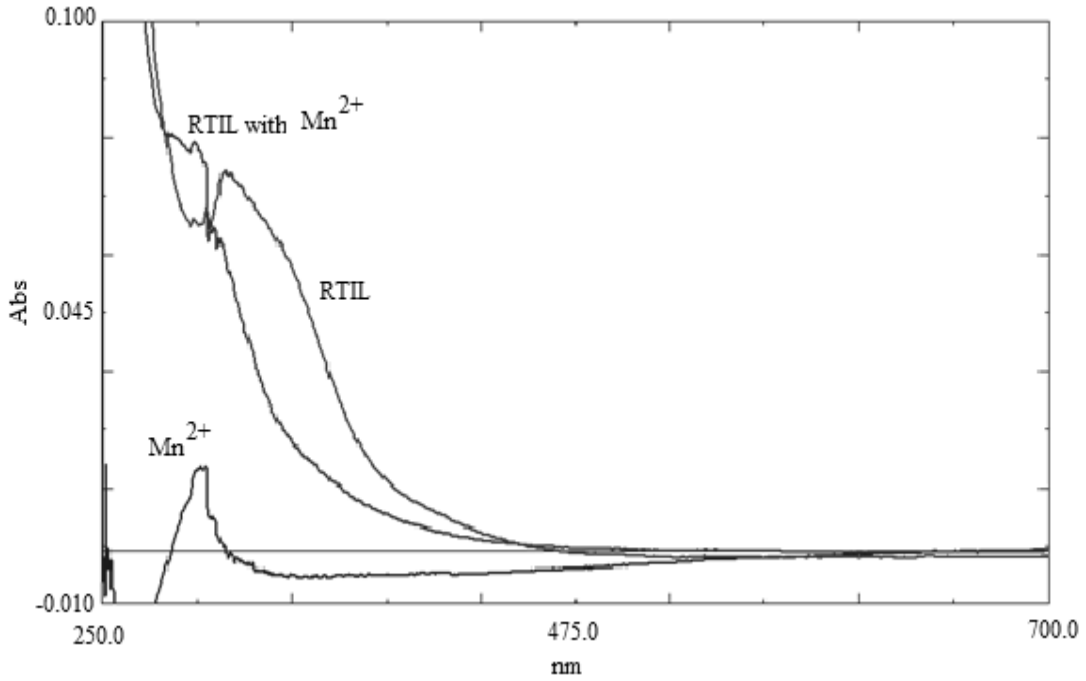

Figure 4.33 Absorption based response of IL-III to Mn^{2+} ion

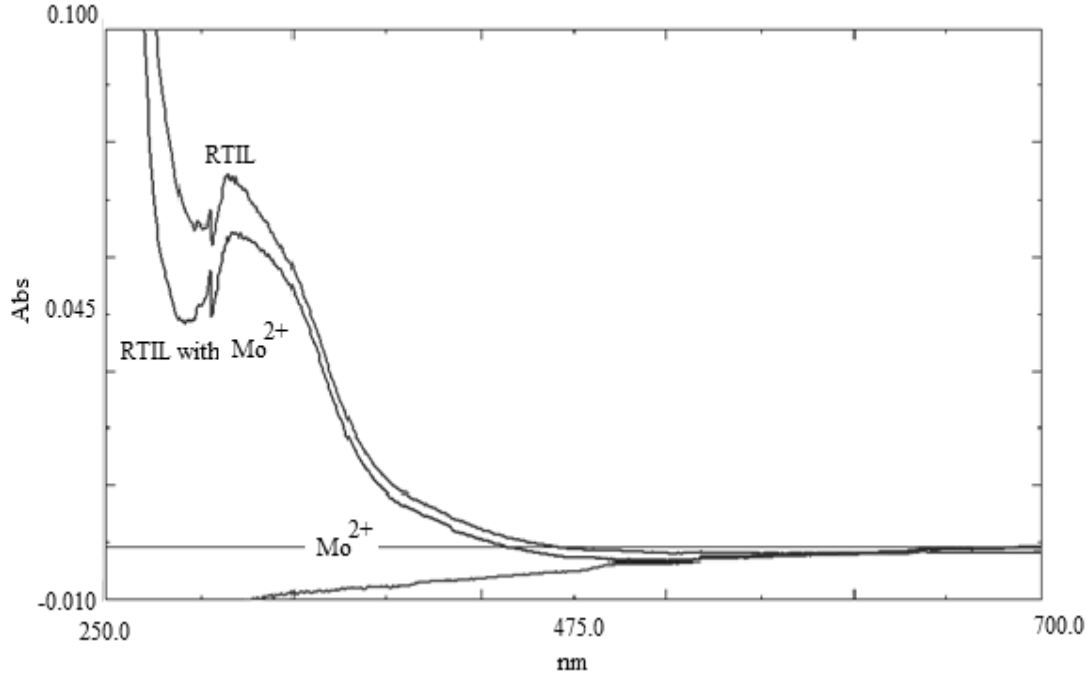

Figure 4.34 Absorption based response of IL-III to Mo^{2+} ion

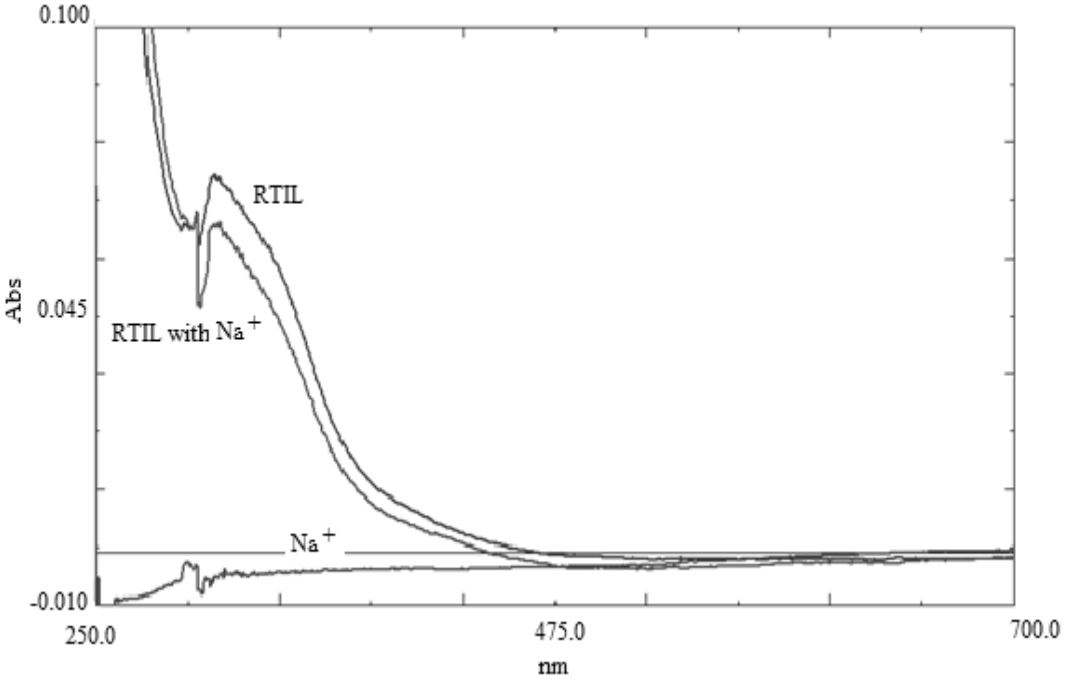

Figure 4.35 Absorption based response of IL-III to Na^{+} ion

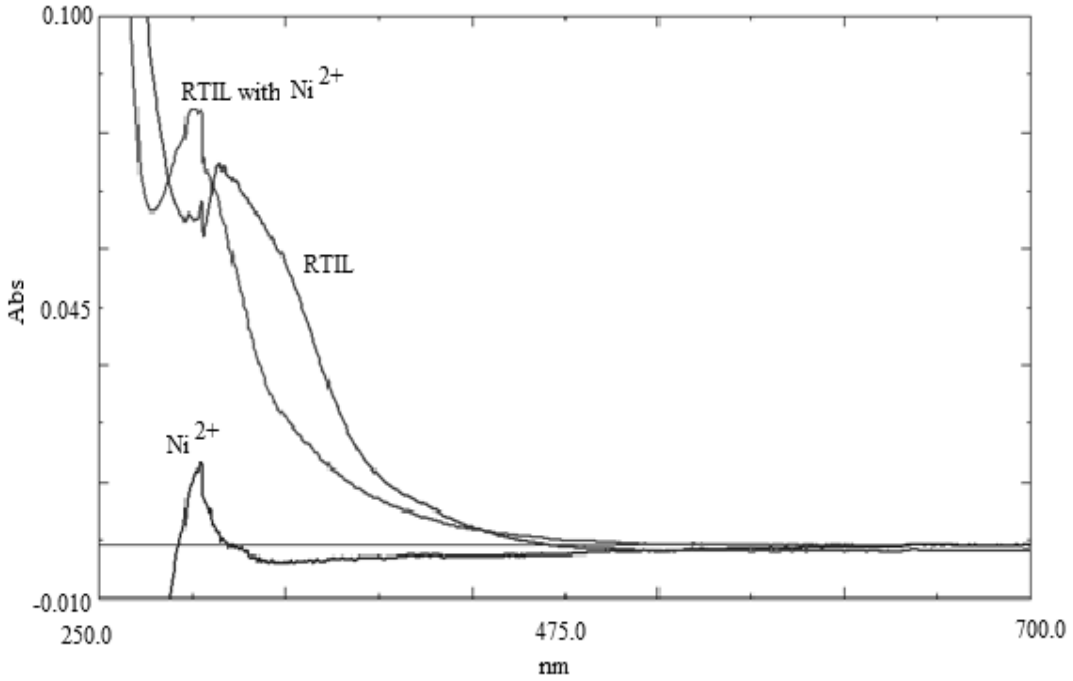

Figure 4.36 Absorption based response of IL-III to Ni^{2+} ion

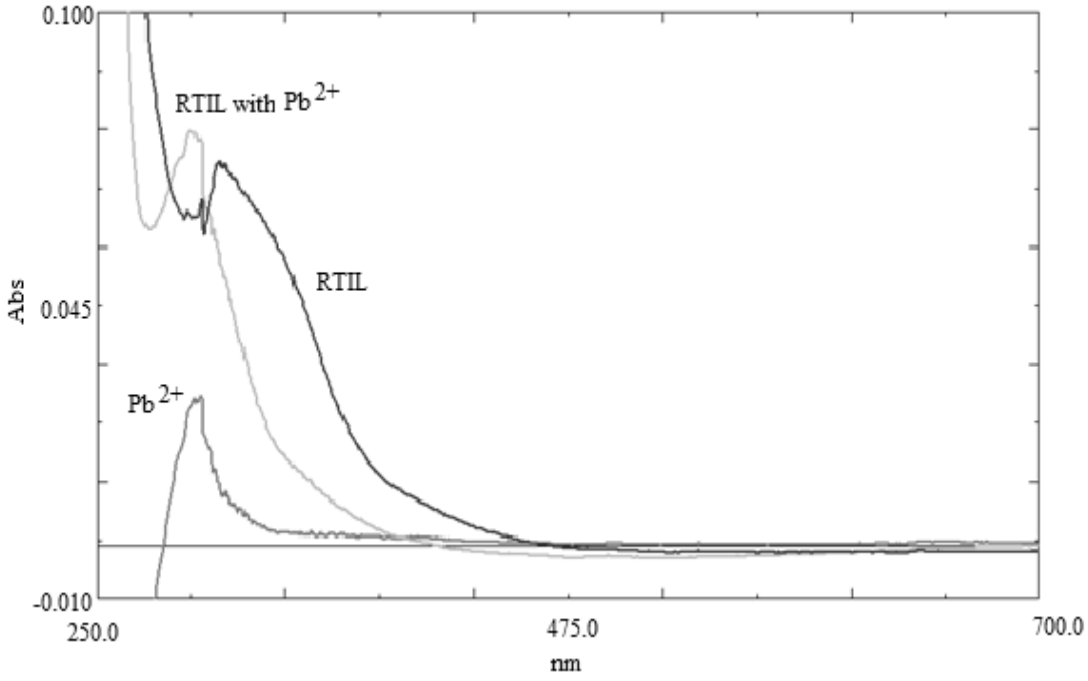

Figure 4.37 Absorption based response of IL-III to Pb^{2+} ion

4.3.4 Response of Different Concentrations of IL-III to Iron Ions

The solutions were freshly prepared prior to experiments to contain 1.0%, 0.8%, 0.2% IL-III. The solutions were diluted with pH 5.0 acetic acid/acetate buffer solution. Figure 4.38 and 4.39 show the response of IL to 1.0 mgL^{-1} Fe^{2+} and Fe^{3+} ions, respectively. The best response was observed for 1.0% IL-buffer mixtures. The next experiments were performed at this ionic liquid concentration (See Table 4.6).

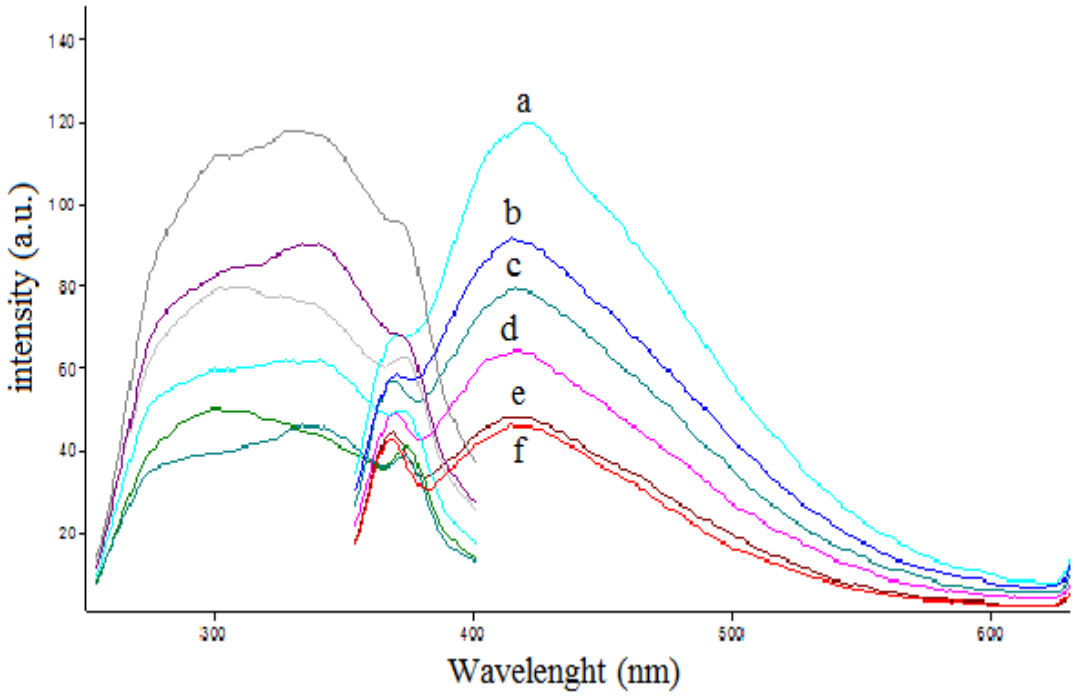

Figure 4.38 Response of different concentrations of IL-III to 1.0 mgL^{-1} Fe^{2+} ions a) 1%IL-III-buffer mixture(by volume) b) after adding 1 mgL^{-1} Fe^{2+} in 1%IL-III-buffer mixture c) 0.8%IL-III-buffer mixture(by volume) d) after adding 1 mgL^{-1} Fe^{2+} in 0.8%IL-III-buffer mixture e) 0.2%IL-III-buffer mixture(by volume) f) after adding 1 mgL^{-1} Fe^{2+} in 0.2%IL-III-buffer mixture

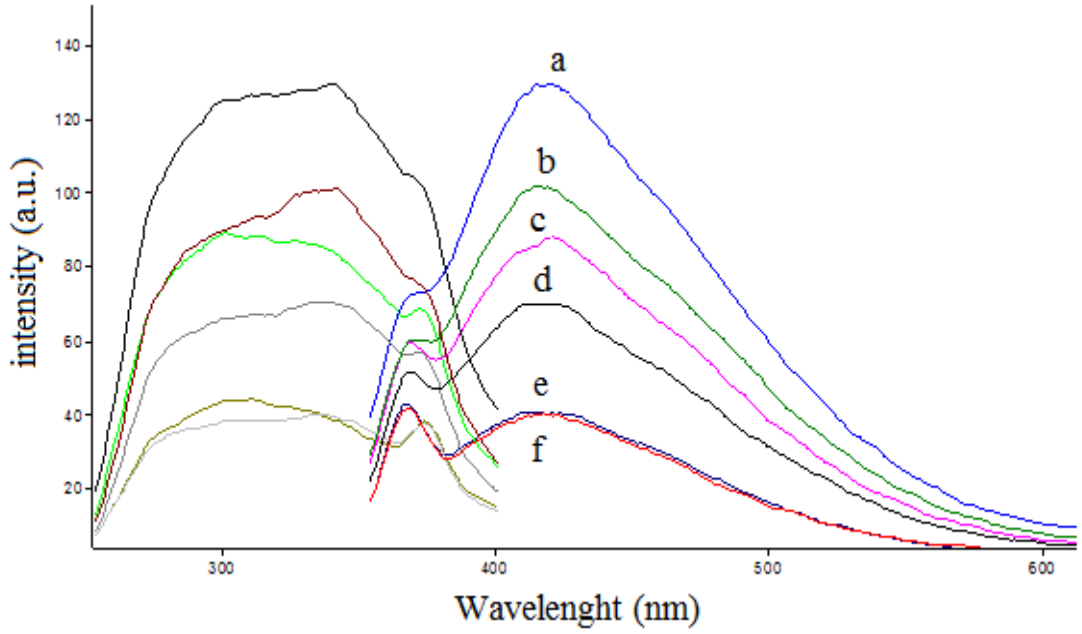

Figure 4.39 Response of different concentrations of IL-III to 1 mgL^{-1} Fe^{3+} ions a) 1%IL-III-buffer mixture(by volume) b) after adding 1 mgL^{-1} Fe^{3+} in 1%IL-III-buffer mixture c) 0.8%IL-III-buffer mixture(by volume) d) after adding 1 mgL^{-1} Fe^{3+} in 0.8%IL-III-buffer mixture e) 0.2%IL-III-buffer mixture(by volume) f) after adding 1 mgL^{-1} Fe^{3+} in 0.2%IL-III-buffer mixture

Table 4.6 % Response of different concentrations of IL-III to 1.0 mgL^{-1} Fe^{2+} and Fe^{3+} ions

	1 mgL^{-1} Fe^{2+}	1 mgL^{-1} Fe^{3+}
1.0% IL-buffer mixture	25	23
0.8% IL-buffer mixture	18	20
0.2% IL-buffer mixture	6	5

4.3.5 Effect of the pH to iron response

Response of IL-III to Fe^{2+} and Fe^{3+} was investigated by exposure to 1.0 mgL^{-1} Fe^{2+} and Fe^{3+} solutions in the different pH buffer (pH 3.0, pH 4.0, pH 5.0, pH 6.0, pH 7.0, pH 8.0, pH 9.0) (See Figure 4.40-4.46). The solutions contain 1% IL-III-buffer mixture and 1mgL^{-} Fe solutions. Absoption based results show that the best

response of IL-III to Fe^{2+} and Fe^{3+} at pH 3.0. The next studies were performed in the buffer at the pH 3.0.

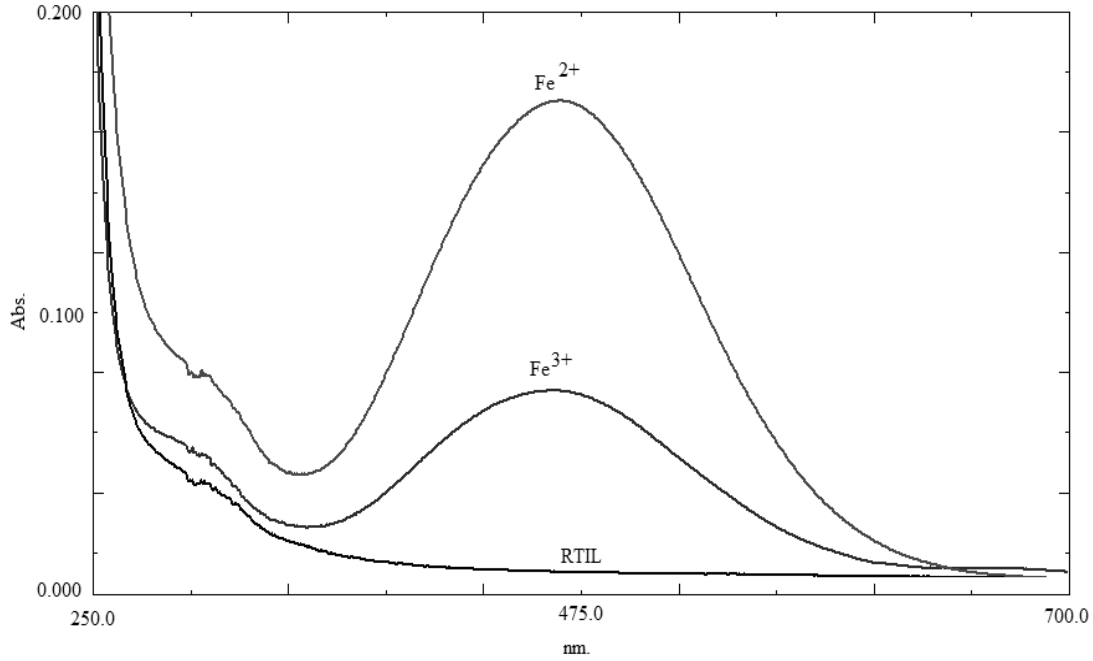

Figure 4.40 Fe^{2+} and Fe^{3+} response of IL-III at pH 3.0

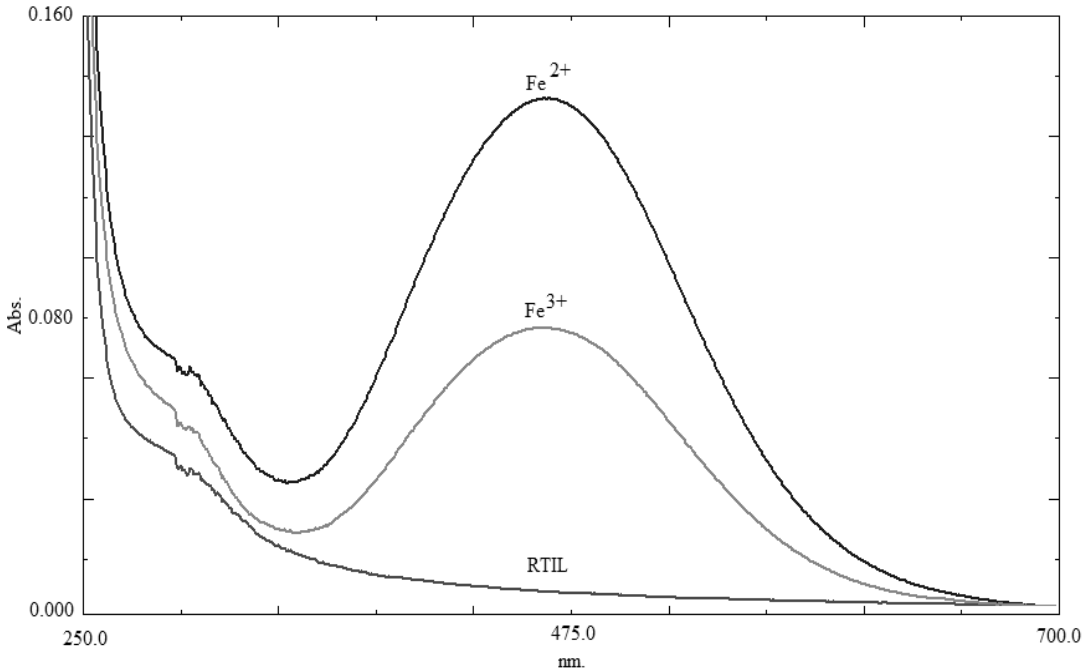

Figure 4.41 Fe^{2+} and Fe^{3+} response of IL-III at pH 4.0

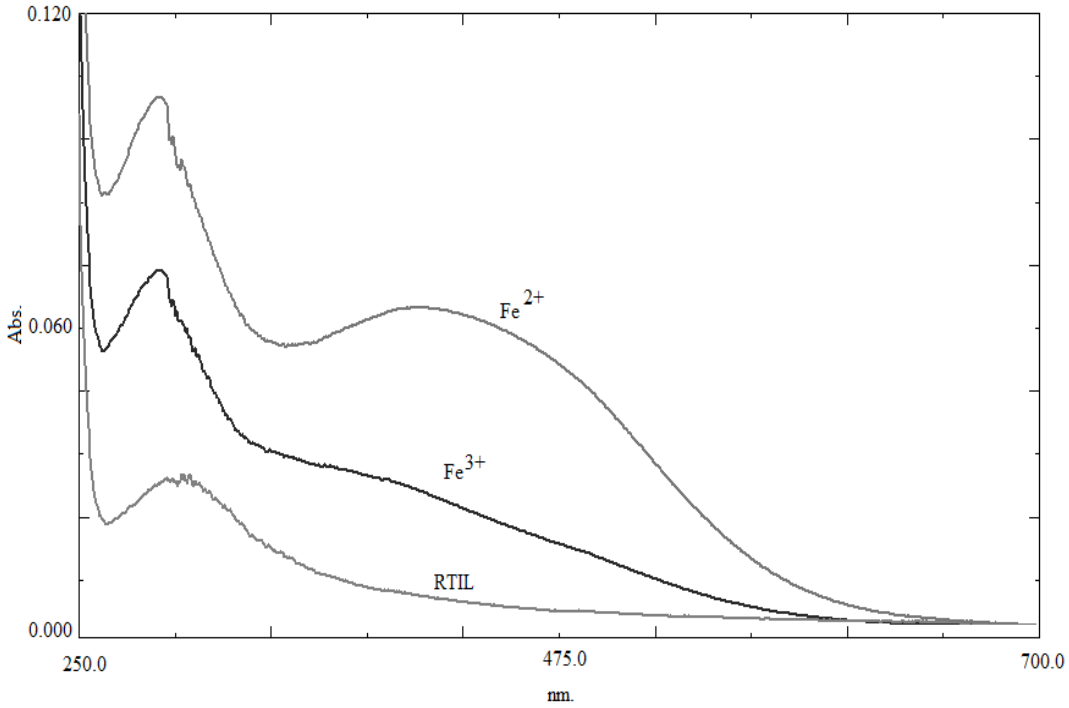

Figure 4.42 Fe^{2+} and Fe^{3+} response of IL-III at pH 5.0

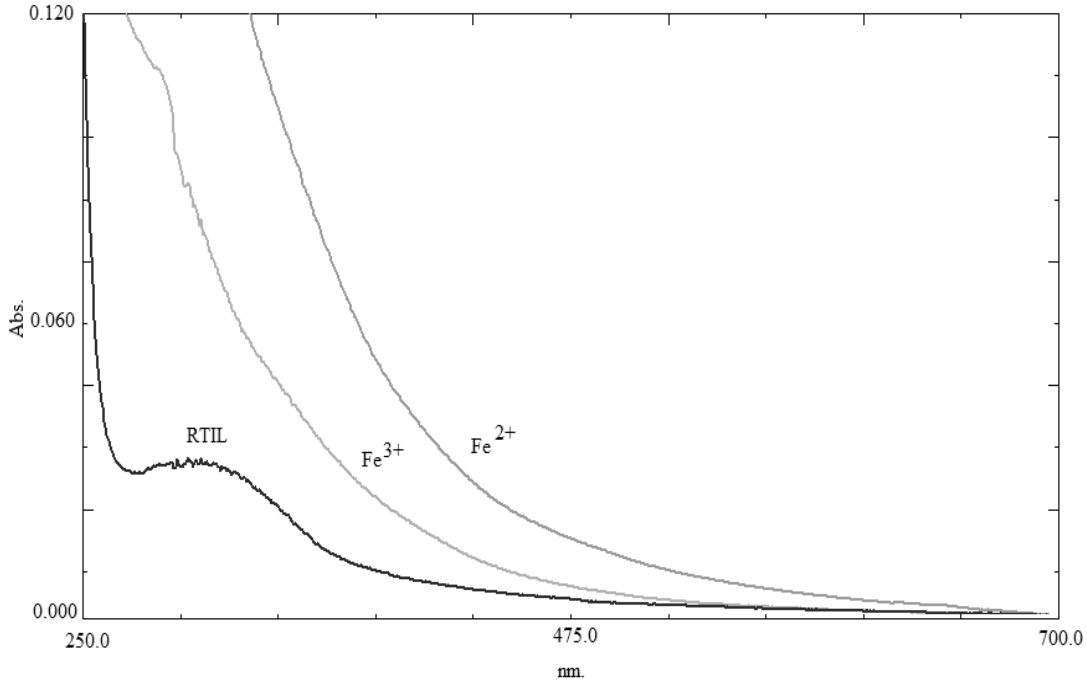

Figure 4.43 Fe^{2+} and Fe^{3+} response of IL-III at pH 6.0

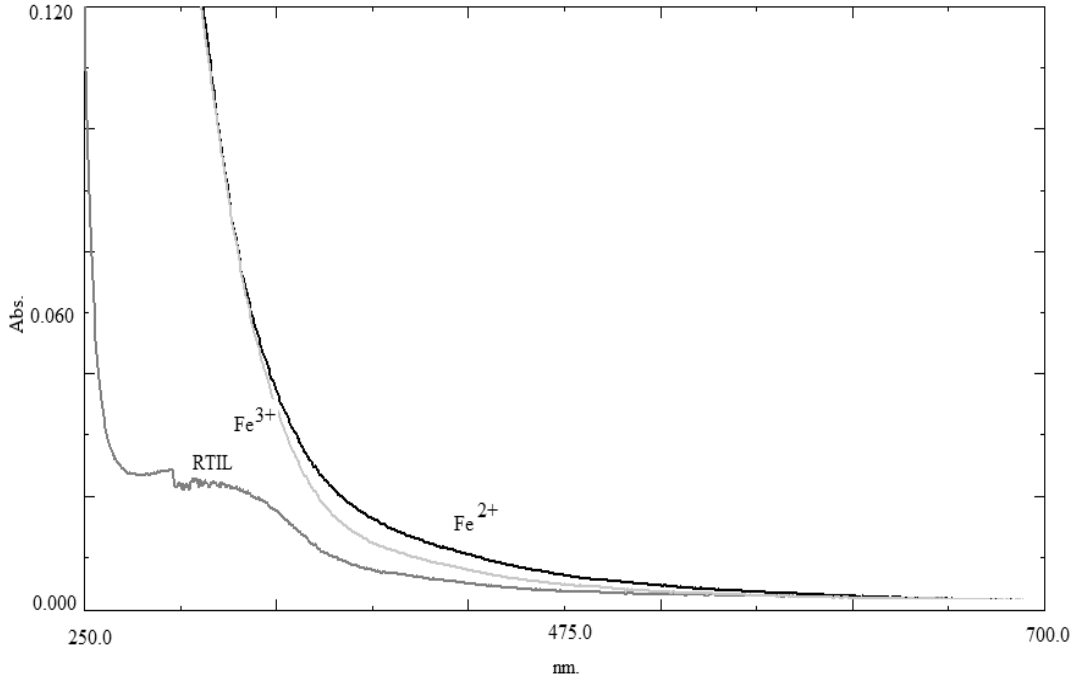

Figure 4.44 Fe^{2+} and Fe^{3+} response of IL-III at pH 7.0

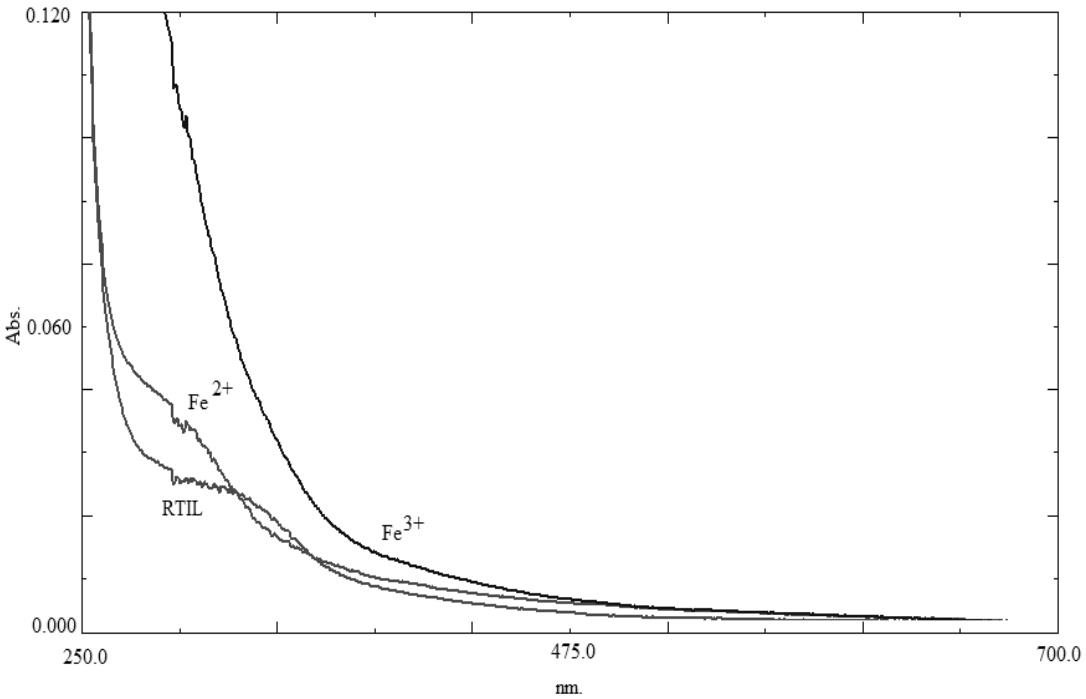

Figure 4.45 Fe^{2+} and Fe^{3+} response of IL-III at pH 8.0

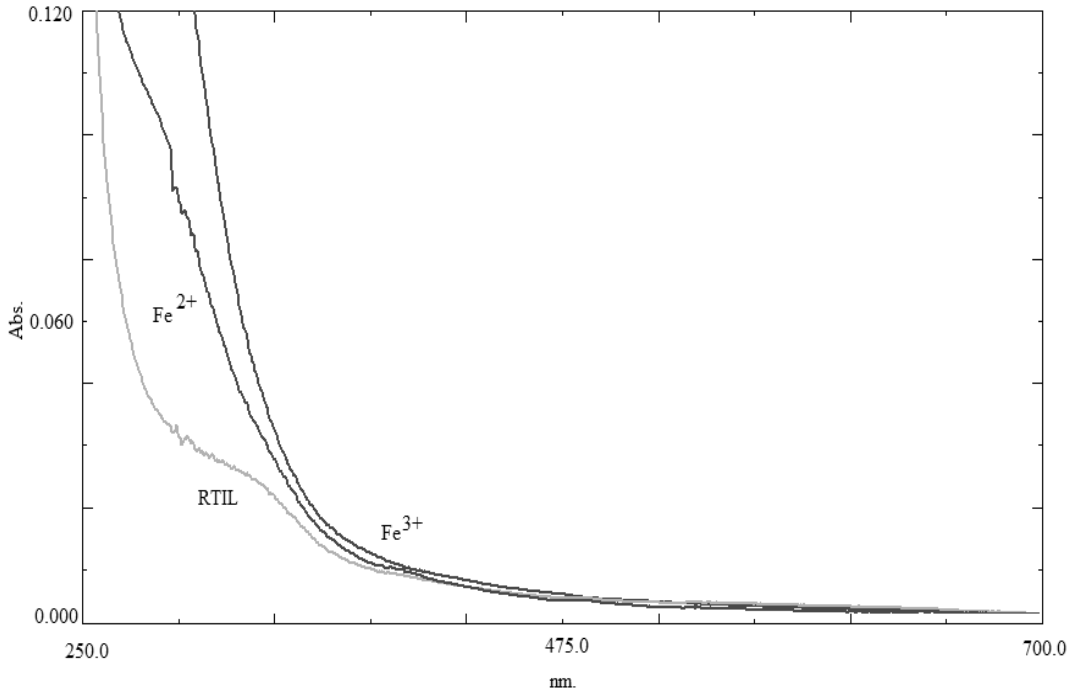

Figure 4.46 Fe^{2+} and Fe^{3+} response of IL-III at pH 9.0

4.3.6 The Response of IL-III to Different Concentrations of Fe^{2+} and Fe^{3+}

4.3.6.1 The response of 1.0% IL-III

Response of 1.0% IL-III to Fe^{2+} and Fe^{3+} was investigated by exposure to different concentrations of Fe^{2+} and Fe^{3+} solutions in pH 3.0 buffer. The solutions contain Fe^{2+} and Fe^{3+} in the concentration range of 0.01– 5.0 mg $L^{-}1$. Figure 4.47-4.50, Table 4.7 and 4.8 show the absorption and fluorescence based data. According to the data absorption based method exhibited better response than fluorescence based method with an increasing response and a higher relative signal change. The inset graphics of Figure 4.48, 4.50 and 4.51 show the absorption based Stern Volmer calibration plot for Fe^{2+} and Fe^{3+} ions.

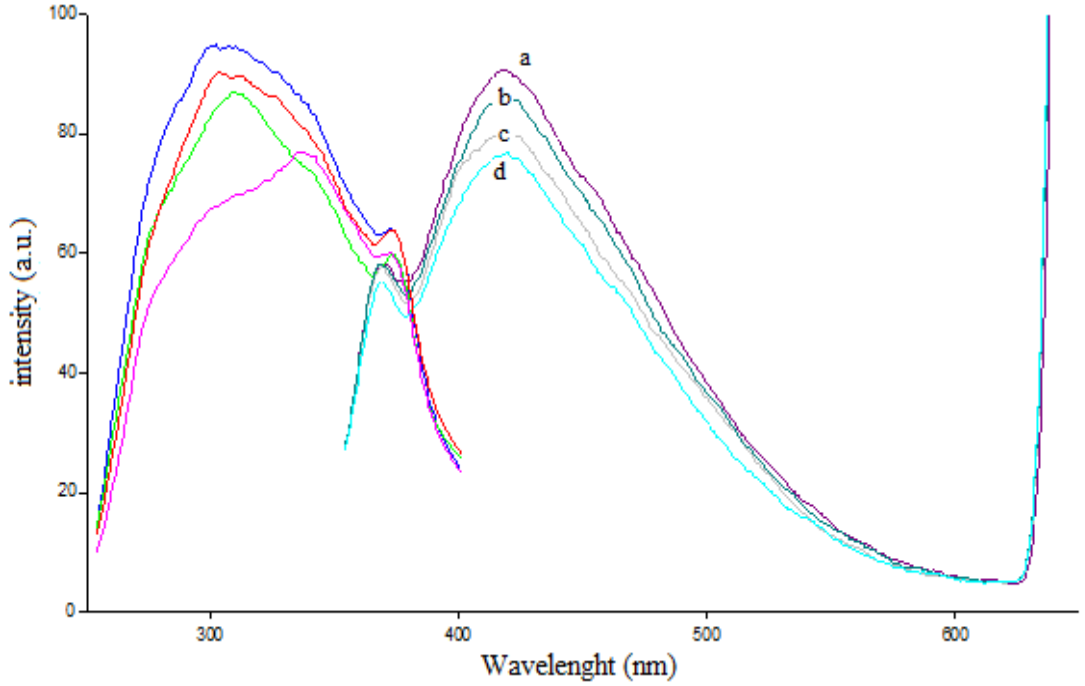

Figure 4.47 Emission and excitation based response of IL-III to Fe^{2+} concentration in the range of 0.0– 1.0 mg L^{-1} Fe^{2+} a) 0.0 mg L^{-1} b) 0.01 mg L^{-1} ^{1} (0, 1.78×10^{-7}M) c) 0.1 mg L^{-1} (1.78×10^{-6}M) d) 1.0 mg L^{-1} (1.78×10^{-5}M)

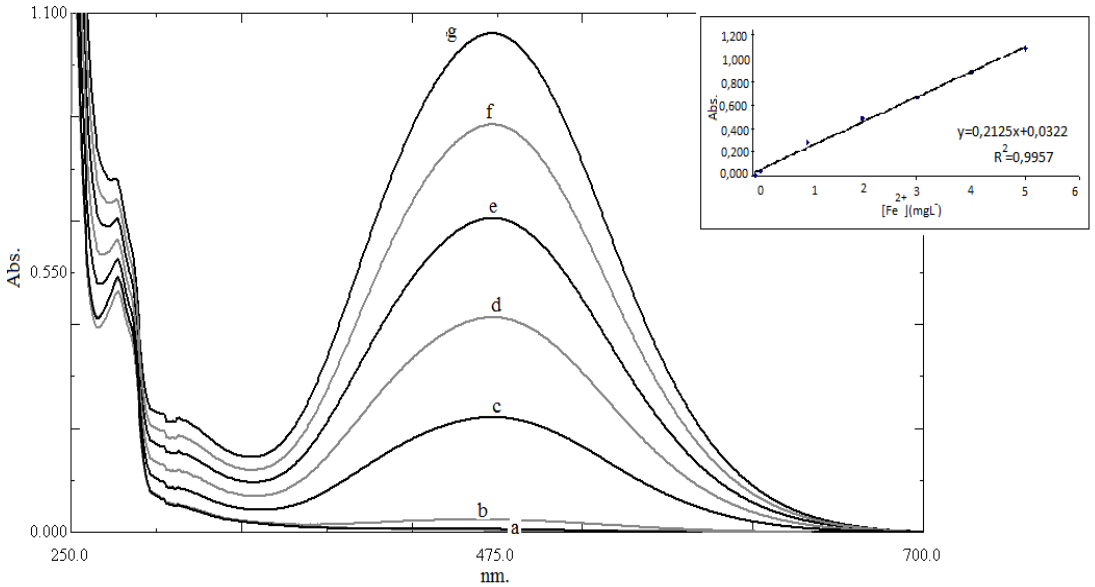

Figure 4.48 Absorption based response of IL-III to Fe^{2+} concentration in the range of 0.0– 5.0 mg L^{-} Fe^{2+} a)0.0 , 0.01 mg L^{-1} (0, 1.78×10^{-7}) b) 0.1 mg L^{-1} (1.78×10^{-6}M) c) 1.0 mg L^{-1} ($1.78\text{x}10^{-5}$M) d) 2.0 mg L^{-1} (3.57×10^{-5}M) e) 3.0 mg L^{-1} (5.34×10^{-5}M) f) 4.0 mg L^{-1} (7.12×10^{-5}M) g) 5.0 mg L^{-1} (8.9×10^{-5}M)

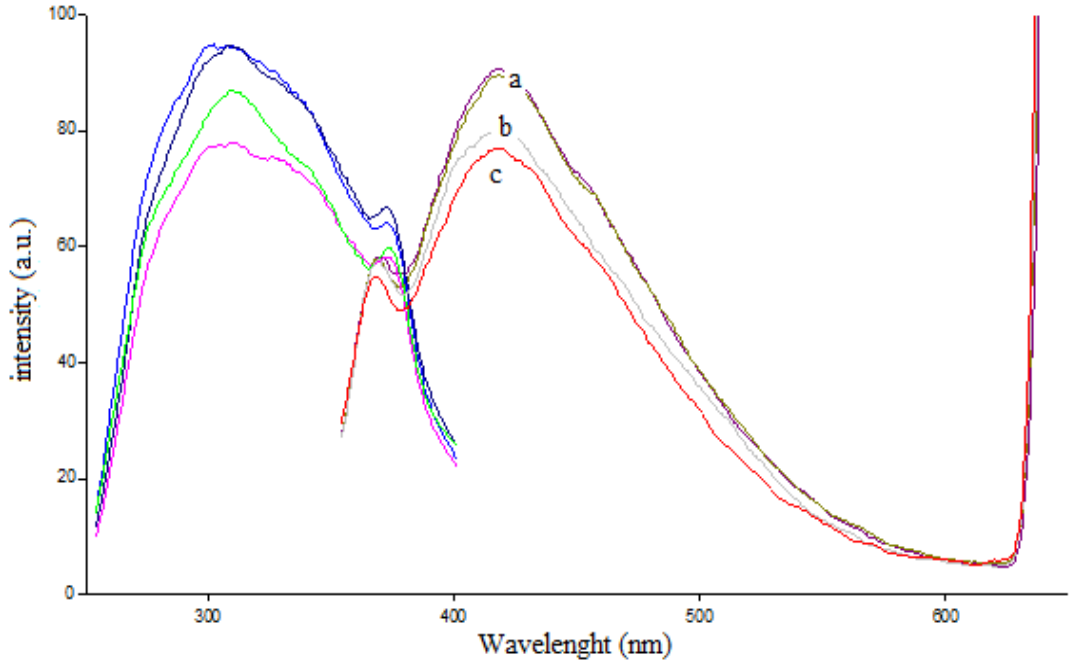

Figure 4.49 Emission and excitation based response of IL-III to Fe^{3+} concentration in the range of 0.0– 1.0 mg L^{-1} Fe^{3+} a) 0.0 mg L^{-1} b) 0.01 mg L^{-1} ^{1} (0, 1.78×10^{-7} M) c) 0.1 mg L^{-1} (1.78×10^{-6}M) d) 1.0 mg L^{-1} (1.78×10^{-5}M)

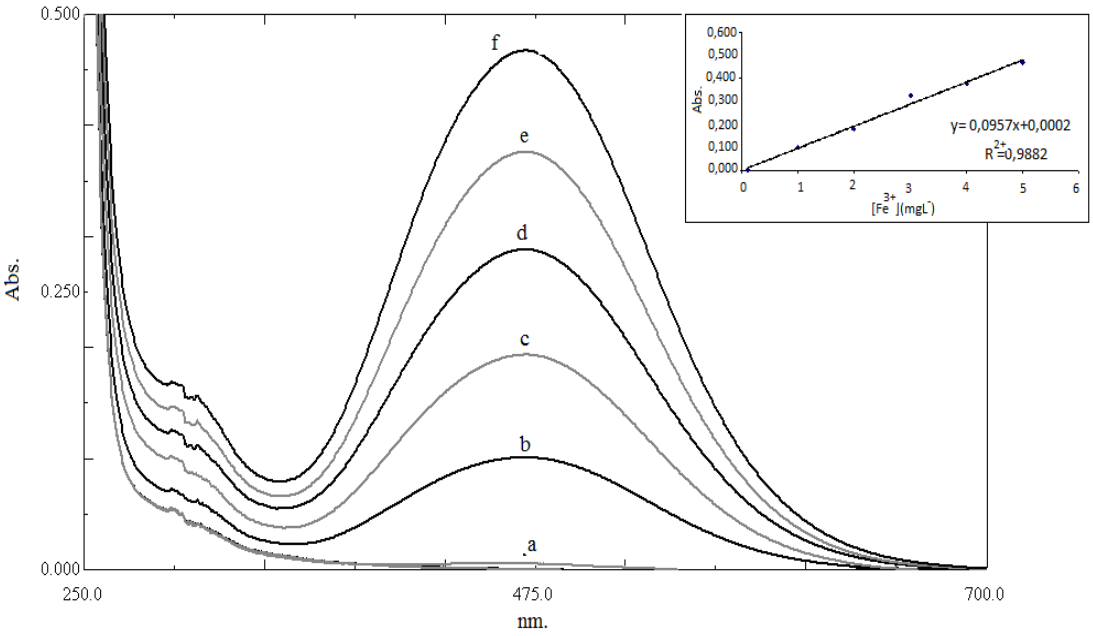

Figure 4.50 Absorption based response of IL-III to Fe^{3+} concentration in the range of 0.0– 5.0 mg L^{-1} Fe^{3+} a) 0.0, 0.01, 0.1 mg L^{-1} (0, 1.78×10^{-7}, 1.78×10^{-6}M) b) 1.0 mg L^{-1} (1.78×10^{-5} M) c) 2.0 mg L^{-1} (3.57×10^{-5}M) d) 3.0 mg L^{-1} (5.34×10^{-5}M) e) 4.0 mg L^{-1} (7.12×10^{-5}M) f) 5.0 mg L^{-1} (8.9×10^{-5}M)

Table 4.7 Absorption spectra related data of response of IL-III to the Fe^{2+} and Fe^{3+}

Metal concentration mgL^{-1} (M)	Abs. (a.u.) for Fe^{2+}	Abs. (a.u.) for Fe^{3+}
0.01 mgL^{-1} (1.78×10^{-7}M)	0.000	0.000
0.10 mgL^{-1} (1.78×10^{-6}M)	0.038	0.012
1.00 mgL^{-1} (1.78×10^{-5}M)	0.287	0.100
2.00 mgL^{-1} (3.57×10^{-5}M)	0.488	0.180
3.00 mgL^{-1} (5.34×10^{-5}M)	0.664	0.325
4.00 mgL^{-1} (7.12×10^{-5}M)	0.880	0.375
5.00 mgL^{-1} (8.9×10^{-5}M)	1.080	0.467

Table 4.8 Emission and excitation spectra related data of response of IL-III to the Fe^{2+} and Fe^{3+}

Metal concentration mgL^{-1} (M)	Em (nm) for Fe^{2+}	F.I.(a.u.) for Fe^{2+}	Em (nm) for Fe^{3+}	F.I. (a.u.) for Fe^{3+}
0.01 mgL^{-1} (1.78×10^{-7}M)	412	89	415	85
0.10 mgL^{-1} (1.78×10^{-6}M)	413	80	415	82
1.00 mgL^{-1} (1.78×10^{-5}M)	411	75	413	71

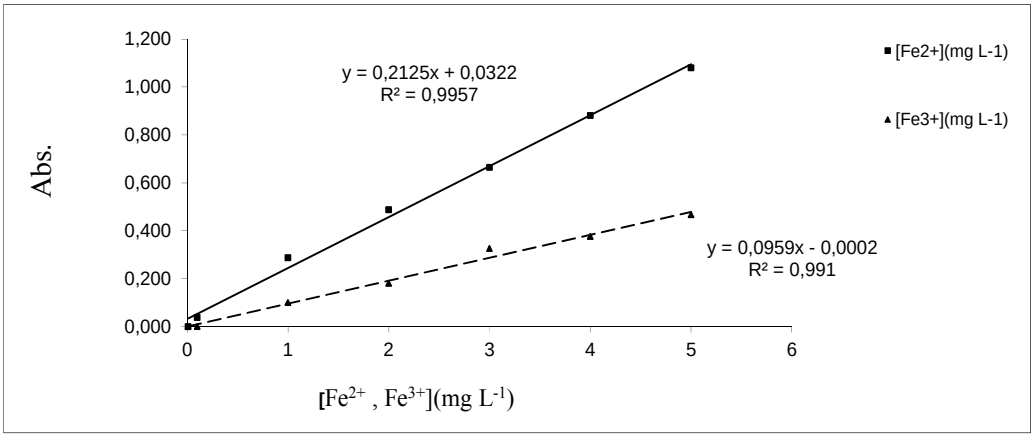

Figure 4.51 Absorption based calibration plot of Fe^{2+} and Fe^{3+} selective composition in the concentration range of 1.79×10^{-7}–8.95×10^{-5} M in IL-III in acetic acid/acetate buffered solutions at pH 3.0.

4.3.6.2 The response of 40% IL-III

Response of 40% IL-III to Fe^{2+} and Fe^{3+} was investigated by exposure to different concentrations of Fe^{2+} and Fe^{3+} solutions in pH 3.0 buffer. The solutions contain Fe^{2+} and Fe^{3+} in the concentration range of 0.001– 5.0 mg $L^{-}1$. Figure 4.52 and 4.53, Table 4.9 show the absorption based data. Figure 4.54 show the absorption based calibration plot of Fe^{2+} and Fe^{3+}

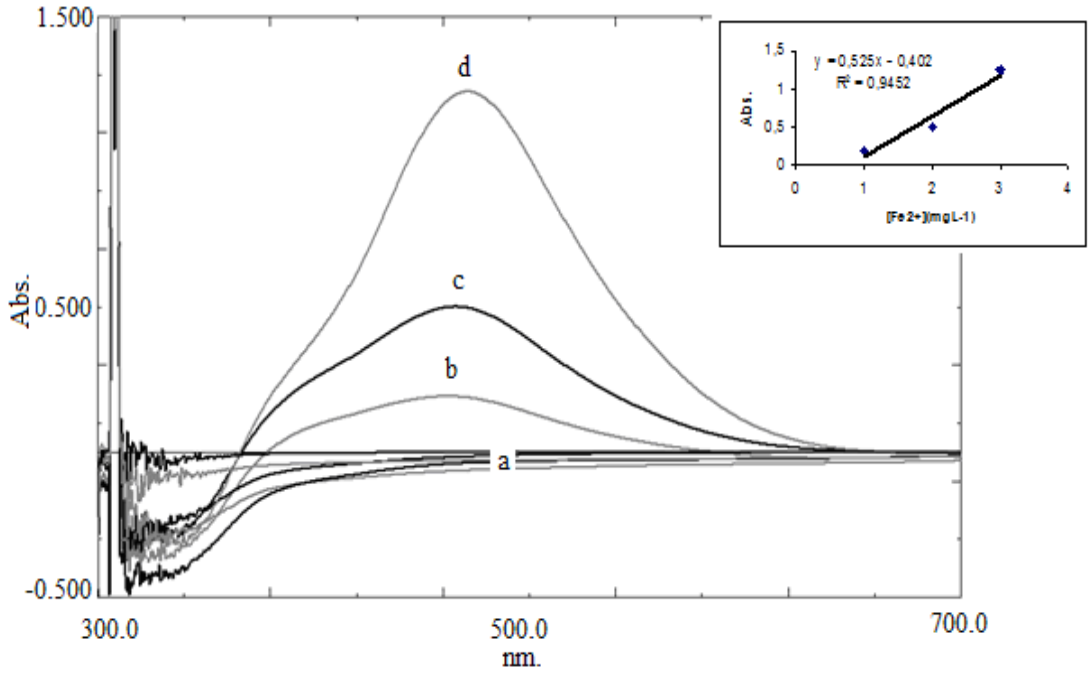

Figure 4.52 Absorption based response of IL-III to Fe^{2+} concentration range of 0.0– 3.0 mg L^{-1} Fe^{2+} a) 0.0, 0.01, 0.1 mg L^{-1} (0, 1.78×10^{-7}, 1.78×10^{-6}M) b) 1.0 mg L^{-1} (1.78×10^{-5} M) c) 2.0 mg L^{-1} (3.57×10^{-5}M) d) 3.0 mg L^{-1} (5.34×10^{-5}M)

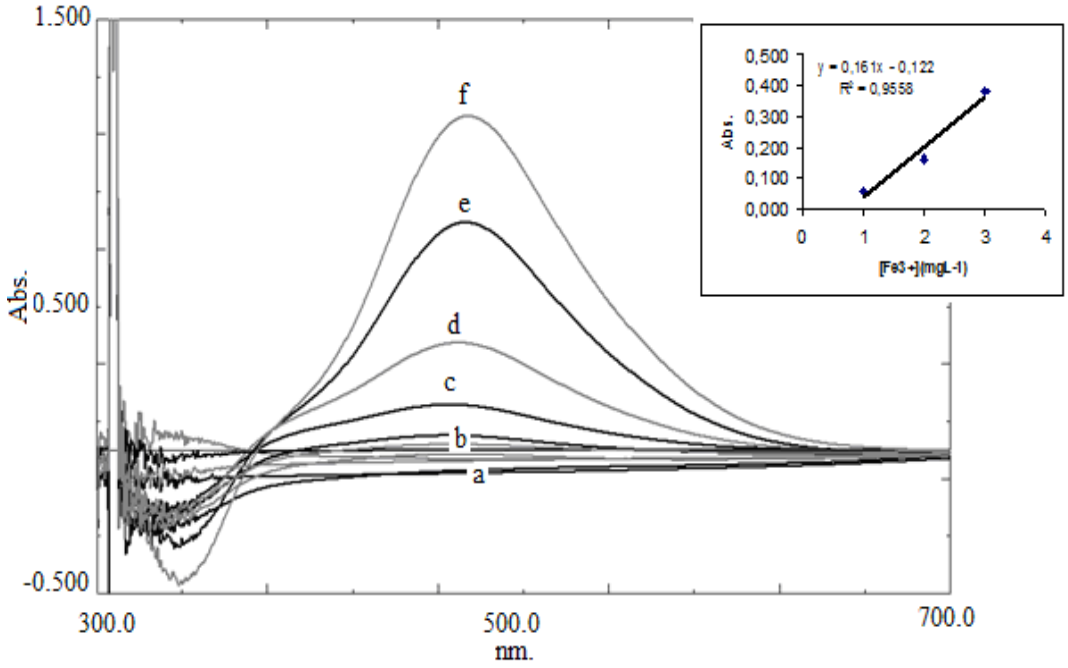

Figure 4.53 Absorption based response of IL-III to Fe^{3+} concentration range of 0.0– 5.0 mg L^{-1} Fe^{3+} a) 0.0, 0.01, 0.1 mg L^{-1} (0, 1.78×10^{-7}, $1.78x10^{-6}$M) b) 1.0 mg L^{-1} (1.78×10^{-5} M) c) 2.0 mg L^{-1} (3.57×10^{-5}M) d) 3.0 mg L^{-1} (5.34×10^{-5}M) e) 4.0 mg L^{-1} (7.12×10^{-5}M) f) 5.0 mg L^{-1} (8.9×10^{-5}M)

Table 4.9 Data of the absorbance value of IL-III to Fe^{2+} and Fe^{3+} in 40%IL-buffer solution, concentration range of 0.1– 5.0 mg L^{-1}

Metal concentration mgL^{-1} (M)	Abs. (a.u.) for Fe^{2+}	Abs. (a.u.) for Fe^{3+}
0.0 mgL^{-1}	0	0
0.1 mgL^{-1} (1.78×10^{-6}M)	0.015	0.027
1.0 mgL^{-1} (1.78×10^{-5}M)	0.0196	0.059
2.0 mgL^{-1} (3.57×10^{-5}M)	0.502	0.160
3.0 mgL^{-1} (5.34×10^{-5}M)	1.246	0.381
4.0 mgL^{-1} (7.12×10^{-5}M)	-	0.796
5.0 mgL^{-1} (8.9×10^{-5}M)	-	1.170

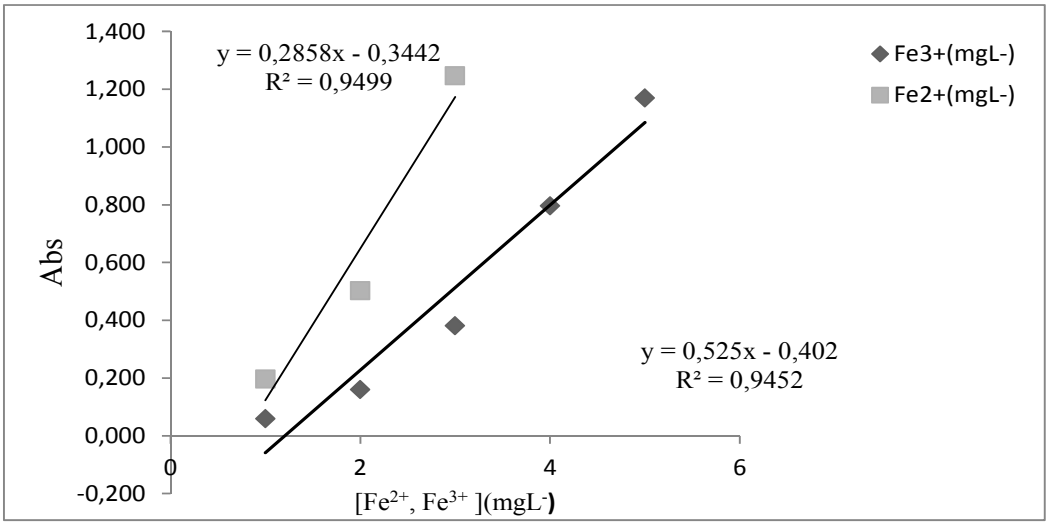

Figure 4.54 Absorption based calibration plot of Fe^{2+} and Fe^{3+} selective composition in the concentration range of 1.79×10^{-6}–8.95×10^{-5} M in IL in acetic acid/acetate buffered solutions at pH 3.0.

Table 4.10 Analytical characteristics of solutions

Solution	Linear working range (mg L^{-1})	Regression equation	Limit detection (mgL^{-1})	*r* (*n=3)*
1%IL-III (Fe^{2+})	0.1-5	y=0.2125x+0.0322	0.1	0.9957
1% IL-III (Fe^{3+})	0.1-5	y=0.0959x-0.0002	0.1	0.9910
40% IL-III (Fe^{2+})	0.1-3	y=0.2858x-0.3442	0.1	0.9499
40% IL-III (Fe^{3+})	0.1-5	y=0.525x-0.402	0.1	0.9452

4.3.7 Photostability of the complex

4.3.7.1 Short Term Stability

The photostability of the $FeSCN^{2+}$ complex was investigated for selected concentration of Fe^{2+} (1.0 mgL^{-}) in 1% IL-buffer mixture and in buffer solution which doesn't contain any ionic liquid (Fig. 4.55 and 4.56). The short term photostabilities were recorded as a function of time for 60 minutes. The $FeSCN^{2+}$ complex was stable during this period for the both media.

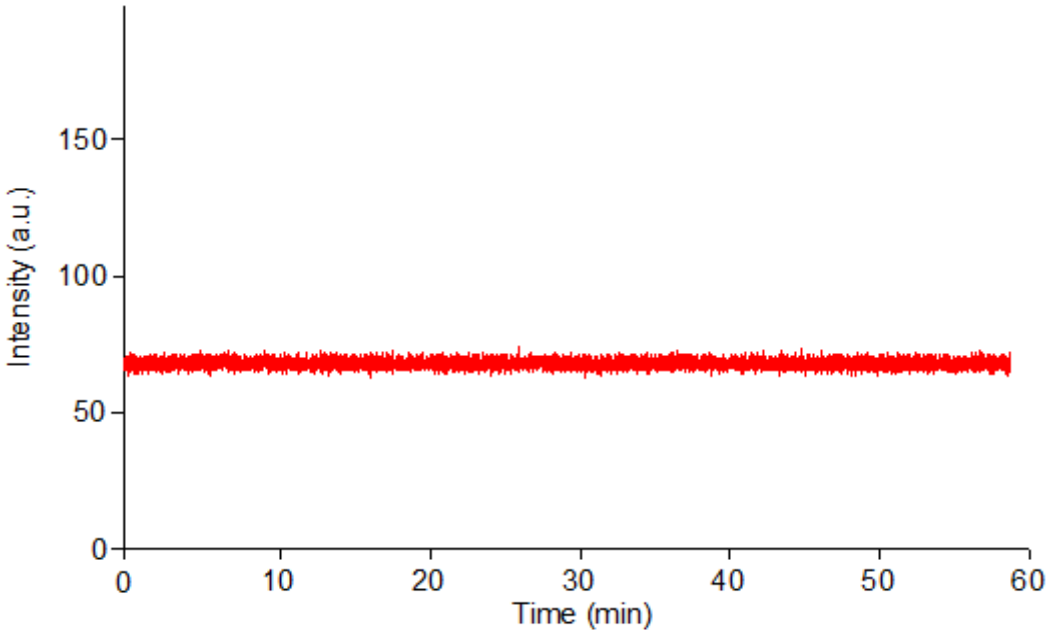

Figure 4.55 Kinetics of $FeSCN^{2+}$ complex in 1% IL-III-buffer media

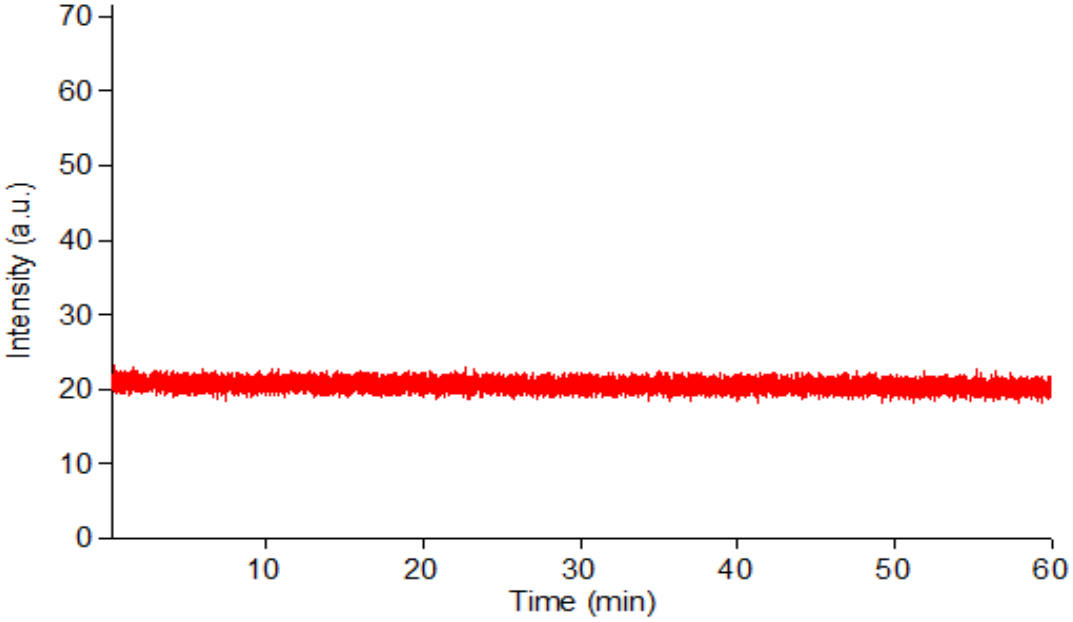

Figure 4.56 Kinetics of $FeSCN^{2+}$ complex in buffer media without any ionic liquid.

4.3.7.2 Long Term Stability

Its known that the color of aqueous solutions of Fe^{3+} thiocyanate complexes is unstable owing to the reduction of Fe^{3+} by thiocyanate, fading by 50% in six hours (Marczenko, Balcerzak, 2000) When the sensing cocktails were stored in sealed

cuvettes protected from sunlight 50% decrease for Fe^{2+}, 35% decrease for Fe^{3+} was observed after 2 weeks. Figure 4.57 and 4.58 illustrate the stability of complex with Fe^{2+} and Fe^{3+}, respectively.

.

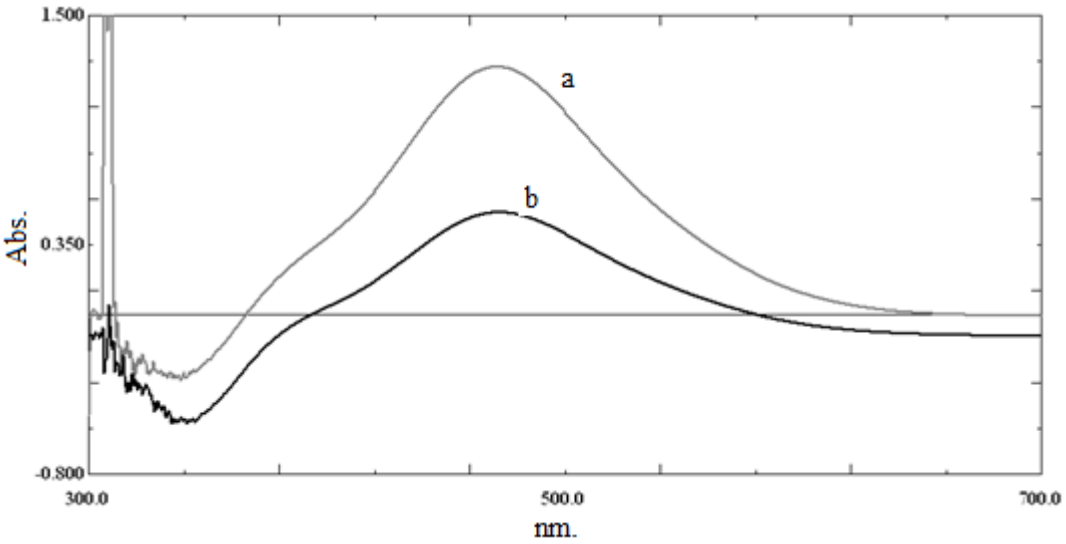

Figure 4.57 Long term stability of complex with Fe^{2+}a) IL-III with Fe2+ solution b) IL-III with Fe2+ solution two weeks later

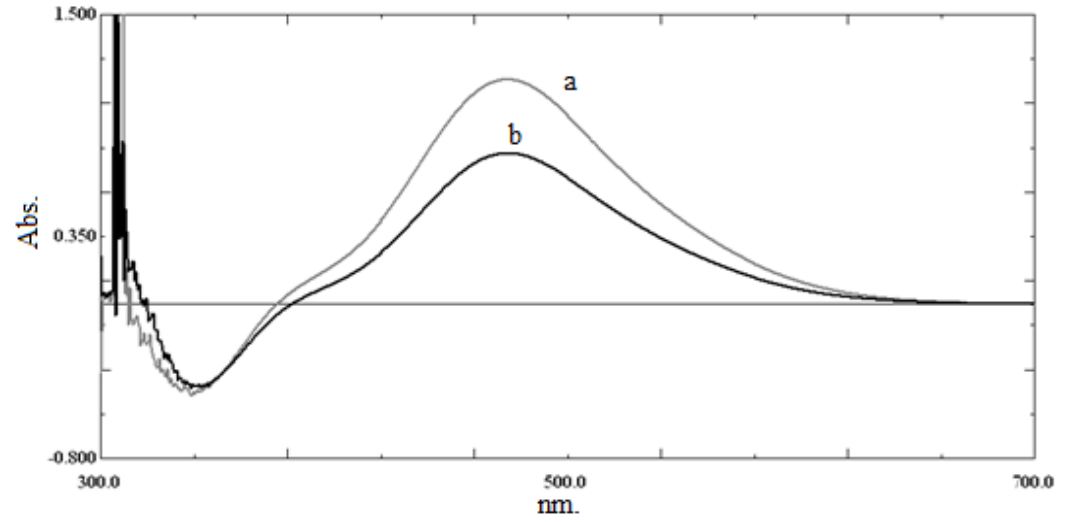

Figure 4.58 Long term stability of complex with Fe^{3+} a) IL-III with Fe^{3+} solution b) IL-III with Fe^{3+} solution two weeks later

4.4 Conclusion

In the absorption spectra of ILs, a broad absorption band between 350-700 nm was observed. In the absorption spectra of [BMIM][SCN], new absorption maxima at 460 nm was observed by the addition of Fe^{2+} and Fe^{3+} ions, which is due to the complex formation of iron ions with SCN group of the ionic liquid. All of the ILs exhibited emission bands between 350-600 nm. The fluorescence intensity of IL-I decreased by the addition of the metal ions was between 8 %-25 %. The maximum response was seen for iron ions. The fluorescence intensity of IL-II was effected as a decrease in fluorescence intensity for all of the ions except mercury ions in the range of 5%-8%. The maximum response was observed for iron ions. Mercury ions caused an 8 % increase in fluorescence intensity. The fluorescence intensity of IL-III was affected as a decrease in fluorescence intensity in the range of 7 %-26%. The maximum response was observed for iron ions and for IL-III. According to the data, absorption based method exhibited better response than fluorescence based method with an increasing response and a higher relative signal change. Limit of dedection was found 0.1 mgL^{-} Fe^{2+} or Fe^{3+} for IL-III. The Linear working range was between 0.1-5.0 mgL^{-}. When the sensing cocktails were stored in sealed cuvettes protected from sunlight 50% decrease for Fe^{2+}, 35% decrease for Fe^{3+} was observed after 2 weeks. This storage time is higher than the storage time in aqueous media (in absence of IL).

CHAPTER FIVE
CONCLUSIONS

In the first part, we have employed tree ionic liquids (1-butyl-3-methylimidazolium thiocyanate ([BMIM][SCN]), 1-butyl-3- methylimidazolium tetrafluoroborate ([BMIM][BF_4]), 1-ethyl-3-methylimidazolium tetrafluoroborate ([EMIM][BF_4]) and two micelles (sodium dodecyl sulfate (SDS) and Triton X-100) as new additives for the determination of Mn^{2+} with Eosin Y in aqueous solutions by spectrofluorimetric method. The results revealed that the spectra of Eosin Y in all media exhibited broad emission bands ranging from 510 to 650 nm. The emission maximum of the dye was between the range of 545-554 nm. TX-100 (0.2×10^{-2} M) caused moderately longer red shift of 9 nm and a slight decrease in fluorescence intensity.

In absence of additives we have observed response for the the metal ions of Ca^{2+},Cu^{2+}, Hg^{+}, Hg^{2+}, As^{5+}, Li^{+}, Al^{3+}, Cr^{3+}, Co^{2+} and Ni^{2+} while we have observed no response in the additive containing solutions ions. Thus, the presence of both the ionic liquids and the surfactants increased the selectivity of the dye. Besides, they have decreased the % response of the other metal ions except Mn^{2+}.

The dye exhibited decreasing response in signal intensity in the concentration range of 0.01–3.0 mg L^{-}(1.85×10^{-7}M–5.56×10^{-5}M) Mn^{2+} in S-1, S-2, S-3, S-4, S-5, S-6 solutions. However, the detection limit decreased to 0.001 mg L- in 40 % ionic liquid containing solutions. In higher concentrations of ionic liquids (> 40%), no response to Mn^{2+} was seen. This result reveals that ionic liquids behaves like surfactants and the response increases at a critical miscelle concentration and decreases again after this concentration. The decrease in fluorescence intensity of Eosin Y after a critical concentration of ionic liquid can be attributed to the competing complex formation of IL the dye.

The presence of surfactants of SDS (S-5) and TX-100 (S-6) didn't change the detection limit but significantly enhanced the fluorescence decrease from 63 % (no additive) to 78 % (in presence of Triton X-100). The relative signal changes of Eosin Y to 3.0 mg L- concentration of Mn2+ in S-1, S-2, S-3, S-4, S-5, S-6, S-7, S-8 and S-9 solutions were 63 %, 61 %, 62 %, 58 %, 60 %, 78 %, 56 %, 60 % and 60 %, respectively. The best response of Mn2+ to Eosin Y was seen in S-6 (with TX-100) solutions. The presence of ionic liquid lowered the detection limit of Mn^{2+} by nearly ten times. The interference effect of the other metal ions (Ca^{2+},Cu^{2+}, Hg^{+}, As^{5+}, Mo^{2+}, Li^{+}, $Pb^{2+,}$ Al^{3+}, Cr^{3+},Na^{+}, $Mg^{2+,}$ Zn^{2+}, Cd^{2+}, Fe^{3+},Co^{2+} and Ni^{2+}) to the fluorescence intensity was also investigated. The results showed that Na^{+} and Zn^{2+} ions exhibited less interfering effect in the presence of employed ionic liquids and micelles. The tolerance limit of Na^{+} increased 6 times in presence of [EMIM][BF_4] and the tolerance limit of Zn^{2+} increased 5 times in presence of SDS.

The optimum response was observed at pH 5.0. Because of this the experimens were performed in buffered solutions. One advantage of the IL is that the IL containing solution strongly resisted pH changes due to its buffering effect. Similar behavior of ILs was reported earlier. Formation of such a buffer system enhances the stability of analysis system more than the classical buffer systems and the presence of IL in the analysis solution acts as a sink for acidic or basic species.

In the second part, the absorption spectra of ILs, a broad absorption band between 350-700 nm was observed. In the absorption spectra of [BMIM][SCN], new absorption maxima at 460 nm was observed by the addition of Fe^{2+} and Fe^{3+} ions, which is due to the complex formation of iron ions with SCN group of the ionic liquid. All of the ILs exhibited emission bands between 350-600 nm. The fluorescence intensity of IL-I decreased by the addition of the metal ions was between 8 %-25 %. The maximum response was seen for iron ions. The fluorescence intensity of IL-II was effected as a decrease in fluorescence intensity for all of the ions except mercury ions in the range of 5%-8%. The maximum response was

observed for iron ions. Mercury ions caused an 8 % increase in fluorescence intensity. The fluorescence intensity of IL-III was affected as a decrease in fluorescence intensity in the range of 7 %-26%. The maximum response was observed for iron ions and for IL-III. According to the data, absorption based method exhibited better response than fluorescence based method with an increasing response and a higher relative signal change. Limit of dedection was found 0.1 mgL^{-} Fe^{2+} or Fe^{3+} for IL-III. The Linear working range was between 0.1-5.0 mgL^{-}. When the sensing cocktails were stored in sealed cuvettes protected from sunlight 50% decrease for Fe^{2+}, 35% decrease for Fe^{3+} was observed after 2 weeks. This storage time is higher than the storage time in aqueous media (in absence of IL).

REFERENCES

Anthony, J. L, Maginn, E. J., Brennecke, J. F. (2001). Solution thermodynamics of imidazolium-based ionic liquids and water. *J. Phys. Chem. B, 105* (44), 10942.

Behera, K., Dahiya, P. & Pandey, S. (2006). Effect of added ionic liquid on aqueous Triton X-100 micelles. *J. Colloid Interface Sci.*.

Berthod, A. & Carda-Broch, S. (2002). Uses of Ionic Liquids in Analytical Chemistry. *Laboratoire des Sciences Analytiques.*

Boccio, M., Sayago, M., Agust, G. (2006). A bilogarithmic method for the spectrophotometric evaluation of stability constants of 1:1 weak complexes from mole ratio data. *Elseiver Science Direct 318* , 70–77.

Brennecke, J. F. & Maginn, E. J. (2001), Ionic liquids: innovative fluids for chemical processing. *Aiche J.*, *47*, 2384–2389.

Brunschwig, B. S., Cruetz, C. & Sutin, N. (1998). Electroabsorption spectroscopy of charge transfer states of transition metal complexes. *Coord. Chem. Rev., 177*, 61.

Buzzeo, M. C., Hardacre, C. & Compton, G. R. (2004). Use of Room Temperature Ionic Liquids in Gas Sensor Design. *Analitical Chemistry., 76,* 4583-4588.

Camman, K., Guibault, G., Hall, E., Kellner, R., Schmidt, H. L., & Wolfbeis, O. S. (1996). The Cambridge Definition of Chemical Sensors.

Chan, W. H., Yang, R. H., *&* Wang, K. M. (2001). Development of a mercury ion-selective optical sensor based on fluorescence quenching of 5,10,15,20-tetraphenylporphyrin. *Anal. Chim. Acta.,* 444, 261.

Diaz Garcia M.E. & Sanz-Medel, A. (1986) Dye-surfactant interaction: a review. *Talanta 33:*255–264.

Earle, M. J. & Seddon, K. R. (2000). Ionic liquids Green solvents for the future. *Pure Appl. Chem. 72* (7), 1391-1398.

Eggins, B.R., (2002). Chemical Sensors and Biosensors. *England: Wiley*.

Endres, F. & Abedinw, Z. (2006), Air and water stable ionic liquids in physical chemistry. *Physical Chemistry Chemical Physics 8*, 2101–2116.

Fernandez, D., Gramatges, A., Calvo, S., Mangano, C., Pallavicini, P. (2004). Structure and dynamics of micelle-based fluorescent sensor for transition metals. *Chem. Phys. Lett.,1-3*(398), 245-249.

Galster, H. (1991). *pH Measurements: Fundamentals, Methods, Applications, Instrumentatio.* Weinhein,VCH: Germany.

Gerber, G.B., Leonard, A., Hantson, P., (2002) Carcinogenicity, mutagenicity and teratogenicity of Manganese compounds." Crit Rev Oncol Hematol. 25-34.

Hein, R. J., Warnke, M. M. & Armstrong, W. (2009). Ionic Liquids in Analytical Chemistry. *Annual Review of Analytical Chemistry*, 145-68

Hess, M., Meier, H.& Zeeh, B. (2002). Spektroskopische Methoden in der organischen Chemie (7th ed.), *Thieme*

Holbrey, J. D. & K. R. Seddon (1999). Ionic liquids, Review. *Clean Products and Processes* , 223-236.

Idriss, K.A., Sedaira, H., Abdel-Aziz, M.S. & Ahmad, H.M. (1999). Rapid test methods for minor components analysis of hydraulic cement. Spectrophotometric determination of manganese oxide content of Portland cement and cement raw meal. *Talanta* 50, 913–919.

Liu, J., Jhonsson, J. A. & Jiang G. (2005). Application of ionic liquids in analytical chemistry. *TrAC Trends in Analytical Chemistry 24*(1) 20-27.

Khania, H, Rofoueia, M. H., Arabb, P., Guptac, V. K. & Vafaeia, Z. (2010) Multi-walled carbon nanotubes-ionic liquid-carbon paste electrode as a super selectivity sensor: Application to potentiometric monitoring of mercury ion(II). *Journal of Hazardous Materials*, 402–409.

Kitai, A., (2008). Limunescent Materials and Aplication . *England: Wiley.*

Kohler, H., Klimant, I., Kunz, W., Wolfbeis, O. S., (1996) . New Fluorescent Optical pH Sensors with Minimal Effects of Ionic Strength.

Kuswandi, B. (2000). Optical Chemical Sensors for the Determination of Heavy Metal Ions: A mini review**.** *Jurnal Ilmudasar, 1* (2), 18 – 29.

Lakowicz, J. R. (1993). *Principles of Fluorescence Spectrocopy.* Plenum Press: New York and London.

Liu, J.F., Jönsson, J.A., Jiang, G.B. (2005). Application of ionic liquids in analytical chemistry. *Trends Anal. Chem.* 24, 20-27.

Malcik, N., Oktar, O., Ozser, M. E., Caglar, P., Bushby, L., Vaughan, A., Kuswandi B., *&* Narayanaswamy, R. (1998). Immobilised reagents for optical heavy metal ion sensing. *Sens. Actuators* B, 53, 211.

Marczenko, Z., Balcerzak, M. (2000) Seperation, preconcentration and spectrophotometry in inorganic analysis, *Elsevier science B.W*.

Mayr, T. (2002). Optical Sensors for the Determination of Heavy Metal Ions. *Institut für Analytische Chemie:* Chemo- und Biosensorik an der Universität Regensburg.

Meites, L., McGraw-Hill, E., (1963) "Handbook of Analytical Chemistry", 1st ed., L. Meites, Ed.. McGraw- Hill, New York, p 6-28.

Merrigan, L., Bates, E.D., Dorman, S.C., (2000) New fluorous ionic liquids function as surfactants in onventional room-temperature ionic liquids. *Chem Commun 2051–2052.*

Miskolczy, Z., Sebök-Nagy, K., Biczok, L., Göktürk, S., (2004) Aggregation and micelle formation of ionic liquids in aqueous solution. *Chem Phys Lett 400:296–300.*

Mohr, J., Murkovic, I., Lehmann, F., Haider, C. & Wolfbeis, S. O. (1997) Application of potential-sensitive fluorescent dyes in anion- and cation-sensitive polymer membranes. *Sensors and Actuators* 38-39 , 239-245.

Moreno, A., Silva, M., Perez Bendito D., & Valcarcel, M. (1983) Application of a modified catalytic effect: determination of nanogram amounts of zinc in milk samples using a kinetic-fluorimetric method *Analyst*, , 108, 85-91.

Oehme, I., *&* Wolfbeis, O. S. (1997). Fundamental Review – Optical Sensors for Determination of Heavy Metal Ions. *Microchim. Acta,* 126, 177-192.

Oter, O., Ertekin, K., Kırılmıs, C. & Koca, M., (2007). Spectral characterization of a newly synthesized fluorescent semicarbazone derivative and its usage as a selective fiber optic sensor for copper(II) . *Analytica Chimica Acta,* 584 (2) ,308-314.

Oter, O. (2007). *Investigation of Sensor Characteristics of Some Chromoionophore Structures in Polymer and Sol-Gel Matrices*. Ph.D thesis. Izmir.

Oter, O., Aydogdu, S., (2010) Determination of Aluminum Ion with Morin in a Medium Comprised by Ionic Liquid–Water Mixtures. *J Fluoresc 21:43–50.*

Ou, G., Zhu, M., She, J. & Yuan, Y. (2006) Ionic liquid buffers: a new class of chemicals with potential for controlling pH in non-aqueous media. *Chem Commun* (44):*4626–4628.*

Park, S., Kazlauskas, R. (2003). Biocatalysis in ionic liquids—advantages beyond green technology. *Curr. Opin. Biotechnol*., 14, 432–437.

Pramanik, R., Ghatak, C., Rao, V. G., Sarkar, S. & Sarkar N. (2010). Room Temperature Ionic Liquid in Confined Media: A TemperatureDependence Solvation Study in [bmim][BF4]/BHDC/BenzeneReverse Micelles. The Journal of Physical Chemistry.

Praveen, A., Kumar1, P., Reddy, V. (2009). Direct and First Derivative Spectrophotometric Determination of Manganese (II) in Tap Water, Milk, Alloy Steels and Plant Samples. *Eurasian J. Anal. Chem. 4*(1): *66 – 75.*

Reddy, K., Kumar, J.R., Ramachandraiah, C., Thriveni, T., & Reddy A. (2005) Spectrophotometric determination of zinc in foods using *N*-ethyl-3-carbazolecarboxaldehyde -3-thiosemicarbazone: Evaluation of a new analytical reagent *Food Chemistry* p. 585-591.

Ruiz, M.C., Rodriguez, M.H., Perino, E., & Olsina R.A., (2002) Determination of Nb, Ta, Fe and Mn by X-ray fluorescence *Minerals Engineering p. 373-375.*

Safavi A, Abdollahi H, Maleki N, Zeinali S (2008) Interaction of anionic dyes and cationic surfactants with ionic liquid character. J Colloid Interface Sci *322*(1) 274–280.

Salager, L. J. (2002), *Surfactants Types and Uses* Venezuela – Merida 2, 2-5.

Seddon, K. R, Stark, A., & Torres MJ. (2000) Influence of chloride, water, and organic solvents on the physical properties of ionic liquids. *Pure Appl. Chem.*, 2275–2287.

Seiler, K. & Simon, W. (1992). Theoretical aspects of bulk optode membranes. *Anal. Chim. Acta*, 73-87.

Seleim, M. M., Abu-Bakr, M. S., Hashem, E.Y., El-Zohry, A. M. (2009) Spectrophotometric determination of manganese (II) withMordant Brown 33 in the presence of Tween 20 in some foods. *Canadian Journal of Analytical Sciences and Spectroscopy.*

Shvedene, N. V., Chernyshov, D. V.& Pletnev, I. V., (2008) Ionic Liquids in Electrochemical Sensors. *Russian Journal of General Chemistry, 78*(12) 2507.

Spichiger-Keller, U. E. (1998). Chemical Sensors and Biosensors for Medical and Biological Applications. *Wiley-VHC*. Weinheim.

Sten, A., Richard, G. (1975). Spectrophotometric Determination of Manganese (II) and Zinc(II) with 4-(2-Pyridylazo)resorcinol (PAR). *Inorganic Chemistry 1, Chemical Center, University of Lund, P.O.B. 740, S-220 07 Lund, Sweden.*

Sweeny, B. K. & Peters, D. G. (2001). Cyclic voltammetric study of the catalytic behavior of nickel(I) salen electrogenerated at a glassy carbon electrode in an ionic liquid (1-butyl-3-methylimidazolium tetrafluoroborate, BMIM+BF4-). *Electrochemistry Commun. 3* (12), 712-715.

Tantaru, G., Dorneanu, V. & Stan, M. (2002). Schiff bis bases: analytical reagents. II. Spectrophotometric determination of manganese from pharmaceutical forms. *Journal of Pharmaceutical and Biomedical* Analysis *27* , 827–832.

Tatiana, D., Pierre, S., Roldão, R.U., Ivan, G., & Gomes, A., (1996) Spectrophotometric Determination of Manganese in Steels by On-Line Electrochemical Oxidation. *Journal of the Brazilian Chemical Society.*

Velapoldi, R. A. & Tonnesen, H. H. (2004). Corrected emission spectra and quantum yields for a series of fluorescent compounds in the visible spectral region. *Journal of fluorescence, 14* (4), 465-472.

Wang, Y., Tian, M., Wentao, B.& Row, K. (2009). Application of Ionic Liquids in High Performance Reversed-Phase Chromatography. *International Journal of Molekuler Science 10*(6), 2591–2610.

Wardak, C., (2010) A highly selective lead-sensitive electrode with solid contact based on ionic liquid. *Journal of Hazardous Materials 186*(2-3):1131-5.

Warnken, W., Tang, D., Gill, A. & Santschi, P. H.(2000). Performance optimization of a commercially available iminodiacetate resin for the determination of Mn, Ni, Cu, Cd and Pb by on-line preconcentration inductively coupled plasma-mass spectrometry *Analytica Chimica Acta*, 265–276.

Wei, D. & Ivaska, A. (2008). Applications of ionic liquids in electrochemical sensors. *Analytica Chimica Acta ,* 126-135.

Weidgans, B. M., (2004) . New Fluorescent Optical pH Sensors with Minimal Effects of Ionic Strength. *aus Passau.*

Williams, A. T. R., Winfield, S. A. & Miller, J. N. (1983). Relative fluorescence quantum yields using a computer controlled luminescence spectrometer. *Analyst*, 108, 1067.

Wolfbeis, O. S. (Ed.). (1991). *Fiber Optic Chemical Sensors and Biosensors,* Vol. 1&2, CRC, Boca Raton.

Zatta, P., Lucchini, R., Rensburg S.J., & Taylor, A., (2003) The role of metals in neurodegenerative processes: aluminum, manganese, and zinc. *National enstitues of healthy.*